Universidad Autónoma de Madrid

Departamento de Bioquímica

# Identification and characterization of new proteins associated with autophagy in the model system *Dictyostelium discoideum*


Ana Filipa Pinto Ferreira de Mesquita

Madrid, 2014

Departamento de Bioquímica

Facultad de Medicina

Universidad Autónoma de Madrid

# Identification and characterization of new proteins associated with autophagy in the model system *Dictyostelium discoideum*

Ana Filipa Pinto Ferreira de Mesquita

Licentiate in Biochemistry

Supervisor:

Doctor Ricardo Escalante Hernández

Instituto de Investigaciones Biomédicas “Alberto Sols”, Madrid
Consejo Superior de Investigaciones Científicas-Universidad Autónoma de Madrid

Doctor Ricardo Escalante Hernández, Científico Titular del Consejo Superior de Investigaciones Científicas en el Instituto de Investigaciones Biomédicas “Alberto Sols” de Madrid

CERTIFICA: que Ana Filipa Pinto Ferreira de Mesquita, licenciada en Bioquímica por la Universidad de Oporto, Portugal, ha realizado bajo mi dirección el trabajo de investigación titulado:

**“Identificación y caracterización de nuevas proteínas asociadas a autofagia en el sistema modelo *Dictyostelium discoideum”***

y que éste reúne todas las condiciones requeridas por la legislación vigente, así como la originalidad y calidad científica necesarias, para poder ser presentado y defendido con el fin de optar al grado de Doctor por la Universidad Autónoma de Madrid.

Y para que conste donde proceda, firmo el presente certificado en Madrid, a 1 de Noviembre de 2014.

Doctor Ricardo Escalante Hernández
**Director**

# *ACKNOWLEDGMENTS*

Me gustaría agradecer en primero lugar a Ricardo, mi director de tesis. Ricardo es una persona muy inteligente y científicamente muy bueno pero creo que es en la parte humana que más se destaca. En toda la tesis siempre me ha ayudado con las dificultades y como orientador creo que es lo mejor que alguien puede pedir. Es una persona fantástica y creo que más que un jefe es un líder natural, un mentor. De estas personas que vas a conocer una vez en tu vida. Por todo eso me gustaría darle las gracias y decir que espero que tenga las más grandes felicidades en su vida.

En segundo me gustaría agradecer al doctor Oscar Martinez-Perez con quien afortunadamente he colaborado. He aprendido mucho con su colaboración y creo que es una excelente persona y muy buen investigador.

En tercer lugar me gustaría agradecer a todos que colaboraran con mi tesis, al doctor Olivier Vincent por toda la colaboración en el ensayo de doble hibrido y por disponibilizar su laboratorio para mis experimentos.

Gracias a Elena Izquierdo que ha sido fundamental en el inicio de mi tesis, muchas gracias Eli!

A mis compañeros del laboratorio Sandra, Luis, Montero, Eunice y Sol por vuestra colaboración tanto en experimentos como en toda la vida del instituto, ha sido muy agradable compartir con vosotros. Sandra eres una de las personas más trabajadoras que conozco te va a ir todo muy bien, Luis me encantaría haber compartido más tiempo contigo eres super simpatico, Sol eres super maja espero q todo te va bien en lo que te queda de tesis.
Queria agradecer a Daniela en especial porque por mucho tiempo fue mi única compañera y le valoro mucho por todo lo que me ha ayudado con sus consejos a lo largo de la tesis.

Queria agradecer a tres personas que me ayudaron directamente en la tesis, Diego y Lucia del confocal y Javier de imagen. Muchas gracias por vuestro profesionalismo.

Quiero agradecer a mi amigo Dani Eliche y a Triny porque su amistad fue fundamental para los tiempos más complicados de mi tesis.

Quiero también agradecer a las personas simpaticas y lindas que he conocido en el IIB, Petrina, Leon, Pilar, Lara, Barbara, Carlitos y Hikaro aunque no habemos compartido experimentos vuestra simpatía en las horas de la comida y en la convivencia fueron muy importantes porque sois adorables y me alegro mucho de haberles conocido.

Quiero agradecer a Rosa, Pepa, Claudia, Paco y Ana Guadaño porque siempre fueron muy amables conmigo y como investigadoras más avanzados me han podido dar otras perspectivas de la tesis.

Quero agradecer aos meus pais porque sem eles não podia ter chegado aqui. Ao meu irmão que foi o meu ídolo durante muitos anos.

Quero agradecer ao João, por fazer um programa para eu poder confimar as minhas proteínas, pela ajuda com a tese e porque é espectacular. Realmente sem ele eu podia acabar a tese na mesma, mas não ia ter nem metade da felicidade na minha vida pessoal. Obrigado Noot, eu sei q devia vir um capitulo da tese só para ti, mas os senhores da secretaria não deixaram.

# RESUMEN

Hemos estudiado la red de interacciones proteina-proteina en el proceso de la autofagia en el sistema modelo *Dictyostelium discoideum* usando ensayos de doble hibrido y pull-down de las proteínas conservadas Atg1 y Atg8. Estos análisis confirmaron interacciones esperadas descritas en otros organismos pero también permitieron la identificación de nuevos interactores que ponen de manifiesto la compleja regulación de la ruta autofágica.

El complejo de la serina/treonina quinasa Atg1, un regulador esencial de la autofagia fue investigado en detalle. La composición del complejo Atg1 en *Dictyostelium discoideum* es mas similar a células de mamífero que a las de levaduras ya que además de Atg13, este organismo posee Atg101, una proteína no conservada en hongos.

Hemos descubierto que Atg101 interacciona con Atg13 y que la anulación de estas proteínas en *Dictyostelium* lleva a un bloqueo temprano de la autofagia, aunque la severidad del fenotipo de desarrollo y el grado de bloqueo de la autofagia es más severo en células deficientes en Atg13.

Hemos identificado una proteína conteniendo dominios zinc-finger B-box y FNIP que es un interactor de Atg101. La mutación del gen que codifica esta proteína reduce pero no anula el flujo autofágico, lo que sugiere que funciona como un regulador positivo de Atg101. Describimos además la interación de Atg1 con la enzima de la ruta de las pentosas fosfato transketolasa. Encontramos alteraciones en la actividad de la transketolasa endógena en cepas que sobrexpresan o que son deficientes en Atg1. Esto sugiere la presencia de una nueva vía de regulación entre la autofagia y la ruta de las pentosas fosfato en *Dictyostelium discoideum*.

# ABSTRACT

The network of protein-protein interactions of the Dictyostelium autophagy pathway was investigated by yeast two-hybrid and pull-down of the conserved autophagic proteins Atg1 and Atg8. These analyses confirmed expected interactions described in other organisms but also identified novel interactors that highlight the complexity of autophagy regulation. The serine/threonine kinase Atg1, an essential regulator of autophagy, was investigated in detail here. The composition of the Atg1 complex in Dictyostelium discoideum is more similar to mammalian cells than to yeast since, besides Atg13, it contains Atg101, a protein not conserved in fungi. We found that Atg101 interacts with Atg13 and genetic disruption of these proteins in Dictyostelium leads to an early block in autophagy, although the severity of the developmental phenotype and the degree of autophagic block is higher in Atg13 deficient cells. We have also identified a protein containing a zinc-finger B-box and FNIP motifs that interacts with Atg101. Disruption of this protein reduces but do not abolish autophagic flux suggesting that it functions as a positive regulator of Atg101. We also describe the interaction of Atg1 kinase with the pentose phosphate enzyme transketolase. We found changes in the activity of endogenous transketolase activity in strains lacking or overexpressing Atg1 suggesting the presence of an unsuspected regulatory pathway between autophagy and the pentose phosphate pathway in Dictyostelium.

# INDEX

# ABBREVIATIONS

# ABBREVIATIONS

**Atg:** Autophagy related gene.

**Ax4:** Axenic growth strain number 4.

**Bif-1:** Endophilin B1/Bax-interacting factor 1.

**BS:** Blasticidin

**CMA:** Chaperone mediated autophagy.

**DAPI:** 4',6-diamidino-2-phenylindole.

**Dd:** *Dictyostelium discoideum*.

**DMEM:** Dulbecco's Modification of Eagle's Medium.

**DTT:** Ditiotreitol.

**EBSS:** Earle's Balanced Salt Solution.

**ECL:** Enhanced Chemiluminescence.

**EDTA:** Ethylenediamine Tetraacetic Acid.

**ESI:** Electrospray ionization.

**FIP200:** Focal Adhesion kinase (FAK) family interacting protein of 200 kDa.

**G6P:** Glucose 6-phosphate.

**G6PDH:** Glucose 6-phosphate dehydrogenase.

**GFP:** Green fluorescent protein

**HA:** Epitope tag derived from human influenza hemagglutinin.

**Hek-293T:** Human Embryonic Kidney 293 cells.

**HeLa:** Human Cervical Carcinoma Cell Line

**HL5:** Axenic medium for *Dictyostelium discoideum* growth.

**KO:** Knockout.

**LC3:** Light Chain Microtubule-associated protein 3.

**LIR:** LC3 Interacting Region.

**LTQ:** Linear Trap Quadrupole.

**LB:** Luria Bertani.

**$NAD^+$/NADH:** Nicotinamide adenine dinucleotide.

**$NADP^+$/NADPH:** Nicotinamide adenine dinucleotide phosphate.

**PBS:** Phosphate buffered saline.

**PCR:** Polymerase Chain Reaction.

**PE:** Phosphatidylethanolamine.

**Pgka:** Phosphoglycerate Kinase.

**PI3 kinase:** phosphatidylinositol 3-kinase.

**PI(3)P:** Phosphatidylinositol 3-phosphate.

**PIK:** Phosphatidylinositol kinase.

**PPP:** Pentose phosphate pathway.

**PtdIns3K:** Class III Phosphatidylinositol 3-kinase.

**PtdIns3P:** phosphatidylinositol 3-phosphate.

**PVDF:** Polyvinylidene Difluoride.

**RIPA:** Radio-Immunoprecipitation Assay buffer.

**RFP:** Red Fluorescent Protein.

**RP:** Reverse phase.

**RP-LC-MS/MS:** Reverse phase-liquid chromatography Mass Spectrometry.

**SARs:** Selective Autophagy Receptors.

**SD:** Complete Synthetic Defined Media.

**SDS:** Sodium dodecyl sulfate.

**SDS-PAGE:** Sodium dodecyl sulfate polyacrylamide gel electrophoresis.

**SM:** Selective Medium.

**ThDP:** Thiamin diphosphate.

**TK:** Transketolase.

**TOR:** Target of rapamycin.

**TPP:** Thiamine pyrophosphate.

**TRP1:** Gene that encodes phosphoribosylanthranilate isomerase, an enzyme that catalyzes the third step in tryptophan biosynthesis.

**ULK1 and ULK2:** Unc-51 like autophagy activating kinase 1 or 2.

**UNC-51:** Uncoordinated protein 51.

**URA3:** Gene on chromosome V in *Saccharomyces cerevisiae* .

**UVRAG:** UV radiation resistance associated gene.

**Vps:** Vacuolar protein sorting.

**WD-40:** Structural motif of approximately 40 amino acids often terminating in a tryptophan-aspartic acid dipeptide.

**WIPI1/2:** WD repeat domain phosphoinositide-interacting protein 1 or 2.

**X-GAL:** 5-bromo-4-chloro-3-indolyl-beta-D-galacto-pyranoside.

**Y2H:** Yeast two-hybrid.

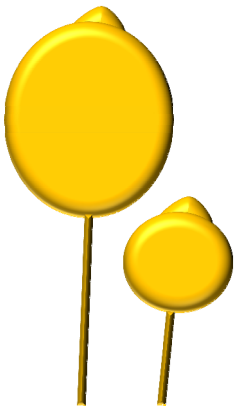

# INTRODUCTION

# INTRODUCTION

## 1. The Autophagic pathway.

Autophagy is a degradation pathway that occurs in all eukaryotic organisms analyzed to date. This route has been associated with numerous pathologies and dysfunctions as cancer, neurodegenerative diseases, aging, heart and liver diseases metabolic dysregulation and oxidative stress. [1-3]

In general autophagy comprises the degradation of parts of the cytoplasm in the lysosomes. There are three forms of autophagy namely chaperone-mediated autophagy, microautophagy and macroautophagy. [4] Chaperone mediated autophagy requires the identification of proteins by a cytosolic chaperone that delivers this proteins to the surface of lysosomes where they unfold and pass through the membrane to be degraded. [5] Microautophagy differs from CMA and macroautophagy because it involves the invagination of the lysosomal membrane which encloses little amounts of material from the cytoplasm. [6,7]

Our work will be focused only in macroautophagy, hereafter referred simply as autophagy. The autophagic process is initiated with the formation of double membrane vesicles (phagophores) that elongate to form a compartment called autophagosome. The autophagosomes enclose parts of the cytoplasm that are then delivered to the lysosomes forming the autolysosomes where the cargo can be degraded. The degraded compounds are transported back to the cytoplasm where they can be recycled and used in other cellular activities. [8-11] This mechanism is tightly regulated by a series of proteins called autophagy-related proteins (Atg proteins). Nowadays approximately 30 Atg proteins have been identified. [12-14]

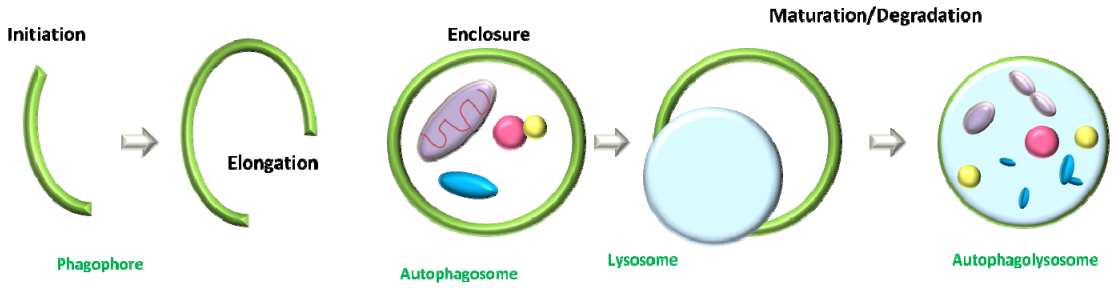


**Figure 1. Autophagosome formation.** The scheme represents the stages of autophagy: the first step is the initiation/nucleation with the formation of the phagophore membrane. At this stage the Atg1/Ulk1 and the class III PI3K complexes are necessary. Secondly, the elongation of the double membrane to form a complete enclosed autophagosome, in which the ubiquitin-like conjugation machinery is fundamental and finally the maturation stage comprising the fusion of the autophagosome to the lysosomes and consequent cargo degradation.[15,16]

Autophagy was for some time sought to be a non-selective, unspecific degradation mechanism. However, it has now become clear that autophagy can be selective, for example the specific targeting of damaged organelles such mitochondria (a process known as mitophagy), peroxisomes (pexophagy) or endoplasmic reticulum (reticulophagy). Selective autophagy is a relatively recent branch of study but the amount of targets of selective autophagy identified is growing and the same can be said about the receptors and adaptor proteins involved in their recognition. [17-19]

Autophagy is tightly controlled by organized complexes formed by Atg proteins that regulate the various stages (induction, nucleation, elongation and maturation) of autophagy. The following sections describe these groups in more detail.

### 1.1. Atg1/ULK1 Complex and the induction stage.

The first Atg protein described was the serine/threonine kinase Atg1 also known as ULK1 in mammals, UNC-51 kinase in *Caenorhabditis elegans* and *CG10967 in Drosophila melanogaster*. These proteins are highly conserved especially in the N-terminal kinase domain. In yeast, Atg1 interacts with the regulatory proteins Atg13, Atg17, Atg29, and Atg31 in response to autophagy-inducing signals. [20] In mammalian cells, ULK1 kinase complex is constituted by ULK1, Atg13 and Atg101. Both the yeast Atg1 and mammalian ULK1 are directly regulated by TORC1 (target of rapamycin complex 1) by phosphoryation. TORC1 complex is a regulator of the nutritional status of the cell. Under nutrient-rich conditions Atg1/ULK1 and Atg13 are hyperphosphorylated. By contrast, in starvation conditions TOR activity is inhibited, which leads to the activation of Atg13 and to its dephosphorylation. The dephosphorylated Atg13 then ligates Atg1/ULK1 activating the kinase activity and leading to autophagy initiation. [1,14,21,22]

Atg101 is a small mammalian protein with approximately 200 amino acids that has not been conserved in yeast. It plays a fundamental role in the stability and basal phosphorylation of Atg13 and ULK1. [23,24]

Mammalian Atg1/ULK1 complex is constituted by another protein fundamental for autophagy, FIP200 - focal adhesion kinase (FAK) family interacting protein of 200 kD - also called RB1CC1 (retinoblastoma 1–inducible coiled-coil 1). This protein directly interacts with ULK1 and has a role in different cellular functions such as cell size, proliferation, and migration. [25] Although there is no FIP200 homologue in yeast it is accepted that the protein Atg17 is the functional equivalent of FIP200. [26] Yeast Atg17 interacts with Atg13 and with Atg1 in a manner dependent on Atg13 and similarly to FIP200 is fundamental for autophagy. [27] Defects in FIP200 in mammalian cells are

associated with accumulation of ubiquitinated protein aggregates and increased apoptosis. [28] Atg17 and FIP200 have other similarities as the fact that both have multiple coiled-coil domains and both are fundamental for Atg1/Ulk1 activity. [25]

Atg17 forms a subcomplex both in basal and starvation conditions with Atg29 and Atg31, these proteins target the pre-autophagosome structure under starvation conditions and their function is to recruit Atg13 and consequently Atg1. [29,30]

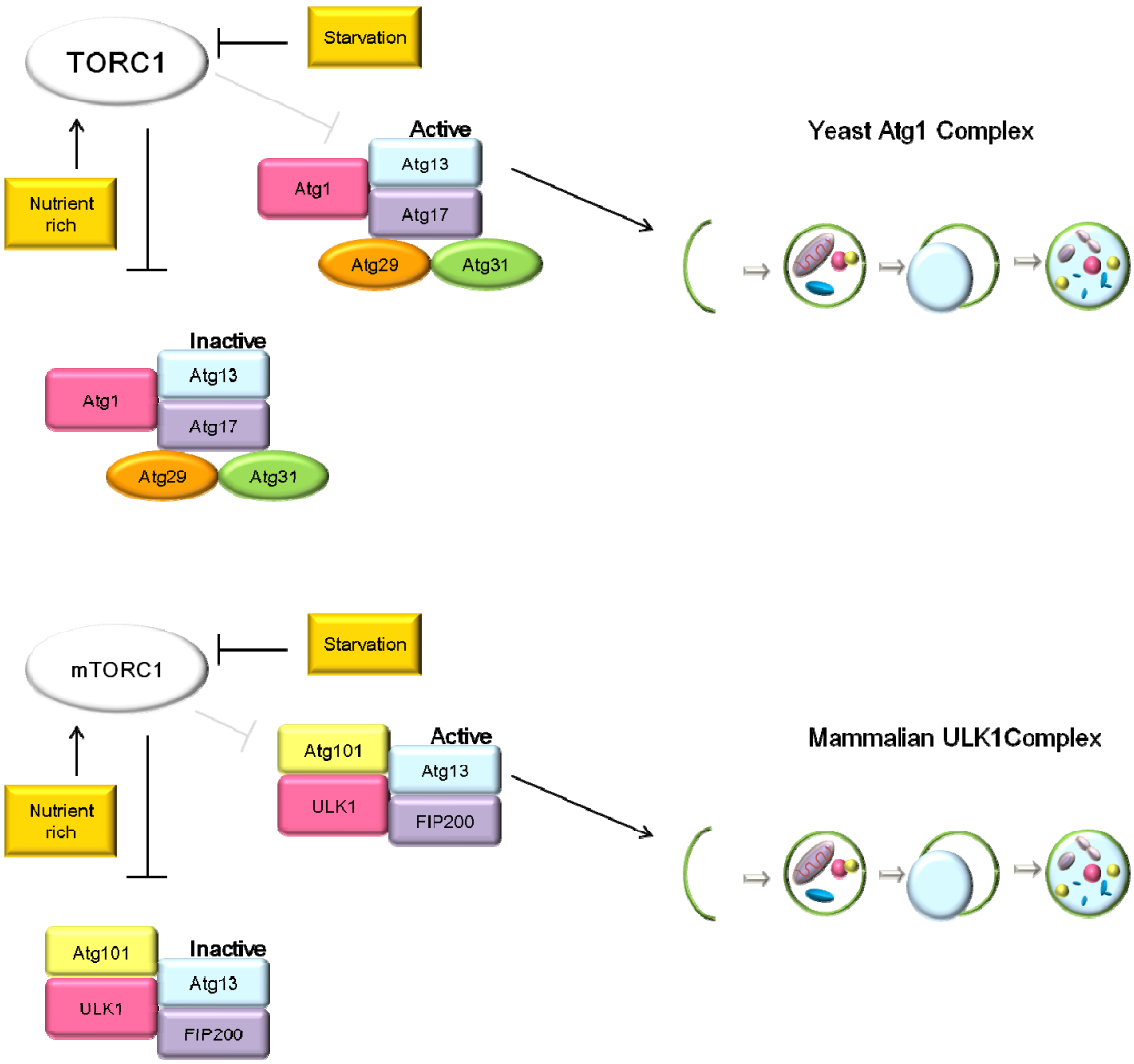


**Figure 2. The protein composition of Atg1/ULK1 complex.** In yeast, the complex contains Atg1, which directly binds to Atg13 and Atg17, while Atg29 and Atg31 are linked to the complex through the interaction

with Atg17. The mammalian complex is formed by ULK1, the ortholog of Atg1, which interacts with Atg13. The two other members of the complex are Atg101 and FIP200. In normal, nutrient rich conditions the mammalian TOR complex 1 (mTORC1) inhibits ULK1 and Atg13 by phosphorylation. Under starvation TORC1 is inhibited and this activates the ULK1 complex. Active ULK1 may take a closed conformation, in which the middle proline/serine-rich regions move the kinase domain to the proximity of its possible targets, Atg13 and FIP200. Their phosphorylation triggers downstream events for autophagosome formation.

### 1.1. PtdIns3-Kinase complex in the initiation stage.

During the formation of the phagophore membrane PtdIns3P is generated at the site of autophagosome formation by the activity of the class III phosphatidylinositol 3-kinase (PtdIns3K) VPS34. This process is essential for the recruitment of other proteins such as the PtdIns3P-interacting protein Atg18 (also known as WD-repeat domain phosphoinositide-interacting protein (WIPI in mammals) (figure 3). [31] Atg18 or WIPI1/2 in mammalians is a protein essential for autophagosome formation and has been reported to interact with other Atg proteins, for example Atg16. [32-34] WIPI1 and WIPI2 share common ancestry with Atg18 and have different complementary functions. [35] Atg18/WIPI includes a WD-40 repeat and seven predicted β-propellers, which may facilitate the scaffold of other proteins involved in recruiting the autophagy machinery. [35]

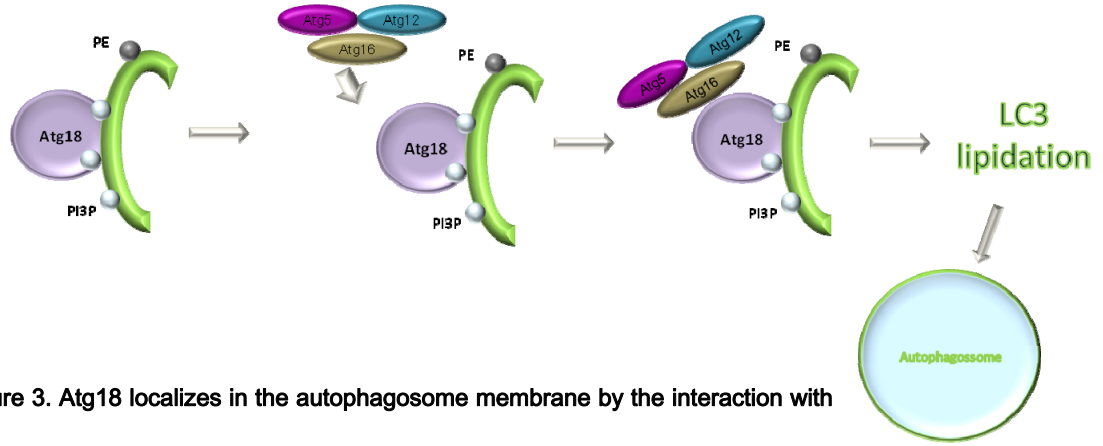


**Figure 3. Atg18 localizes in the autophagosome membrane by the interaction with PtdIns3P.** It requires the activity of Atg1 and VPs34 complexes for correct localization. [31,33,34]

The connection of PtdIns3K to autophagy started with the finding that 3-methyladenine, a PtdIns3K inhibitor impedes the formation of autophagosomes. [36] In yeast there is only one PtdIns3K called Vps34 which forms a stable membrane complex and is regulated by Vps15. [37] Vps34-Vps15 is present in two complexes, but only one of them is associated with autophagy, the complex formed by the proteins Vps34, Vps15, Atg14 and Atg6. [37,38] Beclin 1, the mammalian homologue of yeast Atg6 is a multifunctional scaffold proteins involved in autophagy, apoptosis and cancer that is known to be regulated in autophagy by some co-factors as Atg14 and Bif-1 (Endophilin B1/Bax-interacting factor 1). [39-41] Although most of the Vps34-Atg15 is not bound to beclin 1 the complexes of Vps34 responsible for promoting autophagy contain beclin-1 that acts as an autophagy regulator. [38,42] Atg6 has also been associated with the size and number of autophagosomes in yeast. [41]

Bif-1 is a protein containing an amino-terminal N-BAR domain involved in the induction of membrane curvature although its precise function in autophagosome formation is poorly known. [43] Bif-1 interacts with Beclin-1 through UVRAG and acts as a co-factor, activating autophagy in mammalian cells. [44,45]

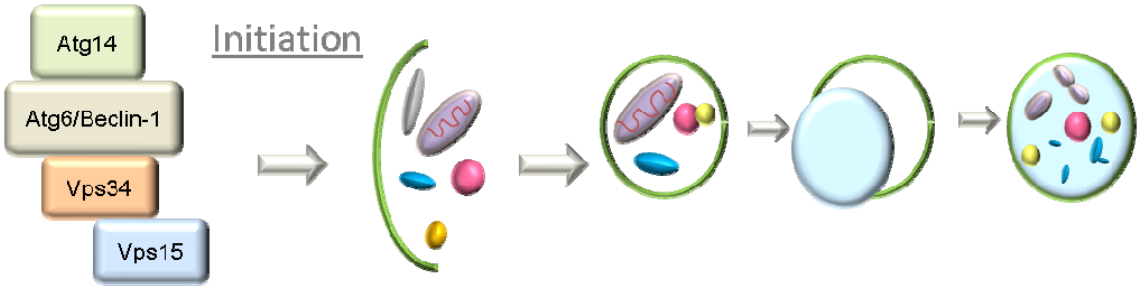


**Figure 4. Vps 34 and associated proteins.** Vps34 is mainly involved in the initiation of autophagy by generating PtdIns3P at the site of autophagosome formation and this promotes the activation and recruitment of other Atg proteins and factors in response to nutrient starvation. This image displays a representation of the arrangement of the VPS34 complex. [38,46-48]

## 1.2. Ubiquitin-like conjugation systems.

Atg8, the yeast counterpart of mammalian LC3 is a protein essential in autophagosome formation that contains a C-terminal ubiquitin-like domain. [49-51] Atg8/LC3 apart from being required for the biogenesis of autophagosome membrane also mediates selective autophagy via the recruitment of LIR-containing autophagy receptors. [51,52] LIR motifs are LC3 interacting regions that ensure the targeting of autophagy receptors to the autophagosome membrane. [51,52]

There are six human homologs for Atg8 grouped in the microtubule-associated protein-1 light chain 3 (MAP1LC3) family (MAP1LC3A, MAP1LC3B, MAP1LC3C; short names LC3A, LC3B, LC3C, respectively, and collectively LC3) and the γ-aminobutyric acid (GABA)-receptor-associated proteins (GABARAP, GABARAPL1, GABARAPL2). [49,50]

One of the most important reactions in autophagy is the covalent attachment of Atg8/LC3 to the lipid phosphatidylethanolamine (PE). This conjugation is mediated by several autophagy-related proteins. [52-55] Atg8/LC3-PE will be localized on both the outer and inner phagophore membrane [52] and its levels have been correlated with the size of autophagosomes implying that Atg8 is actively involved in phagophore expansion. [53] This process is mediated by two ubiquitin-like conjugation systems. In the first the precursor Atg8 is processed by the cysteine protease, Atg4 that cleaves the C-terminus of Atg8/LC3 exposing a conserved cysteine residue. This residue is activated by Atg7 (E1-like) and then transferred to Atg3 (E2-like). Finally Atg8/LC3 is conjugated to phosphatidylethanolamine with the aid of the complex Atg12-Atg5-Atg16 (E3-like). [54,56] The formation of Atg12-Atg5-Atg16 is also dependent on another ubiquitin-like conjugation reaction starting with the covalent ligation of the ubiquitin-like protein Atg12 to Atg5, this interaction is assisted by two sequential reactions catalyzed by Atg7 (E1-like) and Atg10 (E2-like). In the first one of these reactions Atg12 is activated by Atg7 and transferred to Atg10 which makes then the ligation of the C-terminal glycine residue of Atg12 to Atg5. Secondly, Atg12-Atg5 forms a complex with Atg16. [57,58]

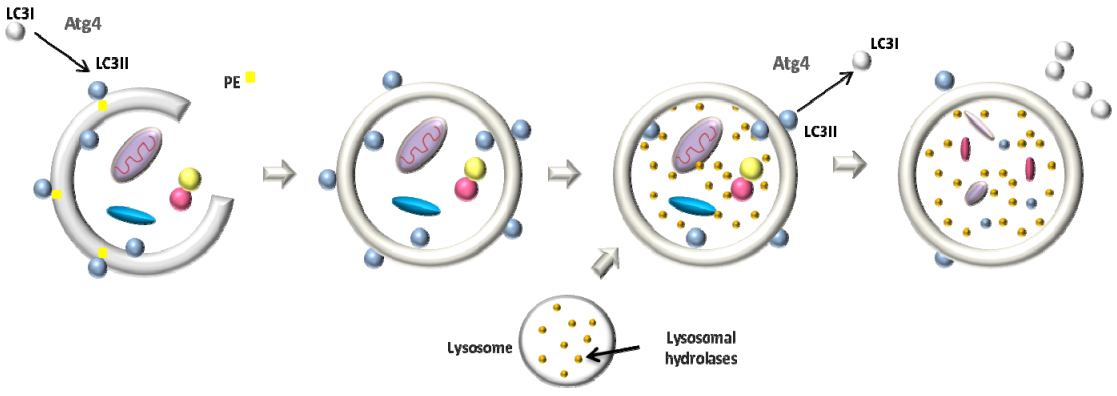


**Figure 5. LC3 localization.** LC3 is converted from LC3-I (non-lipidated) to LC3-II (conjugated to PE) and localized sequentially to the cytosol or to the phagophore, autophagosome and to the autolysosomes. This feature makes LC3 the best autophagosome marker. [59-62]

Once the autophagosome is complete, the Atg8/LC3 located in the external membrane is de-lipidated and recycled by Atg4. After fusion with the lysosomes the cargo and also the lipidated Atg8/LC3 (known as LC3-II) that is trapped inside the autophagosome lumen are degraded. [61]

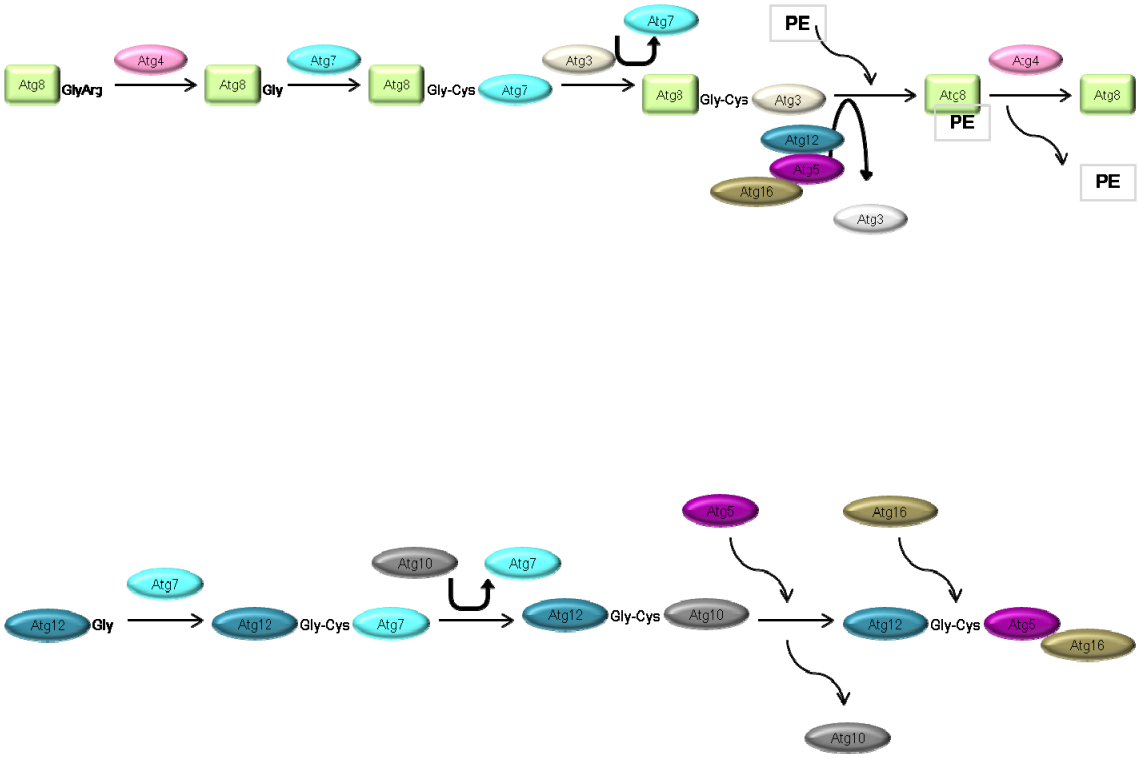


**Figure 6. Atg8 and Atg5-Atg12 conjugation systems.** [31,63]

## 2. Dictyostelium discoideum as a model organism.

The social amoeba, *Dictyostelium discoideum* is a cellular slime mold (Dictyostelid) that forms part of a group of amoeboid protozoa called *Amoebozoa*. [64-66]

The social amoebas can survive in the soil of a very diverse set of habitats, ranging from desert environments to the arctic colds, being usually more prevalent in places rich in bacteria, their main source of nutrition. [67]

Protein similarity studies suggest that phylogenetically Dictyostelium diverged from the animal line before fungi. [68] However, Dictyostelid's cell mechanisms are more similar to the ones encountered in animals than to those in fungi. As a result, there are many cellular processes that are conserved between Dictyostelium and animals that have been lost during fungal evolution, for example cell motility, chemotaxis, phagocytosis and macropynicytosis. [68]

Dictyostelids have been studied for approximately 150 years but it was *Dictyostelium discoideum* the estabilished model to study development and fundamental cell biology. [67]

*Dictyostelium discoideum* genome has been completely sequenced and is organized into six chromosomes that code for approximately 12.500 protein-coding genes. Most of the genes involved in signal transduction pathways and mediate intercellular communication are present in this organism. [69,70]

Multicellularity is considered one of the major improvements in evolution, therefore the transition of *Dictyostelium discoideum* from a unicellular amoeba to a multicelular organism is of most importance. [69,71]

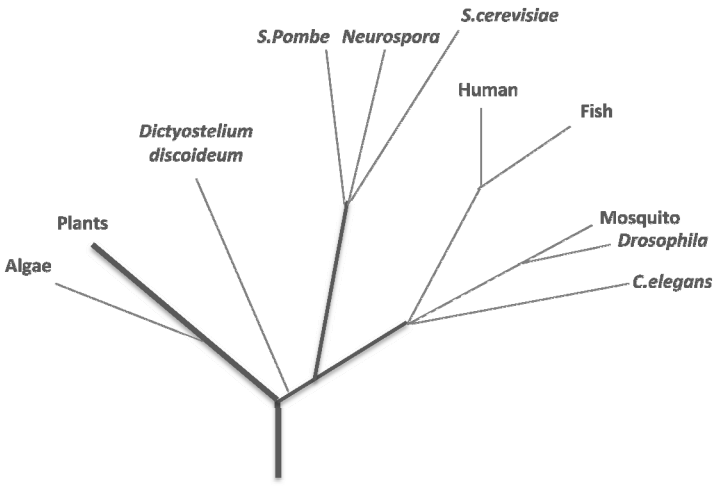


**Figure 7. Phylogeny tree of eukaryotic organisms.** [Adapted from [68]]

*Dictyostelium discoideum* lives as a unicellular amoeba using soil bacteria as nutritional source, in the case of a decrease of available food it uses extracellular signals to communicate and initiate aggregation. [69,71] Approximately 100.000 amoebas come together to form a multicellular organism that goes through a series of stages that compose a multicellular developmental cycle. [69,71] This cycle takes only 24 hours to occur and is initiated with the aggregation of independent amoebas into a mound of cells. [67,71] Soon after aggregation cells differentiate as either prestalk or prespore cells, the first ones tending to move to the distal side of the structure where they form a tip that elongates to form a standing slug (finger). This fingered structure develops into a stage known as "slug" that is capable of migrating phototactically and thermotactically in order to find a better location to culminate into a fruiting body composed by stalk and spores. [72-74] In the suitable conditions the spores can germinate to release unicellular amoebas and complete the life cycle. [75]

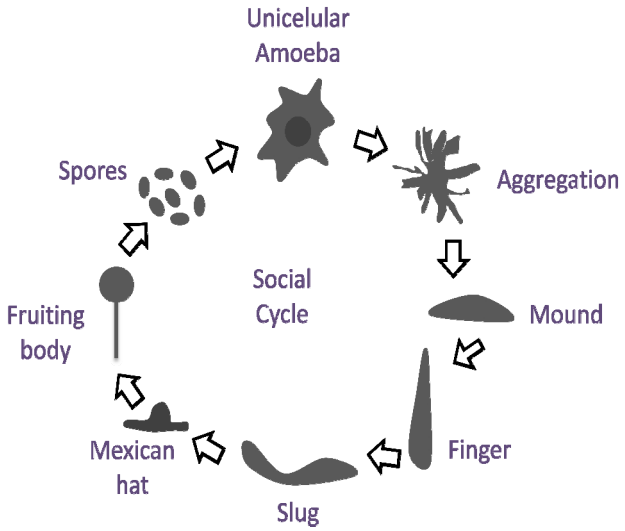


**Figure 8. The developmental life cycle of *Dictyostelium discoideum.*** Under starvation Individual cells aggregate to form a mound of approximately 100.000 cells. These groups of cells go through different stages of development. Dictyostelium cells are haploid throughout the whole process. [67,69,76]

## 3. Autophagy in Dictyostelium discoideum.

*Dictyostelium discoideum* development cycle is energy consuming but takes place in the absence of nutrients and thus, the cells need mechanisms to mobilize internal resources that enable the maintenance of the cellular homeostasis.

Autophagy plays an essential role in the recruitment and recycling of proteins and lipids that will enable the development to occur normally. As a result, when autophagy is impaired, development does not proceed normally. [77,78]

Dictyostelium autophagy is more similar to mammalian cells than to yeast model. Autophagosomes are formed randomly in the cytoplasm in close association with the endoplasmic reticulum (ER) and fuse with the multiple lysosomes. This similarity extend to the molecular mechanisms since there are a number of autophagic proteins conserved between Dictyostelium and mammalian cells that are absent in yeast. [78,79]

One relevant example is Vmp1 (Vacuole membrane protein 1), and endoplasmic reticulum-resident protein that is required for the origin of autophagosomes from the ER in Dictyostelium and mammalian cells. [80] Nevertheless, although some autophagy-related proteins have been studied in *Dictyostelium discoideum*, the extent of these studies are still behind of what is known in mammalians and yeast.

### 3.1. Atg proteins in Dictyostelium discoideum.

*Dictyostelium discoideum* Atg1 is composed by an N-terminal kinase domain very similar to the homologues in other organisms and a C-terminal domain with very limited identity. These two domains are separated by a zone rich in asparagines. [77,78]

Amoebas in which Atg1 has been knocked out show reduced survival in nitrogen starvation and decreased protein degradation in development revealing a fundamental role of this protein in autophagy and in the initiation of multicelularity. [77]

In 2003, Richard Kessin's group mutated Atg5 and Atg7 showing that the disruption of these proteins leads to defects in aggregation upon starvation. During this study it was also demonstrated that the GFP recombinant forms of Atg5 and Atg12 were present in two different forms in starving cells that corresponded to conjugated and not conjugated forms. These data indicate that the conjugation systems may be arranged in the same way in *Dictyostelium discoideum* as previously described for yeast and mammals. [81]

*Dictyostelium discoideum* has homologue forms to autophagosome markers Atg8 (LC3 in mammals) and Atg18 (WIPI in mammals). The first is present in the autophagosome membrane until its degradation and the second labels the nascent autophagic membrane. [82]

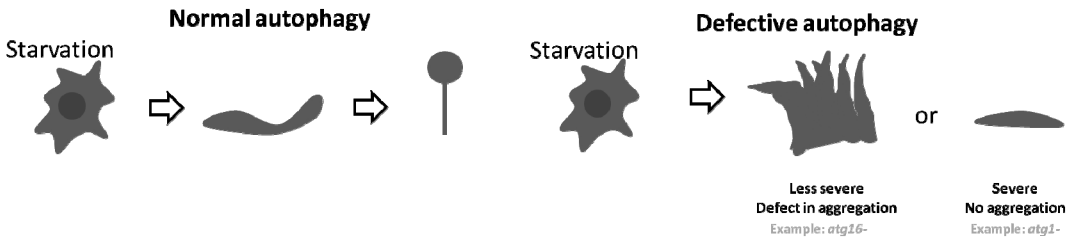


Figure 9. Autophagy impairment is reflected on developmental defects in *Dictyostelium discoideum*.

## 4. The Pentose Phosphate Pathway.

The pentose phosphate pathway is a conserved biochemical pathway closely related to glycolysis. The principal function of pentose phosphate pathway is the generation of ribose 5-phosphate and NADPH that are used in biosynthetic pathways. [83,84] Ribose-5-phosphate can be used in the synthesis of nucleotides and nucleic acids and the NADPH generates reducing power that is required for biosynthetic reactions such the fatty acid synthesis and to prevent oxidative stress. This route is therefore a major source of metabolic intermediates for biosynthetic processes. [85]

There are two different phases in this pathway, the oxidative phase, in which glucose 6-phosphate renders NADPH with the formation of ribose-5-phosphate and the non-oxidative phase in which the pentose phosphates can be transformed again into hexoses phosphates that can be used again in oxidative reactions.

The first step of the pentose phosphate pathway is catalyzed by the glucose 6-phosphate dehydrogenase with the consumption of Glucose-6-phosphate, this reaction depends on NADP+ [83] Glucose 6-phosphate dehydrogenase represents the first step in the oxidative phase of penthose phosphate catalyzing the conversion of glucose-6-phosphate to 6-phospho-D-gluconolactone. This reaction converts $NADP^+$ to NADPH which is fundamental to counterbalance oxidative stress. [86-88] Glucose-6-phosphate has a central importance in cellular physiology not only because it is the major source of NADPH but also due to its requirement in many essential cellular systems including

antioxidant pathways nitric oxide synthase, NADPH oxidase, cytochrome p450 system, and others. Indeed G6PD is essential for cell survival. G&PDH is highly regulated at the level of transcription, translation, posttranslation, and intracellular location. [89] The measurement of this enzyme is fundamental in this case to address the state of the total flux of the PPP.

### 4.1. Transketolase.

This enzyme is the most important enzyme of non oxidative branch of the pentose phosphate pathway and needs thiamin diphosphate and a divalent metal ion for its activity. Thiamin diphosphate (ThDP) is a derivative of thiamin. [90]

Transketolase enzymes have been identified and studied in several organisms, including humans, *Saccharomyces cerevisiae*, Escherichia coli, maize, spinach, *Plasmodium falciparum* and now *Dictyostelium discoideum*. [91]

This protein exists in all animal organs and tissues playing a fundamental role in the metabolism of cells. [92] The name transketolase was adopted due to the function of this enzyme catalyzing the transfer of a 2-carbon fragment from the ketopentose ribulose 5-phosphate to the 5-carbon sugar ribose 5-phosphate generating a ketol linkage in the 7-carbonsugar, sedoheptulose 7-phosphate. [84] Activity of human transketolase has been studied in numerous pathologies as it is the case of cancer, malaria, tuberculosis, Wernicke–Korsakoff syndrome and neurological disorders like Alzheimer disease. [91,93,94] Being connected to many metabolic pathways, transketolase assumes a central role in homeostasis regulation being its inhibition responsible for example of alterations in coenzymes synthesis (ATP, CoA, NAD(P)+, FAD), oxidative stress and the production of genetic alterations in cancer cells. [95]

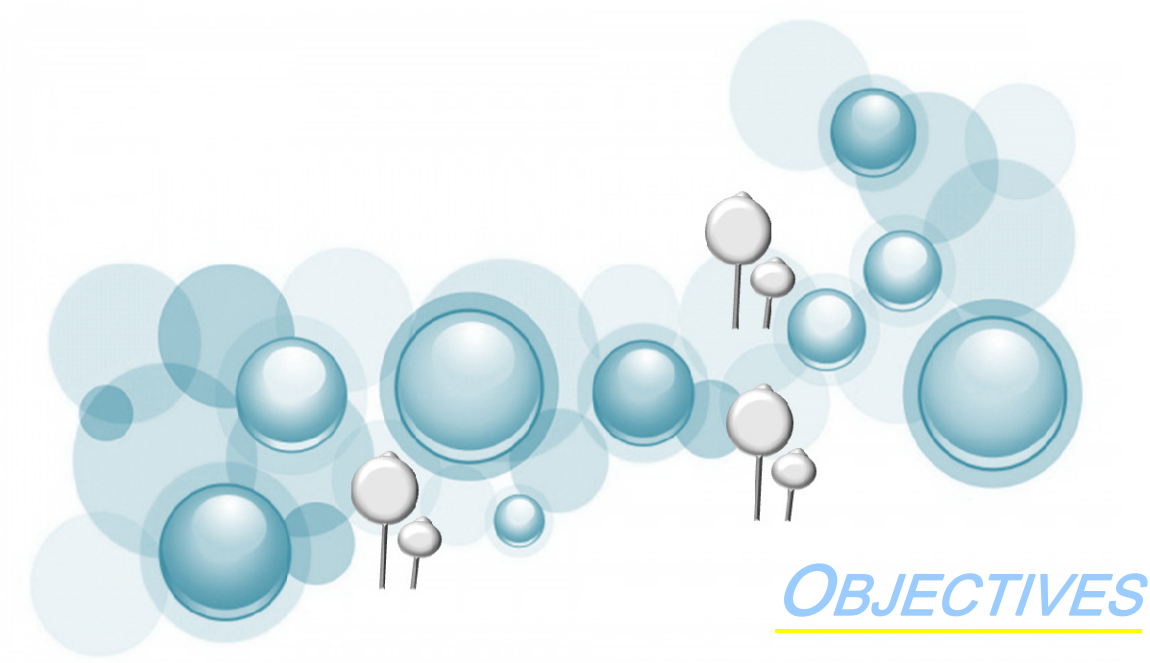

# OBJECTIVES

# OBJECTIVES

1. Identification of the putative proteins involved in *Dictyostelium discoideum* autophagy using bioinformatics analysis.

2. Characterization of the autophagy interaction network in *Dictyostelium discoideum* by yeast-two hybrid.

3. Optimize a suitable method to quantify autophagy flux.

4. Characterize the Atg1 kinase complex and the importance of the putative proteins Atg13, Atg101, Atg17 and FIP200 in autophagy by generation of knockout strains.

5. Study the functional connection between Atg1 kinase and the pentose phosphate pathway enzyme transketolase.

# MATERIALS AND METHODS

# MATERIALS

## 1. Cell Lines.

### 1.1. Bacteria.

In this work we employed the strain of Escherichia coli DH5α in all cloning, overexpression and knock-out constructs. This strain was grown in Luria Bertani, LB medium (1% bacto-tryptone, 1% NaCl and 0.5% Bacto-yeast extract). The medium was complemented with ampicillin (100 µg/ml) since all plasmids used had this resistance.

### 1.2. Yeast.

Yeast two-hybrid assays were carried out in S. cerevisiae TAT7 (MATα ade2–101 his3-Δ200 leu2-Δ1 trp1-Δ901gal4 gal80 LYS2::lexAop-HIS3 URA3::lexAop-lacZ).

### 1.3. Dictyostelium discoideum.

Wild-type Ax4 strain (provided by DictyStock Center, Northwestern University in Chicago, IL, USA) was used for genetic manipulation, knockout generation and over-expression of the different genes analyzed in this study.

### 1.4. Mammalian cell lines.

HEK-293T cells (Thermo Scientific) cell lines were used for activity assays.

## 1.5. Oligonucleotides.

Oligonucleotides for PCR (polymerase chain reaction) were purchased from Sigma-Aldrich.

| Dictybase ID | Name | Oligonucleotides | |
|---|---|---|---|
| DDB_G0292390 | **Atg1** | N terminal Foward | 5′ CGGGATCCGCATGAAACGAGTAGGAG 3′ |
| | | N terminal Reverse | 5′ CGGGATCCGCTTAATTAAAGAAATCTTCCCAAG 3′ |
| | | C terminal Foward | 5′ CGGGATCCACCAAATAGTTTACCATTTGC 3′ |
| | | C terminal Reverse | 5′ CGGATCCGCATTATTTTGAATACTATTG 3′ |
| DDB_G0292390 | **Atg13** | N terminal | 5′ CGGGATCCAAATGGATTCAAGATATTCAG 3′ |
| | | N terminal Reverse | 5′ GGGATCCTTAATCATAGTTATTTCCAGATTG 3′ |
| | | C-terminal | 5′ CGGGATCCTTATTGAGAAGTTGGTTTATTATTAAAG 3′ |
| | | C- terminal Reverse | 5′ CGGGATCCTTATTGAGAAGTTGGTTTATTAAAG 3′ |
| DDB_G0288287 | **Atg101** | Foward | 5′ CGGGATCCGCATGAACAGTAAACAATATG 3′ |
| | | Reverse | 5′ CGGGATCCTTATTTTGTAATTTGAGGAGG 3′ |
| DDB_G0268498 | **FIP200** | Foward | 5′ CGGGATCCAAGATTCAAAAGATGATATTCCCACTTC 3′ |
| | | Reverse | 5′ CGGGATCCTTAATTATCTGAGGAATCAGAAGATAG 3′ |
| DDB_G0295673 | **Atg17** | Foward | 5′ CGGGATCCATTTTTCAAGTAAATCATTAGAATTGTG 3′ |
| | | Reverse | 5′ CGGGATCCTTATTGTTGATTAATTGGTGAAGATC 3′ |
| DDB_G0289601 | **pIKE** | Foward | 5′CGACGAATGAAAGTTTCAAAAGACTTTAAG 3′ |
| | | Reverse | 5′ CGGTCGACTTAAGCTTTCCAATATTGTAACC 3′ |
| DDB_G0288021 | **Atg6b** | Foward | 5′ CGGGATCCTGGATTTATATTGTCAAAAATGTTAC 3′ |
| | | Reverse | 5′ CGGGATCCTTACCAAATTAAATTAAGATCCATTTTAAG 3′ |
| DDB_G0284997 | **Bif1** | Foward | 5′ CGGGATCCATAAAATTACAACACAATTTGCAAG 3′ |
| | | Reverse | 5′ CGGGATCCTGGATTTATATTGTCAAAAAATGTTAC 3′ |
| DDB_G0288895 | **Bif2** | Foward | 5′ GCGGATCCTGTCAAAAGAAAAAACATCTTGG 3′ |
| | | Reverse | 5′ GCGGATCCTTAACCACTTGTATGATTACATG 3′ |
| DDB_G0277319 | **Atg3** | Foward | 5′ CGGTCGACTGTTAACATCATTTCAACAAGCTG 3′ |
| | | Reverse | 5′ CGGTCGACTTATGTATCGAATTCAAGAGTG 3′ |
| DDB_G0273443 | **Atg 4-1** | Forward | 5′ GCGGATCCGCATGTTTACGAAATATTCACACC 3′ |
| | | Reverse | 5′ GCGGATCCTTAGCCAACCATTGTAAAATCATCG 3′ |
| DDB_G0289881 | **Atg5** | Forward | 5′ GCGGATCCGCATGTCATCATTTGACGAAGATATC 3′ |
| | | Reverse | 5′ GCGGATCCTTAGTAGTTATTGCTATTATTATTG 3′ |
| DDB_G0271096 | **Atg7** | Foward | 5′ CGGTCGACTGACAAATACACTTCAGTTTAAAG 3′ |
| | | Reverse | 3′ CGGTCGACTTAAGAAATATCAATATCCCAATC 3′ |
| DDB_G0286191 | **Atg8** | Foward | 5′ CGGGATCCGCATGGTTCATGTATCAAGC 3′ |
| | | Reverse | 5′ CGGGATCCTTATAAATCACTACCAAAAG 3′ |
| DDB_G0268840 | **Atg10** | Foward | 5′ CGGGATCCGCATGTTAACATCCAAAGATTTTAG 3′ |
| | | Reverse | 5′ CGGGATCCCTATATATTATTATTTTTTAATAAATCAAATGG 3′ |
| DDB_G0282929 | **Atg12** | Foward | 5′ CGGGATCCGCATGGAGGAAGAAGAAAAAAATAATAATG 3′ |
| | | Reverse | 5′ CGGGATCCTTAACCCCACGCCATTTGTTGGG 3′ |
| DDB_G0275323 | **Atg 16** | Foward | 5′ CGGTCGACATAATTCATATATGATGATGATGG 3′ |
| | | Reverse | 5′ CGGTCGACTTATTGAATTATATTTTATCTTTATCAGC 3′ |
| DDB_G0285375 | **Atg 18** | Foward | 5′ CGGGATCCGCATGAATGTTGGAGGTAAATTCAATG 3′ |
| | | Reverse | 5′ CGGGATCCTTATAATATTTTTGCTGTAACATC 3′ |
| DDB_G0270098 | **p62** | Foward | 5′ CGGTCGACTGGTAAATCTTATTTTAAAGATCC 3′ |
| | | Reverse | 5′ CGGTCGACTTATTGTTCTTGATTACTTAATAAATGGTC 3′ |
| DDB_G0278351 | **Atg14** | Forward | 5′ CGGGATCCGTGAAGATTTTAATTTATTACAAGAAC 3′ |
| | | Reverse | 3′ CGGGATCCTTATCCAATTTGAATTGAAGTAGTGG 5′ |
| DDB_G0274019 | **Transketolase** | Foward | 5′ GCCTCGAGTAATGTCAAACATTGATTTTAAAGC 3′ |
| | | Reverse | 5′ GCTCTAGATTATTGTTTTGAAATGAAATGTTTACTAAATTTTCAG 3′ |
| DDB_G0279871 | **Interactor Atg101** | Forward | 5′ CGGGATCCGCATGGCAGGTAAATTTGATAATAAATG 3′ |
| | | Reverse | 5′ CGGGATCCGCTTACATTTCAATTTGAGAGTAACC 3′ |

**Table 1.** Oligonucleotides used to amplify *Dictyostelium discoideum* genes necessary for yeast two-hybrid, overexpression and Immunoprecipitation assays.

| Gene Knocked out | Oligonucleotides | |
|---|---|---|
| Atg 13 | Forward C-terminal | 5′ CGGCGGCCGCATGGATTCAAGATATTCAGA 3′ |
| | Reverse C-terminal | 5′ CGGAATTCCCCATAGGAGTTGGAATTGCTG 3′ |
| | Forward N-terminal | 5′ CGAAGCTTGGTTCATCACCACCATTTGG 3′ |
| | Reverse N-terminal | 5′ CGGTCGACGTGGTAATATTACTAAGAAGC 3′ |
| Atg101 | Forward C-terminal | 5′ GGCGGCCGCATCCGGACGTGTACCATTTCATTATGC 3′ |
| | Reverse C-terminal | 5′ CGGAATTCCTACACAATCTAACGTTGTATC 3′ |
| | Forward N-terminal | 5′ CGAAGCTTCGTTACAAAGACAACCATATTCTC 3′ |
| | Reverse N-terminal | 5′ CGGTCGACGGTTGATAATGGTGTTGTAGATGC 3′ |
| FIP200 | Forward C-terminal | 5′ GCGTCTAGACCCACTTCACCATCACCAAACACTTTAG 3′ |
| | Reverse C-terminal | 5′ GCGTCTAGAGTGTGACGATGAACGTATGGTGG 3′ |
| | Forward N-terminal | 5′ GGGAAGCTTCCAGGTCAATTAGATCCAATG 3′ |
| | Reverse N-terminal | 5′ GCGGTCGACGAACCATCTTTGATGGAACC 3′ |
| Atg17 | Forward C-terminal | 5′ GCGGAGCTCGGTGTGAGATTGAACGTTC 3′ |
| | Reverse C-terminal | 5′ GCGTCTAGACTAAGAATCTATTCTCCATCTC 3′ |
| | Forward N-terminal | 5′ GCGAAGCTTCACTTCTCTGATTTATTAACAC 3′ |
| | Reverse N-terminal | 5′ GCGGTCGACCTGTATTCGTAGGTCAACCTC 3′ |
| Int-Atg101 | Forward C-terminal | 5′ CGGCGGCCGCATGGCAGGTAAATTTGATAATAAAATGTACAC 3′ |
| | Reverse C-terminal | 5′ CGGGATCCGAATTCTTTACAAAATCCATTG 3′ |
| | Forward N-terminal | 5′ CGAAGCTTGTTCTGCAACTTATAAAGATCC 3′ |
| | Reverse N-terminal | 5′ GCGTCGACCATTTCAATTTGAGAGTAACCATTTG 3′ |

**Table 2.** Oligonucleotides used in amplification of the C-terminal and N-terminal flanking regions for knockout constructs.

| Gene | Oligonucleotides | |
|---|---|---|
| Transketolase | Forward | 5′ ggccgaattccgccATGGAGAGCTACCACAAGCC 3′ |
| | Reverse | 5′ ggccgaattcCTAGGCCTTGGTGATGAGGCC 3′ |

**Table 3.** Oligonucleotides employed in the amplification of human transketoase gene, used in overexpression and immunoprecipitation assays.

## 2. Plasmids.

### 2.1. *Dictyostelium discoideum* plasmids.

The extrachromosomal plasmid ptx-GFP was used to express Atg1 complex proteins for the analysis of their subcellular localization (Tom Egelhoff, GenBank Accession Number: AF269237). Plasmids with additional tags were made adding HA or FLAG sequences

between the SacI and BamH1 sites of ptx-GFP, originating ptx-GFP-HA and ptx-GFP-FLAG. Two new alterations were introduced to ptx-GFP-HA and to ptx-GFP-FLAG that consisted in the removal of GFP from both plasmids, creating ptx-HA and ptx-FLAG.

| Plasmid name | Inserted between | Use |
|---|---|---|
| pTX-GFP-Transketolase | XhoI-XbaI | Cellular localization of transketolase |
| pTX-HA-Transketolase | | Phosphorylation assay |
| pTX-GFP-HA-Atg1Ct | Inserted in BamH1 | Immunoprecipitation |
| pTX.HA-Atg1Ct | | Immunoprecipitation |
| pTX-GFP-FLAG-Atg1Ct | | Immunoprecipitation |
| pTX-GFP-HA-Atg13ct | | Cellular localization, mass spectrometry and Immunoprecipitation |
| pTX-GFP-FLAG-Atg13ct | | Cellular localization and Immunoprecipitation |
| pTX-GFP-HA-Atg13nt | | Cellular localization and Immunoprecipitation |
| pTX-GFP-FLAG-Atg13nt | | Cellular localization and Immunoprecipitation |
| pTX-GFP-HA-Atg101 | | Cellular localization, mass spectrometry and Immunoprecipitation |
| pTX-GFP-FLAG-Atg101 | | Cellular localization and Immunoprecipitation |
| pTX-GFP-HA-Atg17 | | Cellular localization and Immunoprecipitation |
| pTX-GFP-FLAG-Atg17 | | Cellular localization and Immunoprecipitation |
| pTX-GFP-HA-FIP200 | | Cellular localization and Immunoprecipitation |
| pTX-GFP-FLAG-FIP200 | | Cellular localization, mass spectrometry and Immunoprecipitation |
| pTX-GFP-HA-Atg101i | | Cellular localization and Immunoprecipitation |
| pTX-GFP-FLAGAtg101i | | Cellular localization and Immunoprecipitation |

**Table 4.** Genes inserted in the HA, FLAG and GFP tagged plasmids and their different applications.

| Bait | N-terminal | C-terminal |
|---|---|---|
| Atg13 | NoI- EcoRI | HindIII-SalI |
| Atg101 | NotI-EcoRI | HindIII-SalI |
| Atg17 | SacI-XbaI | HindIII-SalI |
| FIP200 | Xba-Xba | HindIII-SalI |
| Atg101 interactor | NoI-BamHI | HindIII-SalI |

**Table5.** Flanking regions of the indicated genes were cloned into a pBluescript-SK-derived plasmid containing a blasticidin-resistance cassette as described previously . The location of the flanking regions are indicated by the nucleotide number of the gene. The restriction enzymes used for the cloning are also indicated.

The plasmids pDM430 and pSJSK489 (Jason King, Beatson Institute for Cancer Research, Glasgow) expressing GFP-Atg8 and GFP-Atg18 respectively were also used as autophagic markers.

Plasmid pA15/GFP-Apg1 expressing GFP-Atg1 was kindly supplied by DictyStock Center, Northwestern University in Chicago, IL, USA.

## 2.2. Yeast Plasmids.

For yeast two-hybrid screening plasmids encoding LexA fusion proteins were constructed by inserting a PCR fragment containing complete cDNAs of the genes displayed in Table 6 genes coding sequence into the BamHI or SalI sites of pBTM116 with a substitution of TRP1 by URA3 marker (provided by Doctor Olivier Vincent, Instituto Investigaciones Biomédicas Alberto Sols).

Plasmids encoding these genes were co-transformed with a *Dictyostelim discoideum* library ligated into pAD-GAL4-2.1 (Stratagene). For the pair-wise analysis of interactions the atg genes were also inserted in BamHI or SalI sites of pACT2 (Clontech) and co-transformed with pLex202 (URA). Enabling the analysis of specific interactions between each pair of proteins from table 6.

| Gene name | Restriction sites in pLex202 and pBTM116 |
|---|---|
| Atg1 | BamH1 |
| Atg13 | BamH1 |
| Atg101 | BamH1 |
| FIP200 | BamH1 |
| Atg17 | BamH1 |
| pIKE | SalI |
| Atg6b | BamH1 |
| Bif1 | BamH1 |
| Bif2 | BamH1 |
| Atg3 | SalI |
| Atg 4-1 | BamH1 |
| Atg5 | BamH1 |
| Atg7 | SalI |
| Atg8 | BamH1 |
| Atg10 | BamH1 |
| Atg12 | BamH1 |
| Atg 16 | SalI |
| Atg 18 | BamH1 |
| p62 | SalI |
| Atg14 | BamH1 |

**Table 6.** Restriction sites in pLex202 and pBTM116 where the different Atg gnes were inserted.

The yeast two-hybrid library was constructed using mRNA isolated from growing cells and cells starved for 4 hours. mRNA isolation was performed with the kit "absolutely mRNA TM Purification Kit" (Stratagene) following manufacture´s instructions. The cDNA and the library were carried out according with the following kits from Stratagene: HybriZAP-2.1 XR Library Construction Kit and HybriZAP-2.1 XR cDNA synthesis Kit.

## 2.3. Plasmids for expression in mammalian cells.

Three plasmids expressing ULK1 were purchased, pMXs-IP-EGFP-ULK1 (Addgene, 38193) that codes for ULK1 autophagy activating kinase 1 with GFP, HA-hULK1 (Addgene, 31963) that codes for ULK1 tagged with HA and pmX-IP-EGFP-ULK1 (K46N), an ULK1 variant without a functional kinase domain (Addgene, 38197).

## 3. Antibiotics.

| Antibiotic | Reference | Concentration | Use |
|---|---|---|---|
| Geneticin, G418 Sulfate selective Antibiotic | Gibco 10131-027 | 50 mg/mL | Dictyostelium discoideum strain selection |
| Blasticidine S hydrochloride | Sigma 15205-25MG | 10 mg/mL | Dictyostelium discoideum strain selection |
| Hygromycin B from Streptomyces hygroscopicus | SigmaH3274 | 50 mg/mL | Dictyostelium discoideum strain selection |
| Penicillin-Streptomycin | Gibco 15140-122 | 10,000 U/mL | Complementation of HL5 and DMEM medium |

**Table 7. Antibiotics used for selection in Dictyostelium stains.** Penicillin-Streptomycin was used to supply growth media both in Dictyostelium and mammalian cells.

## 4. Antibodies.

Primary and secondary antibodies, as well as their origin and dilution used, are shown in Table 8 and Table 9.

| Antibody | Produced in | Reference |
|---|---|---|
| **Anti-GFP antibody** | Rabbit | G1554, Sigma-Aldrich |
| **LC3B antibody** | Rabbit | mAb #3868, Cell Signaling |
| **LC3B antibody** | Rabbit | #2775, Cell Signaling |
| **Ha-tag antibody** | Mouse | #2367, Cell Signaling |
| **DYKDDDDK Tag antibody** | Rabbit | #2368, Cell Signaling |
| **Transketolase (H-7)** | Mouse | Sc-390179, Santa Cruz Biotechnology |
| **Anti-TKT** | Rabbit | HPA029480, Sigma-Aldrich |
| **ULK1 Antibody Sampler Kit** | Rabbit | #8359, Cell Signaling |

**Table 8. Primary antibodies used during this study and their sources.** The concentrations were adapted according to manufacturer's indications.

| Antibody | Dilution | Reference |
|---|---|---|
| Goat anti-mouse | 1:7000 | Sc-2005, Santa Cruz Biotechnology |
| Goat anti-Rabbit | 1:7000 | Sc-2030, Santa Cruz Biotechnology |

**Table 9.** Secondary antibodies used in Western-blot and immunofluorescence analysis.

## 5. Dictyostelium discoideum specifications.

### 5.1 Growth conditions.

#### 5.1.1 Growth in association with bacteria on SM plates

SM plates are composed by 10g/L Glucose (Sigma), 10g/L Peptone (Difco), 1g/L Yeast Extract, 0,5g/L $MgSO_4$, 1,8g/L $KH_2PO_4$, 0,6g/L $K_2HPO_4$ and 20 g/L agar. A lawn of bacteria *Klebsiella planticola* was seeded before plating Dictyostelium. Plates were maintained in a standard microbiology incubator at approximately 22°C.

#### 5.2.2. Liquid media.

*Dictyostelium discoideum* was grown in HL5 medium (Formedium) supplemented with 10% Glucose and penicillin-Streptomycin 10000 U/ml penicillin and 10000 µg/ml streptomycin (Gibco).

Starvation experiments were performed in PDF medium (20 mM KCl, 9 mM $K_2HPO_4$, 13 mM $KH_2PO_4$, 1 mM $CaCl_2$, 1 mM $MgSO_4$, pH 6.4).

## 6. Mammalian Cells maintenance.

Hek293T and Hela Cells were maintained at 37˚C with 5% C02 in DMEM media (Sigma Aldrich) supplemented with 10% FBS (Gibco), 10000 U/ml penicillin and 10000 µg/ml streptomycin (Gibco). For starvation EBSS medium (Sigma Aldrich) was used.

# METHODS

## 1. Search for homologues to human genes.

Bioinformatic analysis of putative autophagy protein homologues in *Dictyostelium discoideum* was done using Blast at the Dictybase webpage (http://www.dictybase.org/tools/blast). [78] The results of this analysis are shown in table 1 of the results section.

## 2. Cloning.

Autophagy related genes listed in the table 1 were amplified by PCR in full-length with the exception of Atg1 and Atg13, which were divided in two separated fragments due to the high amount of TAA repeats present in these genes. Atg1 N-terminal expand from nucleotides 1 to 783 and Atg1 C-terminal from nucleotides 1172 to 2000. The Atg13 fragments were the Atg13-N-terminal (nucleotides from 1 to 660) and Atg13 C-terminal (nucleotides 1218 to 2397).

For knock-out constructs a blasticidine-resistant cassette was surrounded by two flanking regions of the target gene to allow gene disruption by homologous recombination. The specific oligonucleotides with the appropriate restriction sites have been described in the materials section. After PCR amplification the fragments were purified and digested with the adequate restriction enzymes and cloned in a pBlueScript vector containing a blasticidin-resistance cassette as described previously.[96]

## 3. Polymerase Chain Reaction.

For high fidelity PCR amplifications the enzyme used was KapaHifi Polymerase (KK2101, Kapabiosystems). Genomic DNA and cDNA were used as templates for Dictyostelium expression constructs or yeast two-hybrid respectively. cDNA was generated form RNA using the Absolutely mRNA Purification Kit (Stratagene) and the HybriZAP-2.1 XR cDNA Synthesis Kit (Stratagene). The PCR reaction to amplify *Dictyostelium discoideum* genes consisted in 95°C 5 minutes of initial melting; 98°C/20 seconds; 45°C /2 seconds and 62°C/30 seconds per kilobase extension followed by a 5 minutes final extension step at 62 ºC.

For PCR experiments in which high fidelity was not necessary Taq polymerase (Biotools) was preferred. The cycles for this enzyme consisted in initial melting: 5 min at 95°C; melting: 1 min at 95°C, annealing: 1 min at 45°C, elongation: 5 min at 62°C, 30 cycles; final elongation: 5 min at 62°C. The low extending temperature of 62°C allowed the amplification of highly A+T-rich templates typically found in *Dictyostelium discoideum* genes.

The PCR products were purified with QIAquick PCR purification Kit (Qiagen).

Human enzyme transketolase was also cloned by PCR using kappa Hifi polymerase, altering the elongation temperature to 72˚C during 2 minutes.

## 4. *Dictyostelium discoideum* methods.

### 4.1. Transformation and Clone Selection.

*D. discoideum* cells were grown in axenic medium HL5 to a density of $1x10^6$cells/mL, $5x10^6$ cells were harvested by centrifugation at 500 g for 5 min, washed twice with ice-cold H-50 buffer (19.98 mM HEPES, 50.03 mM KCl, 9.93 mM NaCl, 1 mM MgSO4, 5

mM NaHCO3, 1.3 mM NaH2PO4, pH 7.0), and then resuspended in 100 µL of H-50 buffer. After that 10 µg plasmid DNA were added and the sample was electroporated with a Bio-Rad MicroPulser electroporation apparatus. Electroporation was made at 0.85 kV/25 µF with one pulse.

Transformed cells were then deposited on p100 plates with HL5. Approximately 24 hours after electroporation the adequate antibiotic selection was added to the growth medium containing the transformants. Distinct clones typically appeared about 7 days after the addition of the selection medium. For clonal isolation the transformants were plated in SM-Agar plates over a bacterial lawn. After three days individual colonies are visible and the DNA extracted with QuickExtract™ DNA Extraction Solution (Epicentre), according to manufacturer´s instructions. The screening of the knock-out strains was made by PCR with the appropriate oligonucleotides as described in the results section.

## 5. Transient transfection of mammalian cells.

Cells were transiently transfected at 24 hours post-plating with various plasmids using Lipofectamine 2000 reagent (Invitrogen), following the manufacturers protocol. The amount of DNA relatively to the amount of Lipofectamine was 1:3 and at moment of transfection the cells were at a 50-70% confluence.

## 6. Western-Blotting.

Whole-cell extracts were prepared by washing the monolayers twice in PBS and cell lysis performed by incubation in RIPA buffer (50 mM Hepes pH 7.4, 150 mM NaCl, 1.5 mM $MgCl_2$, 10% glycerol, 4 mM EDTA, 1% Triton X-100, 0.1% SDS, 1% sodium deoxycholate) plus phosphatase- and protease-inhibitor mixture (Sigma Aldrich) for 30

minutes on ice followed by centrifugation at 13000 rpm for 10 min at 4ºC. Protein concentration was measured using the Bio-Rad Protein Assay Dye Reagent Concentrate (500-0006EDU, Bio-Rad). Analysis of cell lysates was performed by electrophoresis in SDS-PAGE gels and protein transfer to PVDF BioTrace membranes (Pall Corporation). Membranes were incubated with blocking solution (5% Milk Powder in TBS 1x Tween-20) at room temperature and, subsequently, with the appropriate primary antibodies prepared in blocking solution at 4ºC overnight. Finally, the membranes were incubated with the secondary antibodies diluted in TBS 1x Tween-20 for 2 hours at room temperature and the antibody binding was visualized using the ECL detection system (GE Healthcare). Films were exposed at different times to ensure the bands were not saturated. Images were acquired with a SNAPSCAN e42 (AGFA).

## 7. Yeast Two-hybrid.

### 7.1. Screening.

Yeast two-hybrid screen for interaction of Atg proteins was initiated with the pre-transformation of pLex202 (URA) derivatives followed by co-transformation of the cDNA library ligated into pAD-GAL4. . The library was constructed using the kits from Stratagene indicated in the materials section.

His+ transformants were selected in the presence of 5 mM 3-aminotriazole and subsequently screened for β-galactosidase activity using a filter assay. Transformants were patched on to selective SD medium and were grown for two days at 30°C. Filter lift assays for blue color were performed in a nitrocellulose filter impregnated with z buffer (16,1 g/L $Na_2HPO4$, 5,5g/L $NaH_2PO_4$, 0,75 KCl, $MgSO_4$, 2% X-Gal, 8,1% β-

mercaptoetanol) during 1 hour at 37°C. [97] β-galactosidase was quantitatively assayed in permeabilized yeast cells grown to mid-log phase in selective SD medium

### 7.2. Yeast two-hybrid protein-protein interaction test.

Yeast cells expressing combinations of each two plasmids described in section 2.2 were grown in SD medium lacking appropriate supplements to maintain selection. β-galactosidase was assayed using a filter assay (as described above).

## 8. Mass Spectrometry.

### 8.1. Sample preparation.

The recombinant proteins GFP, GFP-Atg1-N-termminal and GFP-Atg8 were constitutively expressed in Ax4 Dictyostelium strain.

Cells expressing the cited proteins were washed twice with PDF medium, lysed and the protein was purified with GFP-trap A kit (Chromotek) according with manufacturer's instructions.

### 8.2. Reverse phase-liquid chromatography RP-LC-MS/MS analysis.

For the Ms/MS analysis the samples were sent to proteomics facility in Centro de Biología Molecular-Severo Ochoa, Madrid.

The desalted protein digest was dried, resuspended in 10 μl of 0.1% formic acid and analyzed by RP-LC-MS/MS in an Easy-nLC II system coupled to an ion trap LTQ-Orbitrap-Velos-Pro mass spectrometer (Thermo Scientific). The peptides were concentrated (on-line) by reverse phase chromatography using a 0.1mm × 20 mm C18 RP precolumn (Proxeon), and then separated using a 0.075mm x 100 mm C18 RP column (Proxeon) operating at 0.3 μl/min. Peptides were eluted using a 90-min gradient

from 5 to 40% solvent B (Solvent A: 0,1% formic acid in water, solvent B: 0,1% formic acid, 80% acetonitrile in water). ESI ionization was done using a Nano-bore emitters Stainless Steel ID 30 µm (Proxeon) interface.

The Orbitrap resolution was set at 30.000. Peptides were detected in survey scans from 400 to 1600 amu (1 µscan), followed by fifteen data dependent MS/MS scans (Top 15), using an isolation width of 2 u (in mass-to-charge ratio units), normalized collision energy of 35%, and dynamic exclusion applied during 30 seconds periods. Peptide identification from raw data was carried out using the SEQUEST algorithm (Proteome Discoverer 1.3, Thermo Scientific). The following constraints were used for the searches: tryptic cleavage after Arg and Lys, up to two missed cleavage sites, and tolerances of 10 ppm for precursor ions and 0.8 Da for MS/MS fragment ions and the searches were performed allowing optional Met oxidation and Cys carbamidomethylation. Search against decoy database (integrated decoy approach) using false discovery rate (FDR) < 0.01.

## 9. Confocal microscopy analysis.

### 9.1. *In vivo* analysis of *Dictyostelium discoideum* cells.

*Dictyostelium discoideum* cells expressing fluorescent proteins (GFP and RFP) were plated in p100 plates and grown in low cell density during at least 1 week to a maximum of 2 weeks. For *in vivo* visualization approximately 10.000 cells were transferred to an *in vivo* Ibidi µ-Slide 8 well slide and watched the fluorescence directly in a Confocal Microscope spectral LSM710 (Zeiss). The preferred objective for these experiments was the 63x Plan-APOCHROMAT.

## 10. *Dictyostelium discoideum* pull-down.

$1x10^7$ *Dictyostelium discoideum* cells co-expressing ptx-GFP-transketolase and ptx-HA-Atg1-C-terminal or GFP-Atg1 and Transketolase-HA were suspended in 200µL of GFP-tap Lysis buffer (10 mM Tris/Cl pH 7.5; 150 mM NaCl; 0.5 mM EDTA; 0.5% NP-40) complemented with protease inhibitor cocktail (AEBSF, 104 mM Aprotinin, 80 µM Bestatin, 4 mM E-64, 1.4 mM Leupeptin, 2 mM Pepstatin A, 1.5mM) during 30 minutes. The extract was centrifuged at 13000 rpm during 10 minutes and the pellet was discarded. The extract was diluted with 650 µL dilution buffer (10 mM Tris/Cl pH 7.5; 150 mM NaCl; 0.5 mM EDTA) with protease inhibitor cocktail and incubated overnight at 4 ºC in a rotated wheel with GFP-trap beads (Chromotek), previously washed with dilution buffer three times. The next day the beads were washed five times with dilution buffer and suspended in 30µL running buffer (125mM Tris-HCl pH 6,8, 4% (p/v) SDS, 20% glycerol, 100 mM DTT and 0,004% bromophenol blue). The sample was boiled at 100˚C during 5 minutes and loaded into a SDS-PAGE gel for analysis.

## 11. Autophagic flux in *Dictyostelium discoideum*.

The different Dictyostelium strains transformed with the construct GFP-TK or GFP-PGKA were grown in HL5 with the appropriate antibiotics. The cells were harvested by centrifugation and washed with PDF once. After centrifugation, cells were resuspended in the appropriate volume of PDF (or HL5) and deposited in 6-multiwell plates ($10^6$ cells in 1 ml). $NH_4Cl$ was added to reach a concentration of 150 mM and incubated during 2 hours at 22º C. After two hours the same amount of $NH_4Cl$ was added again and further incubated during 2 additional hours. After the treatment, cells were resuspended in the

wells by pipetting and transferred to eppendorf tubes, pelleted by centrifugation and resuspended in 50 µl of RIPA buffer supplemented with protease inhibitors (Sigma). The cells were kept in ice during 30 minutes to allow complete cell lysis.

The amount of protein in the extract was determined by the Bradford method and 10 µg of protein complemented with the loading buffer was boiled at 100˚C during 5 minutes and the proteins separated in a standard 10% acrylamide SDS-PAGE gel according to western-blot section in this protocol.

## 12. Transketolase activity assay.

Dictyostelium discoideum cells ( $1x10^7$ cells) in exponential growth or HEK 293T cells were scraped into a medium containing 20 mM Tris-HCl, 1 mM dithithreitol (DTT), 1 mM EDTA, 0,2 mM phemylmethanesulfonyl fluoride (PMSF), 0,2 g/L Triton X-100 and 0,2 g/L sodium deoxycholate, at pH 7,5. The cell extracts were allowed to lyse on ice during 30 minutes (pipetting vigorously every 10 minutes) and centrifuged at 13 000 rpm during 5 minutes at 4˚C to eliminate portions of the cell that weren't lysed.

The activity of the enzyme tranketolase was assayed measuring the rate of NADH consumption from 0,2 mM NADH, 5 mM $MgCl_2$, 0,1 mM TPP, 2 mM ribose-5-phosphate and 1 mM xylulose-5-phosphate, at ph 7,6.

G6PDH activity was assayed by measuring the rate of NADPH production from 0,5 mM $NADP^+$ and 2 mM Glucose-6-phosphate at pH 7,6. [86]

# RESULTS

# RESULTS

## A. Autophagy network organization in *Dictyostelium discoideum*.

### 1. Homology studies:

High-throughput screening for protein interactions brings important perspectives in molecular pathways, as the analyses of these interactions provides new insights into protein/gene function in a determinate network of proteins. Such approach usually depends on a series of different experiments connecting different proteomic tools that can together help us to know and comprehend the arrangement of the network under study. Here, we describe the use of three different protein-protein interaction assays in order to describe the autophagy network in *Dictyostelium discoideum* and identify novel binding partners involved in this route. A preliminary homology search using the proteins known to be involved in this process in other systems allowed the identification putative homologues conserved in Dictyostelium [see publication annexes]. From this study a total of 17 were selected (table 10).

| Dictybase ID | Name | Function | Human | S. cerevisiae | E-value Dd-Hu | E-value Dd-Sc |
|---|---|---|---|---|---|---|
| Atg1 DDB_G0292390 | **Atg1** | Serine/threonine-kinase | ULK1 (G.ID: 8408) ULK2 (G.ID: 9706) | Atg1 (YGL180W) | 1e-38 7e-39 | 7e-42 |
| DDB_G0269162 | **Atg13** | Atg1 regulator | Atg13 related protein (NP_001136145.1) | Atg13 (YPR185W) | n.s.** | n.s.** |
| DDB0237867 | **Atg17** | Scaffold protein | - | Atg17 (YLR423C) | - | 2e-3 |
| DDB_G0268498 | **FIP200** | Atg1 complex-interacting protein | FIP200 (G.ID: 9821) | | 1e-3 | 0 |
| DDB_G0288287 | **Atg101** | Atg1 complex-interacting protein | Atg101 (G.ID: 60673) | | 2e-8 | 0 |
| Atg6B (DDB_G0288021) | **Atg6** | Subunit of the PtdIns3K complex | BECN1 (G.ID: 8678) | Atg6 (YPL120W) | 1e-51 2e-27 | 5e-22 1e-10 |
| DDB_G0284997 | **Bif-1** | BAR and SH3-containing protein | SH3GLB1/Bif1 (G.ID: 51100) | | 0.014* | 0 |
| DDB_G0278351 | **Atg14** | Regulates PtdIns3K | KIAA0831 | Atg14 (YBR128C) | 0.03 | n.s.** |
| DDB_G0277319 | **Atg3** | E2-like enzyme | Atg3 (G.ID: 64422) | Atg3 (YNR007C) | 1e-39 | 7e-19 |
| DDB_G0273443 | **Atg4** | Cysteine protease | Atg4B (G.ID: 23192) Other homologues (Atg4A, C, D) | Atg4 (YNL223W) | 3e-19 | 2e-11 |
| DDB_G0289881 | **Atg5** | Conjugates with Atg12 | Atg5 (G.ID: 9474) | Atg5 (YPL149W) | 1e-15 | 5e-6 |
| DDB_G0271096 | **Atg7** | E1-like enzyme | Atg7 (G.ID: 10533) | Atg7 (YHR171W) | 1e-148 | 1e-116 |
| Atg8 (DDB_G0286191) | **Atg8** | Ubiquitin-like protein that conjugates with phosphatidylethanolamine | Other homologues (LC3/MAP1LC3A; GATE16/ GABARAPL2, etc.,) | Atg8 (YBL078C) | 3e-30 | 1e-35 |
| DDB_G0268840 | **Atg10** | E2-like enzyme | Atg10 (G.ID: 83734) | Atg10 (YLL042C) | 4e-18 | 0.97 |
| DDB_G0282929 | **Atg12** | Conjugates with Atg5 | Atg12 (G.ID: 9140) | Atg12 (YBR217W) | 1e-14 | 8e-7 |
| TipD (DDB_G0275323) | **Atg16** | Interaction with Atg12-Atg5 conjugates | Atg16L1 (G.ID: 55054) | Atg16 (YMR159C) | 1e-68 | 1e-4 |
| Atg18 (DDB_G0285375) | **Atg18** | WD repeat domain phosphoinositideinteracting protein | WI PI-3 (56270) Other homologues (WI PI-1; WI PI-3; WDR45L/WIPI-3) | Atg18 (YFR021W) | 1e-37 8e-81 | 4e-35 8e-29 |

*The possible Dictyostelium homologue for Bif1 has low homology but contains the expected C-terminal SH3 domain and an N-terminal BAR domain.
**The putative Dictyostelium Atg13 and Atg14 shows no significant homology (n.s.) with yeast and human homologues but it contains a conserved pfam Atg13 superfamily domain (as determined by a search of conserved domains at NCBI: http://www.ncbi.nlm.nih.gov/).

**Table10.** *Dictyostelium discoideum* putative autophagy proteins and respective homologues in Human and *Sacharomyces cerevisiae*.

## 2. Yeast two-hybrid.

The proteomic analysis of interactors was performed by yeast two-hybrid screening since this method allows the analysis of a large numbers of gene products (encoded in a cDNA library) for their ability to interact with a protein of interest, in this case the proteins described in table 1. This system was also applied in a pair wise mode combining all possible pairs of proteins from table 1 expressed in recombinant bait and prey vectors to enable a more direct consideration.

For the sake of clarity results obtained are presented in two different sections, the first corresponding to the Atg1 complex and the second to the Atg8 conjugation system and related adjacent proteins.

### 2.1. Yeast two-hybrid analysis for Atg1 Complex proteins.

Table 11 shows a summary of the results obtained in the screening of interactors for Atg1 and the different putative proteins of the complex. Atg1 was split in two segments due to the presence of DNA repeats in the middle of the gene. Positive clones were grown and the pray plasmids isolated and sequenced. Recapitulation of the interactions were performed in a fresh yeast strain, by transforming the corresponding bait and pray plasmids. Positive results were obtained for Atg1 and Atg101 and the rest of the baits rendered no positive clones. The pairwise analysis by yeast two hybrid was also performed and the result shown in Table 12.

Our results show substantial agreement between what was expected based on the described organization of this complex in other organisms. The core of this assembly of proteins is formed by Atg1-Atg13-Atg101 that seems to be conserved. However the

putative proteins Atg17 and FIP200 do not appear to interact with any of the other proteins included in this analysis.

(Poner en la tabla el SC del interactor de atg101 que falta)

**Yeast-two hybrid for Atg1 complex subunits**

| Bait | Interactor | Number of clones | SC* |
|---|---|---|---|
| Atg1 (C-terminal) | DDB_G0272618 (TKT) | 5 | 55-666 |
| | DDB_G0269162 (Atg13) | 6 | 591-796 |
| Atg1 (N-terminal) | - | | |
| Atg13 (N-terminal) | - | | |
| Atg101 | DDB_G0279871 | 1 | |
| Atg17 | - | | |
| FIP200 | - | | |

*SC: smallest clone.

**Table 11.** Atg1 complex proteins used as bait in yeast two hybrid assays with the corresponding interactions obtained from a *Dictyostelium discoideum* cDNA library.

In addition to the expected interactions, Atg1 analysis showed an interaction with the protein Transketolase, an enzyme fundamental in the non-oxidative branch of the pentose phosphate pathway. [92] This interaction was confirmed in five different clones in which the common smallest domain comprised the region between amino acids 55 to 666 of Transketolase.

Atg101, an autophagic protein conserved in various eukaryotes, but not in *Saccharomyces cerevisiae* [98] interacts with a new unknown protein, DDB_G0279871, with no homology with any of the previously described Atg proteins. This protein has a zinc finger B-box domain and is an FNIP repeat-containing protein and will be studied in more detail.

**Pairwise Yeast-two hybrid for Atg1 complex subunits**

| pLex \ pACT | Atg1 (C-terminal) | Atg1 (N-terminal) | Atg13 C-terminal | Atg13 N-terminal | Atg101 | Atg17 | FIP200 |
|---|---|---|---|---|---|---|---|
| Atg1 (C-terminal) | | | | + | | | |
| Atg1 (N-terminal) | | | | | | | |
| Atg13 C-terminal | + | | | | | | |
| Atg13 N-terminal | | | | | + | | |
| Atg101 | | | | + | | | |
| Atg17 | | | | | | + | |
| FIP200 | | | | | | | |

**Table 12. Pairwise yeast two-hybrid assay of Atg1 complex constituent proteins.** In these experiments each pair of proteins was overexpressed simultaneously.

## 2.2. Yeast two-hybrid analysis for Atg8 and related ubiquitin-like conjugation proteins.

The two ubiquitin-like conjugation systems described in this chapter are essential for autophagy. The conjugation of Atg8 to phosphatidyl-ethanolamine (PE) is mediated by the proteins Atg4, Atg7 and Atg3 and the Atg12–Atg5-Atg16 complex that functions as an E3-like enzyme to facilitate Atg8–PE formation. Conjugation of Atg5 to Atg12 requires the function of Atg7 and Atg10. P62 is included in the pairwise analysis for its described interaction with Atg8. [99]

Interactions among the ubiquitin-like conjugation proteins have previously been described in higher eukaryotes [100] and our results confirm that most of these interactions also occur in *Dictyostelium discoideum* (tables 13 and 14). [49,101,102]

In a particular, Atg8 interacts with both Atg7 and with the processing protease Atg4. Other expected results obtained in this assay are the Atg12-Atg7 interaction resultant of the activation of Atg12 by Atg7 and the Atg5-Atg16 which is essential for the localization of Atg5 and Atg12 to the autophagosome assembly site. [49,101,102]

A selective mode of autophagy mediated by selective autophagy receptors (SARs) has been previously described. These receptors are characterized by a short linear sequence motif (LIR-motif) responsible for the interaction between SARs and proteins of the Atg8 family. Such motif can be encountered in the selective autophagy adaptor P62 [103], thus it is not surprising the interaction obtained between this protein and Atg8 in our assay.

Interestingly several new Atg8 interactors were identified in this screening (table 13) like the quality control protein calreticulin; CnrK (a protein described in Dictyostelium as a cell number regulator containing a RING zinc finger domain); Dnpep, an aspartyl aminopeptidase that binds two zinc ions per subunit and is highly homologue to the corresponding human protein and the proteins DDB_G0286393, DDB_G0286149 that showed no significant similarity to any other protein from other organisms.

We performed yeast two-hybrid for other Atg proteins (Atg12, Atg18, Atg10) but no positive clones were obtained from these analysis.

**Yeast-two hybrid Atg8**

| Bait | Interactor | Number of clones | SC |
|---|---|---|---|
| Atg8 | Atg7 | 1 | 301-707 |
| | Atg4 | 1 | 471-745 |
| | CrtA, Calreticulin DDB_G0283536 | 2 | 176-424 |
| | CnrK DDB_G0292120 | 2 | 817-1214 |
| | DDB_G0286393 | 1 | 1-280 |
| | Dnpep DDB_G0286149 | 1 | 1-484 |

**Table 13:** Putative interactors of Atg8 obtained by Yeast two-hybrid screening.

**Pairwise Yeast-two hybrid for Atg8 and related proteins**

| pLex \ pACT | Atg8 | Atg7 | Atg8 | Atg5 | Atg12 | P62 | Atg16 | Atg4 | Atg10 | Atg3 |
|---|---|---|---|---|---|---|---|---|---|---|
| Atg8 | | | | | | + | | | | |
| Atg7 | | + | | | | | | | | |
| Atg8 | | | + | | | | | | | |
| Atg5 | | | | | | | + | | | |
| Atg12 | | + | | | | | | | | |
| P62 | | | | | | | | | | |
| Atg4 | | | | | | | | | | |
| Atg10 | | | | | | | | | | |
| Atg3 | | | | | | | | | | |

**Table 14:** Pairwise yeast-two hybrid using Atg8 and related proteins.

## 3. Analysis of interactors by mass spectrometry.

In order to validate the data obtained in the yeast-two hybrid assays and to expand the number of putative interactors we used a pull-down strategy to identify interactors of Atg1 and Atg8 by mass spectrometry. For this GFP-Atg1 and GFP-Atg8 were expressed in Dictyostelium cells and purified with a GFP-affinity resin as described in materials and methods. As a negative control a GFP-expressing strain was used. The lists of interactions obtained are listed in the annex section of this work. The proteins identified in the control were subtracted from the ones identified in the samples

### 3.1. Analysis of Atg1 interacting proteins by mass spectrometry.

As shown above, Atg13 was found to interact with the C-terminal part of Atg1 and with Atg101, although the direct interaction of Atg1 and Atg101 was not detected in the previous analysis. In this particular interaction the mass spectrometry analysis of Atg1 interacting proteins was very valuable since it allowed the confirmation of the interaction

between Atg1 and Atg101. Thus the Atg1-Atg13-Atg101 complex is complete in *Dictyostelium discoideum*, similarly to the described in higher vertebrates. [98]

The putative Atg17 and FIP200 were not present among the identified interactors, in agreement with the negative results from the Y2H assays.

## 3.2. Analysis of Atg8 interacting proteins by mass spectrometry.

The results obtained by mass spectrometry of Atg8 enabled the confirmation of some of the interactions detected by yeast-two hybrid as it is the case of Atg7, Dnpep and DDB_G0286393. Other important result reported in mammals that we now confirm in Dictyostelium is the detection of the interaction between Atg8 and the E2-like enzyme, Atg3. [104]

The fact that we are obtaining results already described in mammalians by two different and independent approaches supports the conservation of the autophagic machinery in *Dictyostelium discoideum* and highlight the value of some of the newly described interactors.

## 4. Interaction between Atg1 and Transketolase.

Once confirmed the conservation of the Atg1 complex subunits in Dictyostelium we next wanted to study in more detail the new putative interactors transketolate and Atg101-interactor protein. To validate the interaction between Atg1 and transketolase we performed different pull-down assays. In the first GFP-Transketolase and Atg1C-terminal-HA were expressed simultaneously in Dictyostelium cells (Figure 10). In the second experiment the complete Atg1 protein was fused to GFP (GFP- Atg1) and expressed together with Transketolase-HA (Figure 11). In both cases GFP-tagged

proteins were pull-down with GFP-trap and the HA-tagged proteins detected by western blot. GFP was used as negative control.

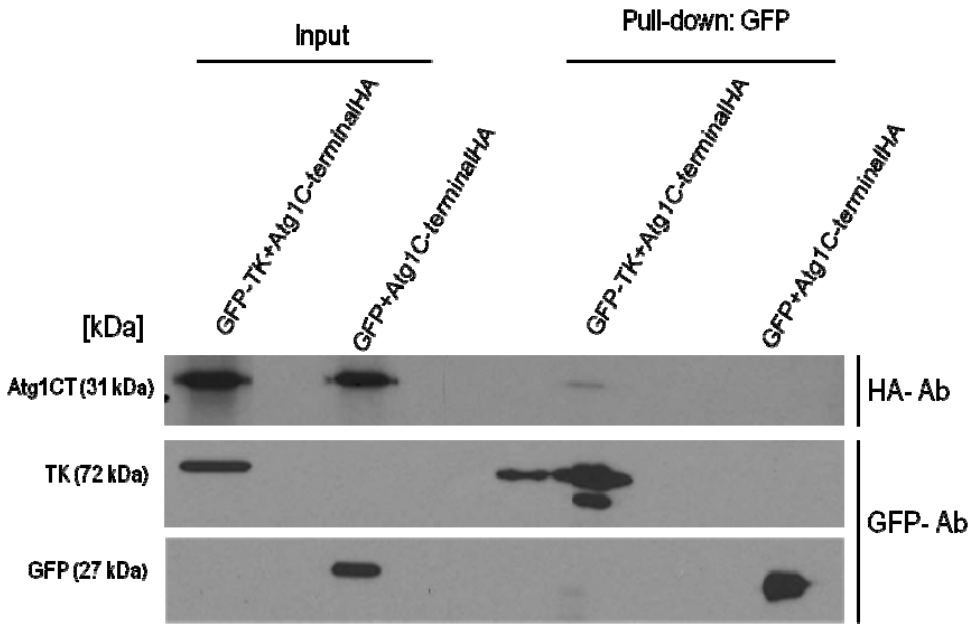


**Figure 10. Pull-down of Atg1Cterminal-HA (Atg1 without the kinase domain) with GFP-TK.** First and second lanes are the input extracts, GFP-TK with Atg1C-HA and control GFP with Atg1C-HA respectively. Third lane presents the pull-down of GFP-TK that results in the detection of Atg1C-HA. The fourth lane presents the control GFP that was unable to pull-down Atg1C-HA.

In the first pull-down assay (figure 10) we encountered some difficulties perfecting the experimental procedure in order to avoid the disruption of the interaction between the C-terminal Atg1 fragment and transketolase. Even with all the caution taken we can see that the band corresponding to Atg1C-terminal is very weak, which might indicate that the interaction is transient or fragile.

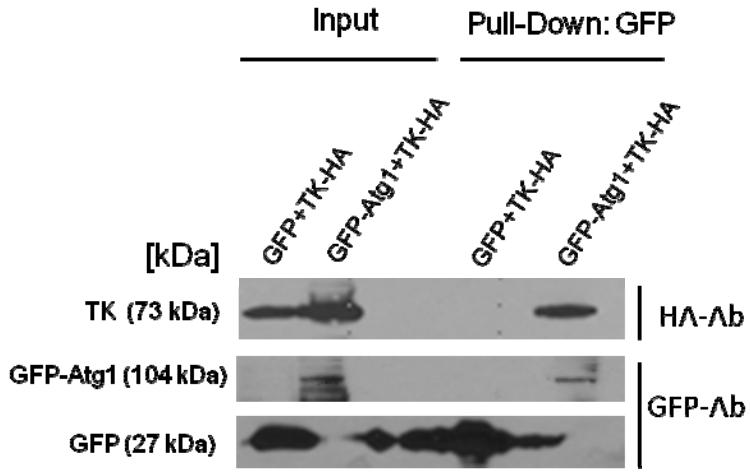


**Figure 11. Pull-down of TK-HA with GFP-Atg1.** Lanes 1 and 2 display the inputs with GFP+TK-HA and GFP-Atg1+TK-HA respectively; lane 3 presents the control of GFP where no interaction is detected and lane 4 shows the interaction of TK-HA with GFP-Atg1. The large expression of the control GFP (lower panel) generated an expansion of the signal to other lanes.

It is important to point out that in the second pull-down experiment (figure 11) the entire Atg1 was used instead of the C-terminal fragment. As we can see this interaction is much stronger than the one using only the Atg1-C-terminal fragment, which suggests that the presence of the kinase domain may favor the stabilization of the interaction.

## 5. Analysis of the interaction between Atg101-interactor and Atg101.

This experiment enabled the confirmation of the interaction previously detected by yeast-two hybrid between Atg101 and its new interacting protein named Atg101-interactor (DDB_G0269162). We found difficulties to express both tagged proteins simultaneously *in vivo*. Therefore, the different proteins were expressed in separated Dictyostelium cells, and the extracts mixed prior to the pull-down assay.

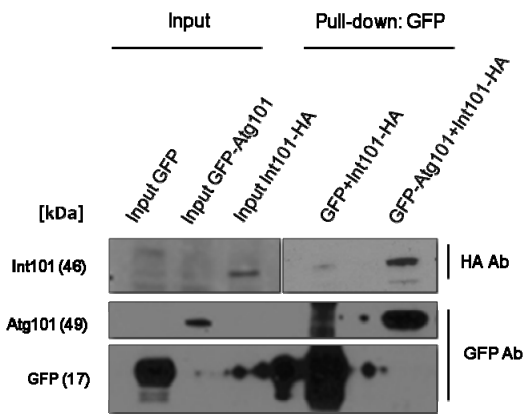


**Figure 12. Pull-down of Atg101-interactor with GFP-Atg101.** Lanes 1, 2 and 3 are the inputs of cells expressing GFP; GFP-Atg101 and Atg101-interactor-HA respectively. Lane 4 presents the negative result of the pull-down of Atg101-HA with GFP. Lane 5 presents the positive interaction of Atg101-interactor-HA with GFP-Atg101. There is a strong interaction between these two proteins which confirms the results previously obtained by yeast two-hybrid assays. Note: the upper part of the gel appears divided since the first incubation with anti-HA antibody rendered a big smear due to unspecific binding to input proteins and thus the gel was stripped and re-incubated with a cleaner HA antibody. Therefore, although it is the same gel the two parts are the result of two different incubations.

# B. Functional analysis of the Dictyostelium Atg1 protein kinase Complex.

## 1. Atg1 complex proteins cellular localization.

We next wanted to examine the subcellular localization of the putative autophagy related proteins Atg13, Atg101, Fip200, Atg17 and Atg101-interactor to determine if these proteins localize to autophagosomes. For this, the Atg proteins were tagged with GFP, expressed in wild-type Ax4 cells and analyzed by confocal microscopy (figure 13).

From this analysis, we found that Atg101, Fip200, Atg13 and Atg101-interactor are uniformly distributed in the cytoplasm. None of them gave the typical punctuated pattern or labeled any particular structure even when exposed to 30 minutes of starvation. Although several Atg proteins, such as Atg8 and Atg18 localize to the autophagosomes, giving a typical punctated pattern [78] others show no localization. In particular, Atg1 fused to GFP has been shown previously to have a general cytoplasmic pattern in Dictyostelium cells with no specific puncta localization. [105] Therefore, our results show that the rest of Atg1-complex subunits have a similar non-localized cytoplasmic pattern that the kinase Atg1.

However there is an exception since Atg17 localizes preferentially in nuclei, although it also marks the cytoplasm but with less intensity. This feature is not expected for a protein associated to autophagy since autophagosome vesicles are formed in the cytoplasm.

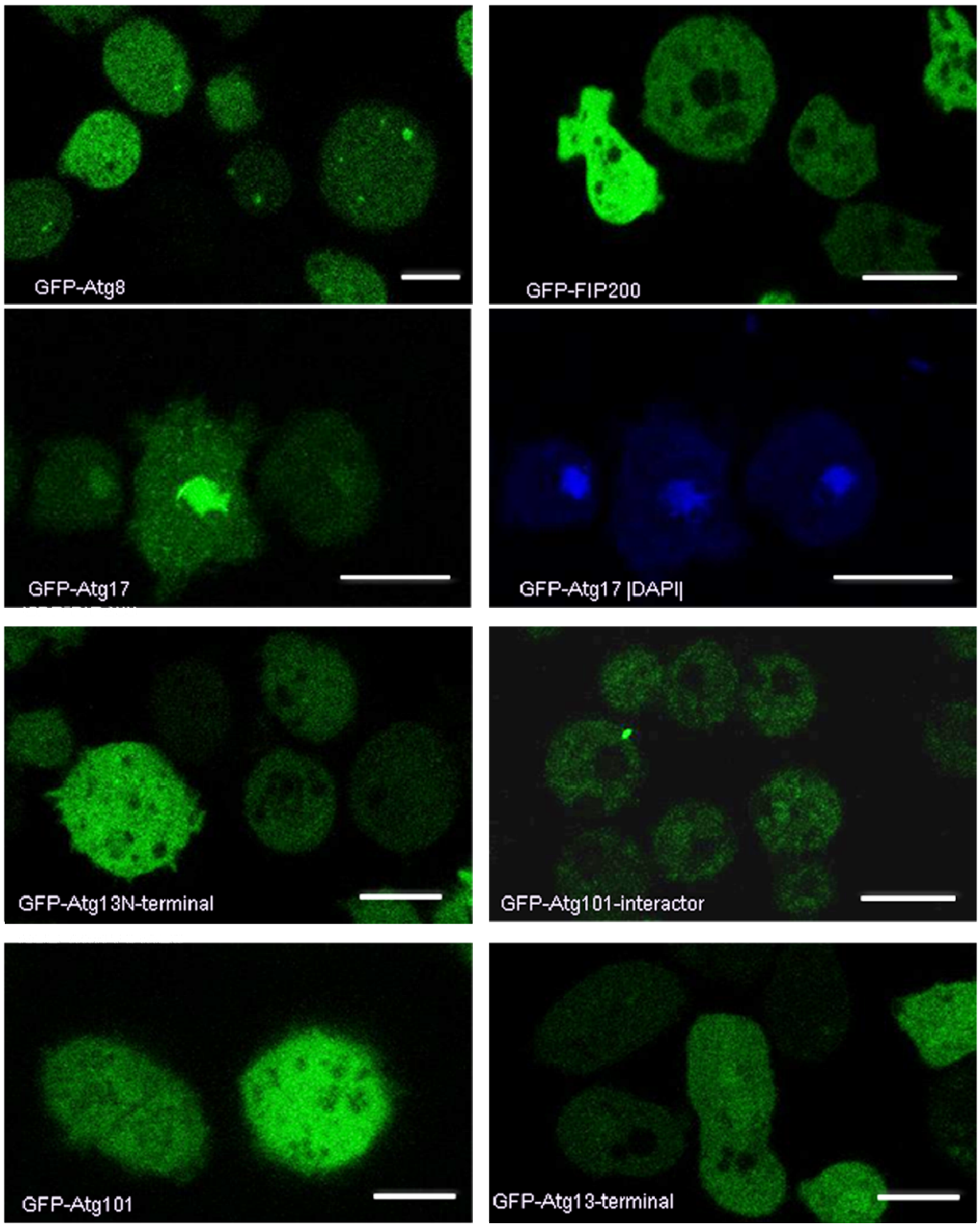


**Figure 13. Cellular localization of Atg1 complex proteins by confocal microscopy.** For comparison the autophagic marker GFP-Atg8 is included, which show the typical autophagosome punctated pattern. Atg101, Atg13-C-terminal, Atg13-N-terminal, FIP200 and Atg17 -GFP tagged proteins were expressed and visualized *in vivo* by confocal microscopy. GFP-Atg17 expressing cells were also strained with DAPI for nucleus co-localization. Scale bars correspond to 10 µm.

## 2. Generation of knock-out strains by homologous recombination.

A series of knockouts were generated to investigate the roles of the Atg1 complex proteins in autophagy regulation. These alterations were introduced by homologous recombination in Ax4 wild-type strain and confirmed by PCR. The detailed information of this procedure is displayed in figure 14.

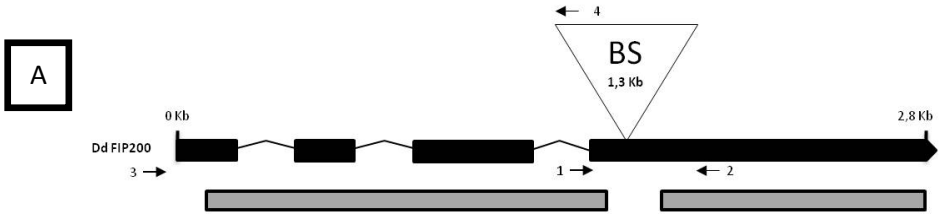


| Oligonucleotides | 1-2 | 3-4 |
|---|---|---|
| Wild-type | 1070 bp | None |
| Knock-out | 2370 bp | 1517 bp |

| Control of PCR DDB_G0288287 | 561 bp | None |
|---|---|---|

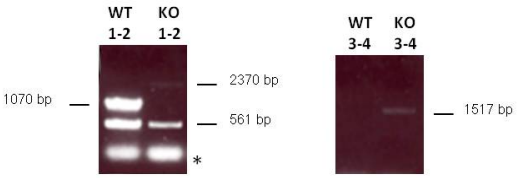


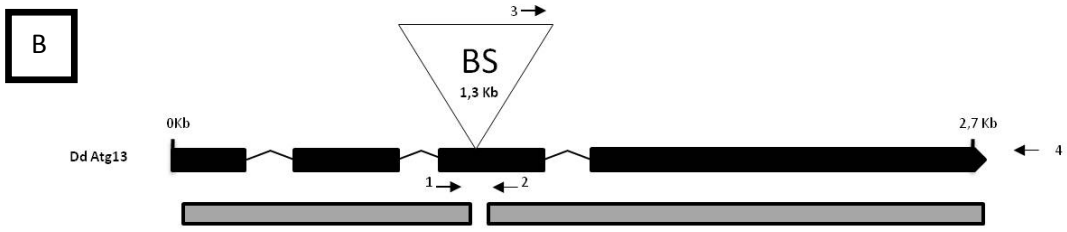


| Oligonucleotides | 1-2 | 3-4 |
|---|---|---|
| Wild-type | 419bp | None |
| Knock-out | 1819 bp | 1057 bp |

| PCR Control DDB_G0289881 | 1141 bp |
|---|---|

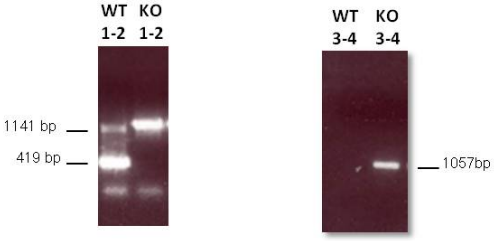

C


| Oligonucleotides | 1-2 | 3-4 |
|---|---|---|
| Wild-type | 480bp | none |
| Knock-out | 1880 bp | 1189 bp |

| PCR Control DDB_G0289881 | 1141 bp |
|---|---|

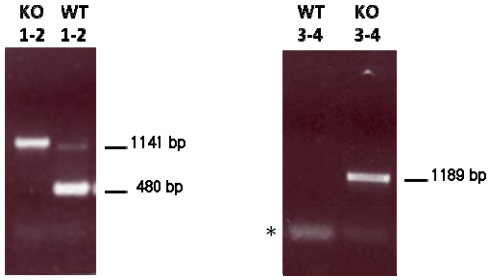


D

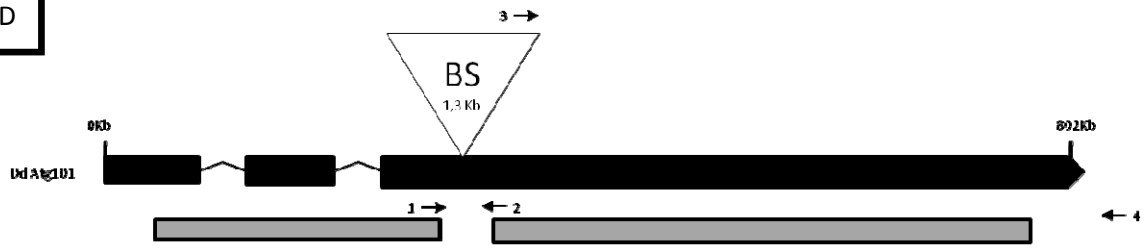


| Oligonucleotides | 1-2 | 3-4 |
|---|---|---|
| Wild-type | 436bp | None |
| Knock-out | 1736 bp | 1100 bp |

| PCR Control DDB_G0285375 | 1119 bp |
|---|---|

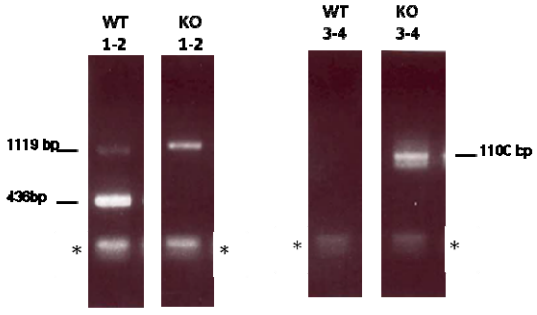

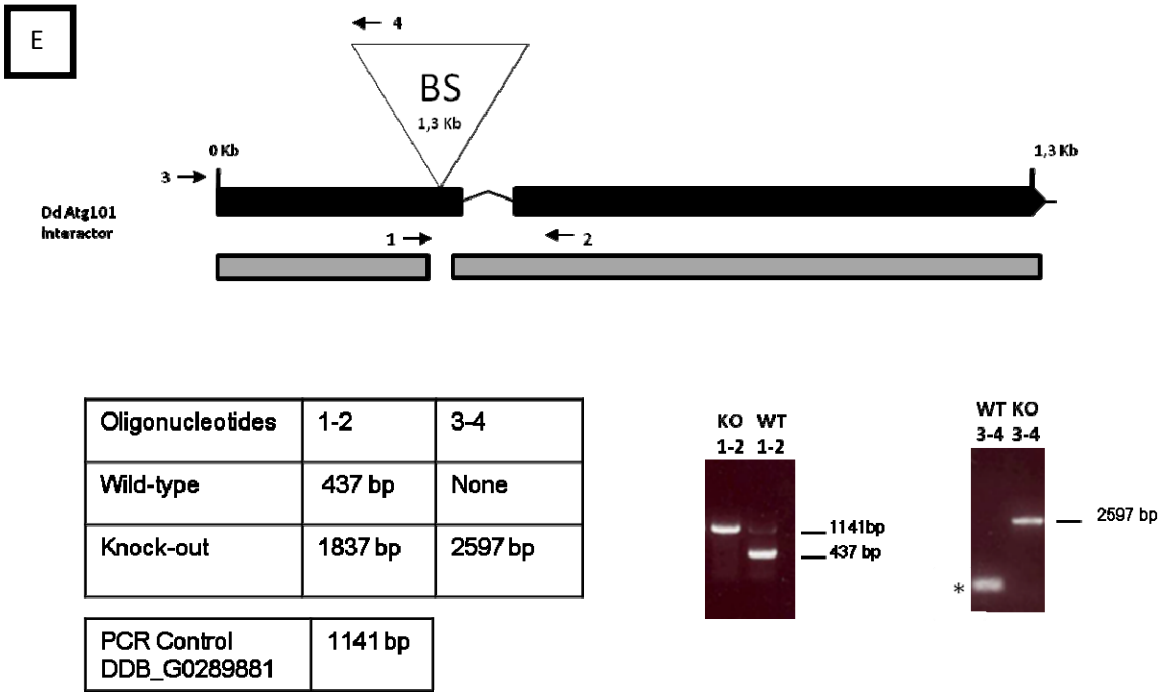


| Oligonucleotides | 1-2 | 3-4 |
|---|---|---|
| Wild-type | 437 bp | None |
| Knock-out | 1837 bp | 2597 bp |

| PCR Control DDB_G0289881 | 1141 bp |
|---|---|

**Figure 14.** Figures A, B, C, D and E represent FIP200; Atg13; Atg101 and Atg101-interactor knockout constructs and analysis of homologous recombination. The black boxes represent the original gene, the introns and the location of the BS cassette after homologous recombination. Grey boxes correspond to the location of the flanking N and C-terminal fragments used to allow homologous recombination. The arrows with the respective numbers indicate the different oligonucleotides used for verification of the recombinant strains. Below the scheme the expected sizes of PCR products for wild-type and mutant strains are displayed in the table. Examples of the expected PCR pattern for wild-type and mutants are shown on the right. For this, DNA extracted from wild-type and knockout strains was subjected to PCR using oligos 1 and 2 or 3 and 4. Unrelated genes were used as PCR controls. . PCR amplifications from the KO strains with oligos 1-2 do not usually generate the expected whole fragment containing the BS cassette due to the large size of the amplicon. Asterisks indicate non-specific bands.

## 3. Analysis of multicellular development in Knockout strains.

Dictyostelium development takes place in the absence of nutrients and therefore the autophagic pathway is required for Dictyostelium development since the nutrients and the energy needed for the development are in part mobilized by autophagy. [105]

To determine whether the mutant cells were capable of carrying out the full program of multicellular development, we evaluated wild-type and mutant cells by plating each strain in SM-agar. The resulting phenotypes were analyzed six days after plating.

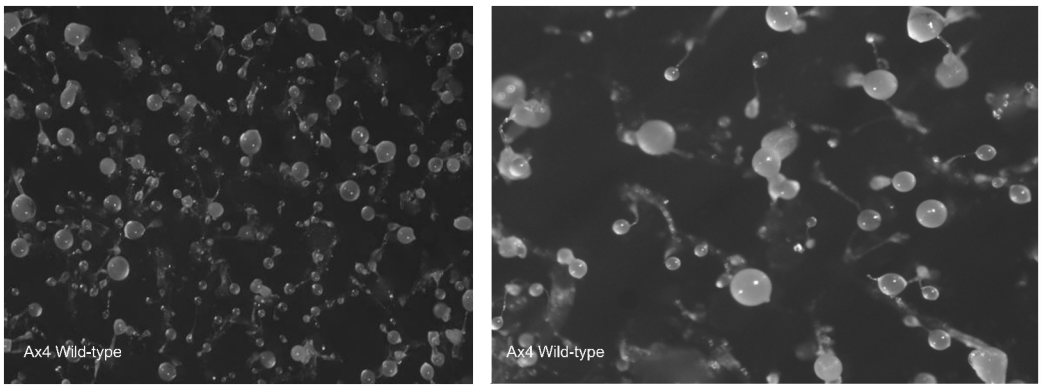


**Figure 15.** Ax4 wild-type parental strain cells were deposited in SM-agar plates in association with bacteria. Both images illustrate what is expected in normal developing *Dictyostelium discoideum* specimens. Fruiting bodies with stalks and spore heads are perfectly formed.

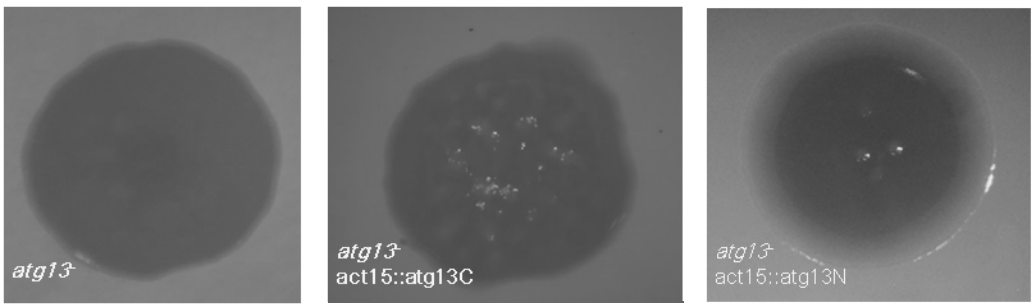


**Figure 16.** Atg13 mutant shows a defect in aggregation. *atg13*- strain (left) lacks aggregation, without the formation of mounds or stalk structures. *atg13*- complemented with Atg13-C-teminal (middle) is not capable of rescuing the wild-type phenotype although it forms little mound structures that are not able to

complete aggregation. Atg13-N-terminal overexpression in *atg13*⁻ (right) does not rescue any of the wild-type features.

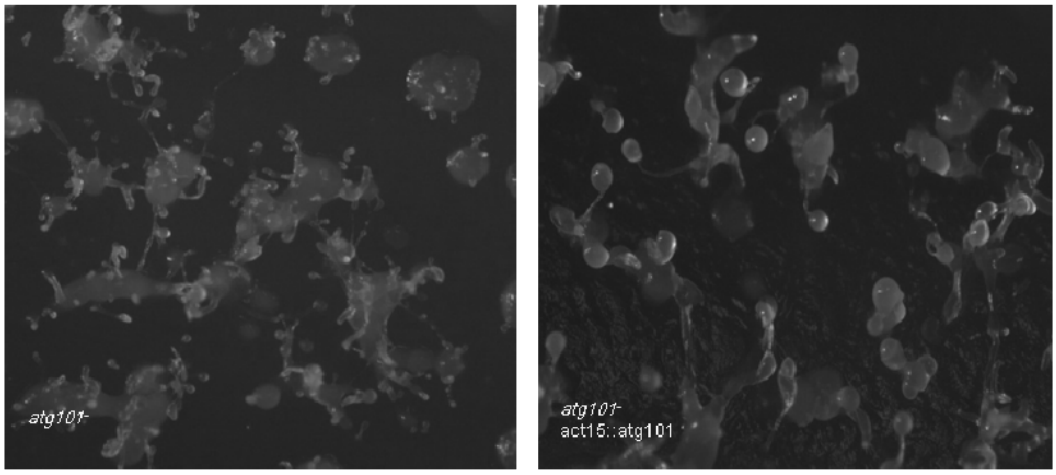


**Figure 17.** Atg101 knockout colonies display a multi-tip phenotype. Left: *atg101*⁻ develops a characteristic "multitip" phenotype [106] in which big mounds split up in multiple tips. These structures never form normal-looking fruiting bodies. Right: The expression of a recombinant GFP-Atg101 in the mutant fully recovers the defects presented; the resulting colonies have a wild-type phenotype.

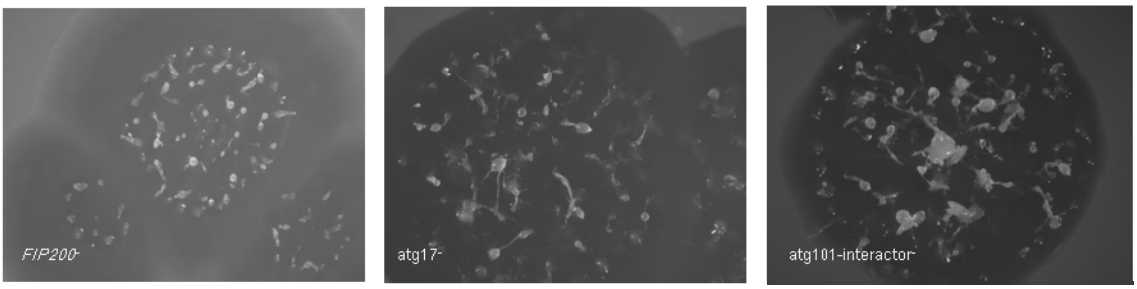


**Figure 18.** Normal phenotypes in the strains *FIP200*; *atg17*⁻ and *atg101-interactor*. The phenotype observed in these three knockout colonies is morphologically normal with fully formed fruiting bodies.

Of the analyzed phenotypes, *atg13*⁻ displayed the most accentuated one characterized by the lack of aggregation and the absence of fruiting bodies, similar to what was

previously described for Atg1 mutants. [77] This phenotype is in agreement to what was expected given that Atg1 and Atg13 interact and work in closed dependence.

*atg101*$^{-}$ shows a multi-tip aggregate, which is indicative of autophagy impairment as demonstrated for other Dictyostelium autophagic mutants. [107] These mutants initiate development and form big mounds that are unable to complete normal fruiting bodies. Instead they form aberrant tips on their surface.

The rest of the mutants (atg17, FIP200 and Atg101-Interactor) did not show a developmental phenotype defect. This suggests that either they affect autophagy marginally to a level that is not sufficient to affect development, or alternatively, they are dispensable for the process. More sensitive and direct assays to monitor autophagy will be used to address this in the next sections.

## 4. Autophagic flux measurements in Atg1 mutant strains.

### 4.1. Optimizing an autophagy flux assay in *Dictyostelium discoideum*.

As the research of autophagy continues to evolve, methods for monitoring autophagy have been perfected. The flux of autophagic vesicles reflects the dynamic process of autophagosome formation, maturation and fusion to lysosomes [108], we can thus define autophagic flux as the rate in which this series of events occur. [109]

Autophagy flux cannot be determined by the simple visualization of autophagosomes. [109] For example, the presence of numerous autophagosome vesicles can reflect either increased autophagy or low autophagic flux due to impairment of lysosome fusion. [PMID: 18216495]. For this reason it was essential to develop a technique that enabled the measurement of autophagic flux in *Dictyostelium discoideum* [82,110] that represented the rate at which intracellular material is being degraded via autophagy.

The method developed in out laboratory to determine autophagic rate in *Dictyostelium discoideum* consisted in the overexpression of the recombinant protein phosphoglycerate kinase (PgkA) ligated to GFP. This cytosolic protein is taken up passively by autophagy and degraded rapidly in normal conditions. However if the cells are exposed to ammonium chloride ($NH_4Cl$) autophagy is slowed down due to the increase in lysosomal pH and this allows the detection of cleaved GFP, which is more resistant to degradation than PgkA (Figure 19). The amount of cleaved protein is assessed by western blotting analysis. This work was published and has been included in the annex section.

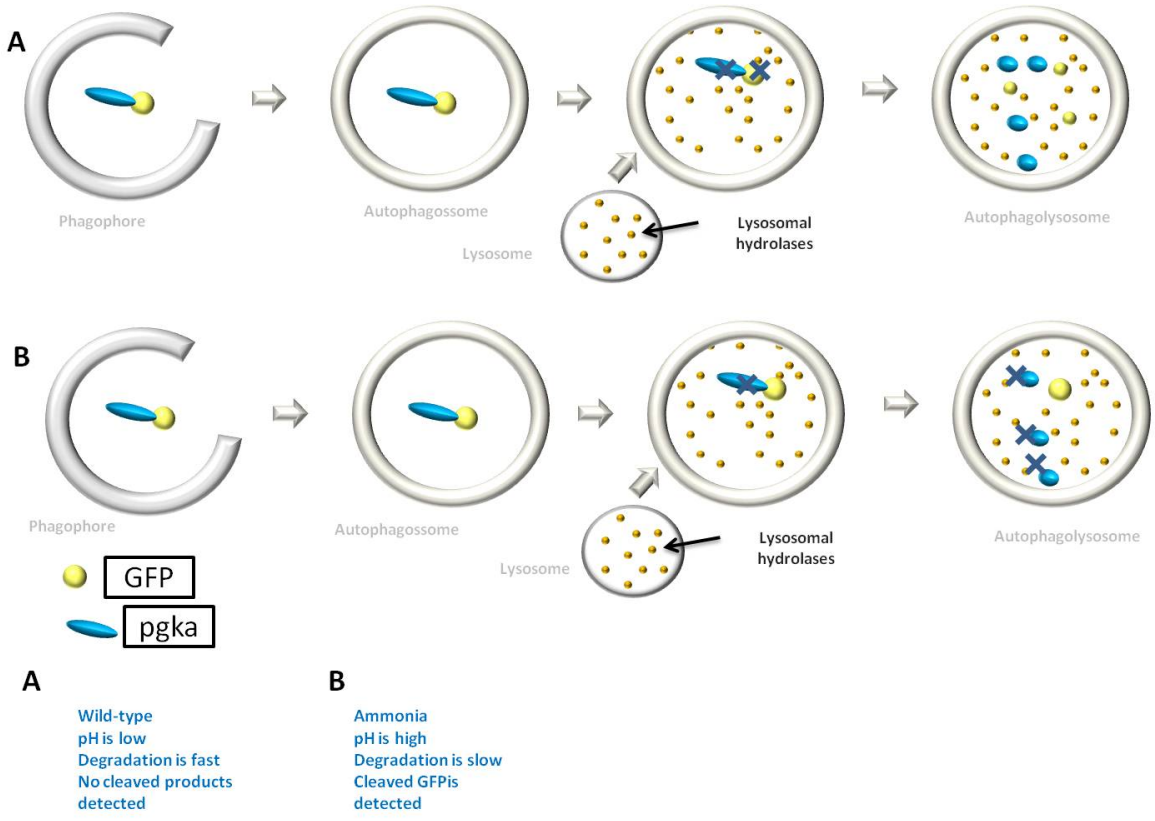


**Figure 19. Decrease in autophagic flux resultant of the addition of $NH_4Cl$.** A. Cells expressing the marker GFP-PgkA in the absence of $NH_4Cl$ proceed with normal autophagic flux rate. Due to the fast degradation no GFP band is visible. B. Cells exposed to $NH_4Cl$ tend to decrease the autophagic flux velocity. This decrease is enough to detect cleaved GFP in a western-blotting analysis.

## 4.2. Autophagy flux in Atg1 kinase complex mutants.

The autophagic flux assay was used to monitor autophagy flux in all Atg1-complex mutants.

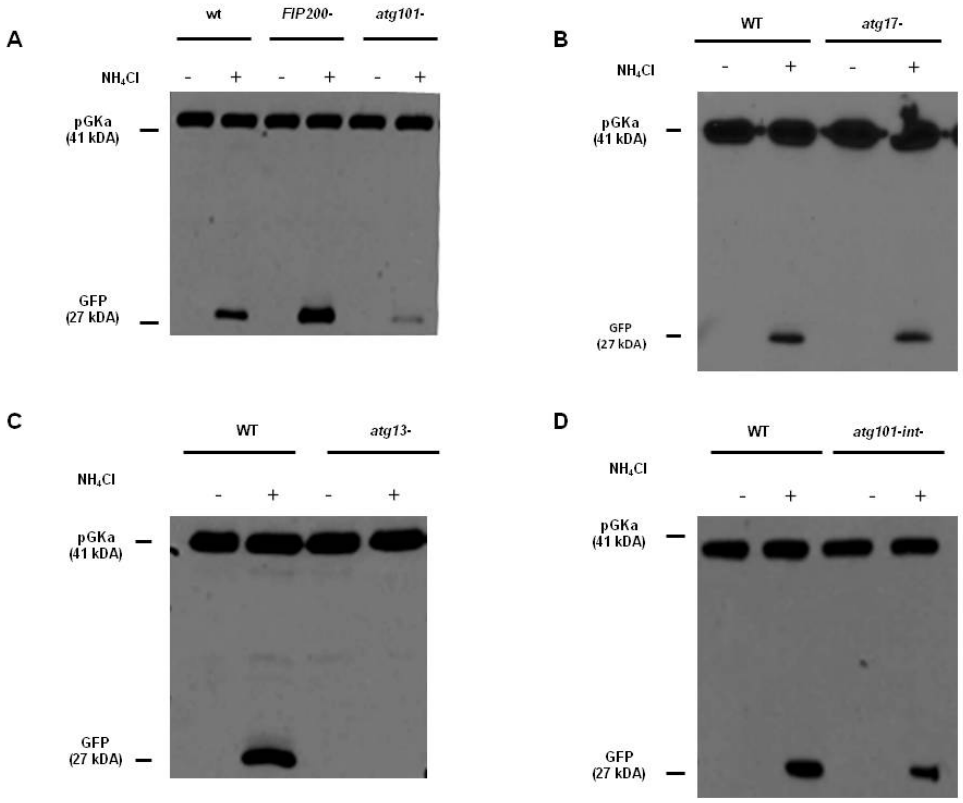


**Image 20.** The recombinant protein phosphoglycerate kinase (Pgka) ligated to GFP was overexpressed in wild-type Ax4 strain and in A) FIP200$^{-}$ and *atg*101$^{-}$ cells or B) *atg* 17$^{-}$ cells or C) *atg* 13$^{-}$ cells or D) *atg101 -interactor-* cells and incubated twice with 150 µM ammonium chloride during 2 hours at 21° C. Each well was loaded with 10 µg of total protein. All the membranes were incubated with anti-GFP antibody. The samples were quantified using ImageJ viewer gel quantification tool.

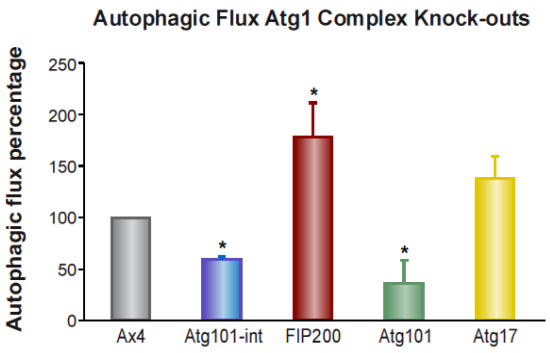


Figure 21. Quantitative analysis of autophagic flux measurements of the strains Ax4*; atg101-interactor-; Fip200-; Atg101-; Atg13- and Atg17-*. Three independent experiments were quantified. Standard-deviation bars are shown. Asterisks indicate the significance of the student t-test ( * for p<0,05).

As shown in Figures 20 and 21, knocking-out Atg1 complex genes affected autophagic flux in different degrees. The most extreme case was *atg13*⁻ , in which autophagy was completely abolished.

Yeast Atg17 is described as being essential for the induction of Atg1 [21], which is in itself fundamental for autophagy activation. The fact that there is no significant alteration in autophagy flux in Dictyostelium cells lacking Atg17 suggest that this protein is not the functional homologue of Atg17 from *Sacharomyces cerevisiae*.

*atg101*⁻ and *atg101-interactor* ⁻ presented a decrease ranging between 38%-50%, which indicates that autophagy is partially down regulated in these strains. The fact that Atg101-interactor renders similar results than Atg101 may suggest a close interplay between these two proteins. Although not significant in this analysis, the level of autophagy tend to be lower in *atg101*- in comparison with *atg101-interactor*- and this might explain the presence of the typical multitipped phenotype in *atg101*- strain while atg101-Interactor mutant had no phenotype. It is possible that there is a threshold level of autophagy, below which normal progression in development is affected.

Surprisingly, the putative FIP200 protein showed a strongly induced autophagic flux that suggests a function as a negative modulator of autophagy. This result is unexpected since FIP200 has been described in mammalian cells as a protein required for autophagy. [111] Our results so far indicate that the proposed Dictyostelium FIP200 protein can be an evolutionary divergent protein that evolved to a different function, or alternatively it may correspond to a different protein not related to FIP200. The fact that we could not detect interactions between this protein and any of the other Atg1- complex subunits makes the second possibility more plausible.

## 5. Analysis of autophagic markers GFP-Atg8 and GFP-Atg18 in the knock-out strains.

A more detail characterization of the autophagic defects was carried out using confocal visualization of autophagic markers. The autophagosome markers GFP-Atg8 and GFP-Atg18 were expressed in wild-type and the different *Dictyostelium discoideum* Atg1-complex mutant strains.

GFP-Atg8 puncta label autophagosomes throughout their initial stages to the degradation stage, since the GFP-Atg8 attached to inner membrane is degraded in the autolysosomes. [112,113] In contrast GFP-Atg18 labels autophagosomes at the initial stages since it is recruited to the site of autophagosome formation as soon as PtdIns3P is generated by the class III PtdIns-3-P kinase VPS34. [35,114,115]

Figures 22 and 23 illustrate representative experiments under starvation conditions. *atg13*- mutant showed the most altered pattern with the formation of large aberrant aggregates of GFP-Atg8 and the absence of GFP-Atg18 puncta. This indicates a strong impairment of autophagy that corroborates the results of the flux assay. *atg101*- mutant strain also showed some abnormal aggregates of GFP-Atg8 although not as large as the ones in *atg13*-. On the opposite, *FIP200*- showed a large number of autophagosomes with both markers that were also large in size. In this case a clear vesicle-like structure can be seen in some of the puncta suggesting that they are functional autophagosomes. This result together with the increased flux observed strongly suggests that *FIP200*- mutant has an increased autophagy. As for *atg17*- and *atg101-interactor*- we did not detect clear differences in the patterns. A summary of these findings from at least three independent experiments are shown in table15.

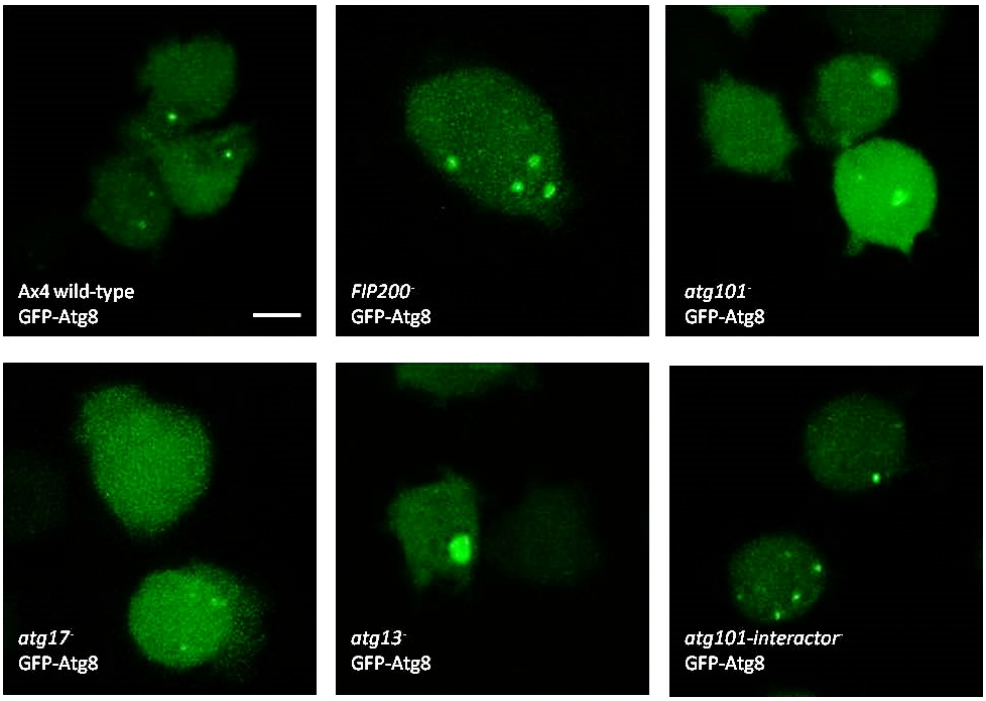


**Figure 22.** Confocal microscopy analysis of autophagy marker protein Atg8 tagged with GFP on Atg1 complex knockout strains (FIP200-; *atg* 101-; *atg* 17-; *atg* 13- and *atg* 101-*interactor* -) subjected to 30 minutes of PDF starvation inducing medium.

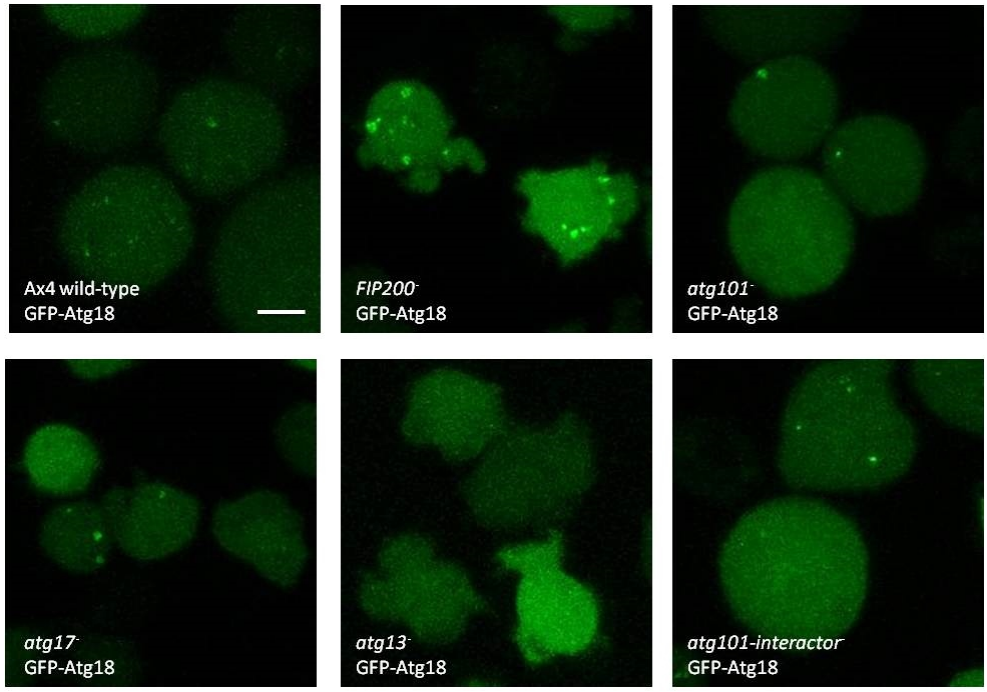


**Figure23**. Confocal microscopy analysis of autophagy marker protein Atg18 tagged with GFP on Ax4 parental strain and Atg1 complex knockout strains subjected to 30 minutes PDF starvation inducing medium.

**Knock-out phenotypes**

| Knock-Out | Atg8-GFP | Atg18-GFP |
|---|---|---|
| Atg13 | Big aggregate; no autophagosomes | No autophagosomes |
| Atg 101 | Little aggregates and some (few) autophagosomes | Few autophagosomes |
| FIP 200 | Large autophagossomes, increased number | More autophagosomes than the wild-type |
| Atg17 | Similar to wild-type | Similar to wild-type |
| Atg101-interactor | Similar to wild-type | Similar to wild-type |

**Table 15.** Summary of the analysis of confocal microscopy of the different strains using the markers GFP-Atg8 and GFP-Atg18.

## 8. Transketolase and Autophagy.

Transketolase (TK), a thiamine diphosphate-dependent enzyme is the key rate-limiting enzyme of the non-oxidative branch of the pentose phosphate pathway. [92,93] The fact that this enzyme interacts with Atg1 opens a whole new set of questions. Does TK have an influence in autophagy? Is Atg1 regulating TK activity?

To verify the first possibility the behavior of autophagy markers GFP-Atg8 and RFP-Atg18 was analyzed by confocal microscopy in wild-type and TK overexpressing cells (figures 24 and 25).

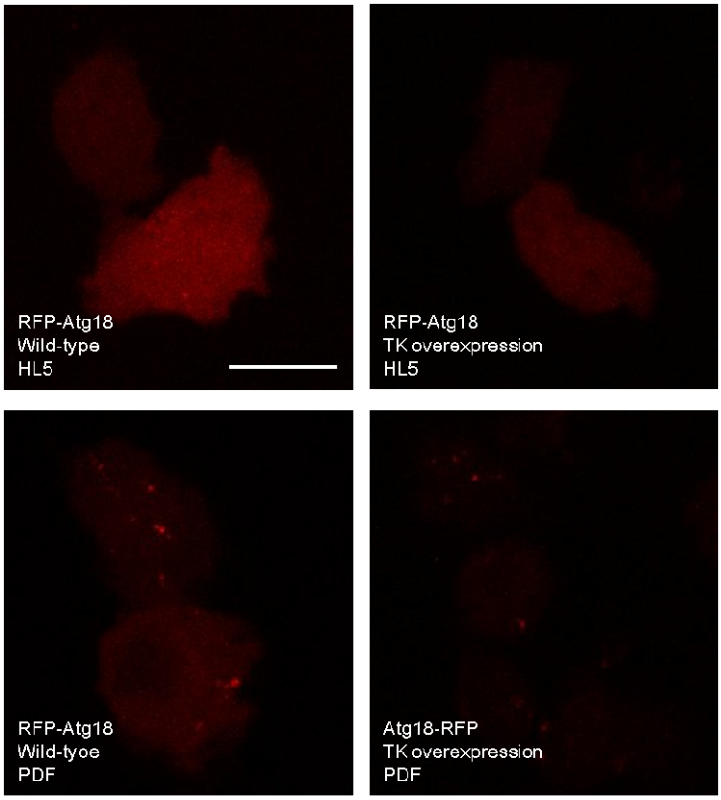


**Figure 24.** *In vivo* confocal analysis of RFP-Atg18 in Ax4 strain and cells overexpressing transketolase in HL5 and PDF starvation medium.

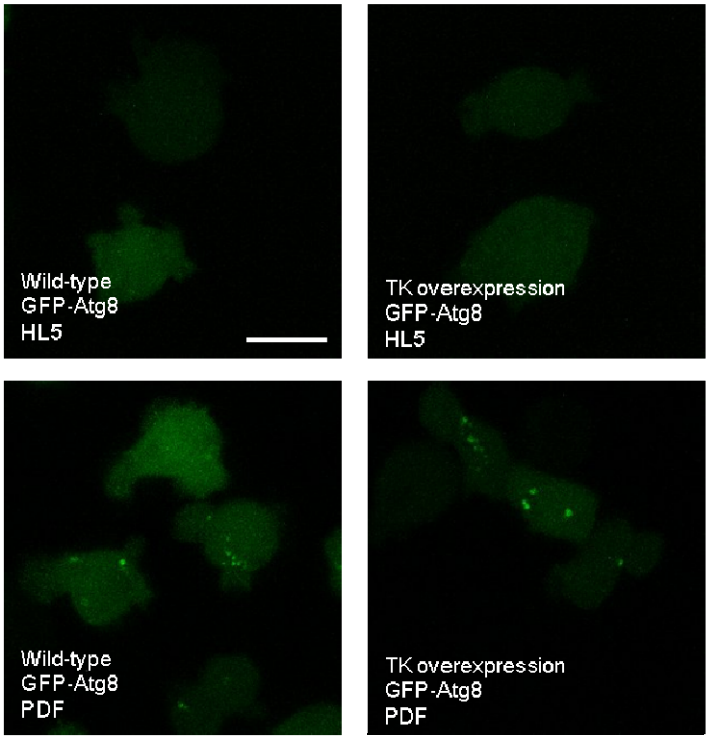


**Figure 25.** *In vivo* confocal analysis of GFP-Atg8 in Ax4 strain and cells overexpressing transketolase in HL5 and PDF starvation medium.

The overexpression of TK did not induce GFP-Atg8 or GFP-Atg18 puncta in HL5 growth media. In addition, the overexpression of TK did not alter the puncta pattern under starvation compared with wild-type, which suggests that TK does not regulate autophagy neither in basal nor in starvation conditions.

## 9. Effect of Atg1 in Transketolase Activity.

In order to study the possible functional connection between Atg1 and TK we measured the activity of TK and another key enzyme of the pentose phosphate pathway, glucose 6-phosphate dehydrogenase (G6PDH) in conditions of altered Atg1 activity.

### 9.1. Transketolase activity measurements in *Dictyostelium discoideum*.

Transketolase activity was determined measuring the rate of NADH consumption from a 0.2 mM NADH, 5 mM $MgCl_2$, 0.1 mM TPP, 2 mM ribose-5-phosphate and 1 mM xylulose-5-phosphate, at pH 7.6. [86,87]

G6DPH activity was assayed by measuring the rate of NADPH production from 0.5 mM NADP and 2 mM Gluc-6-Phosphate at pH 7.6. [86,87]

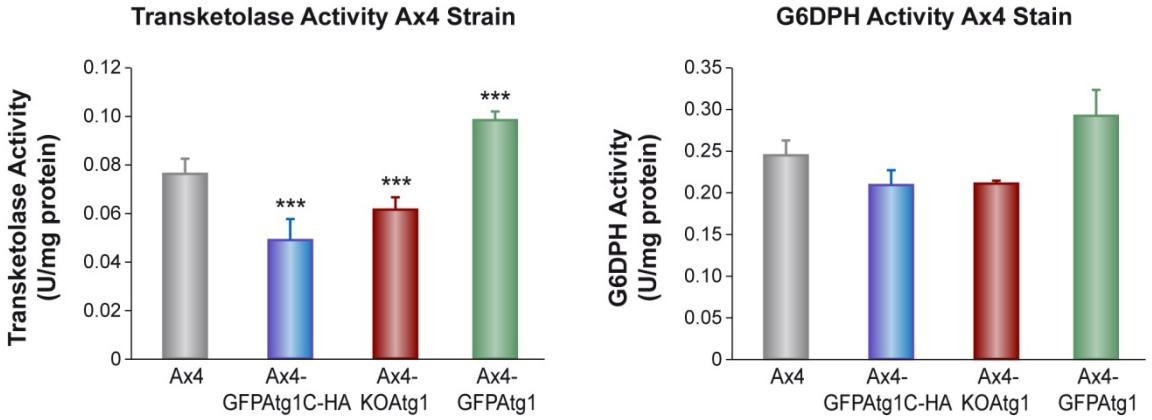


**Figure 26.** Left: Effect of Atg1 in Transketolase Activity. Grey column: wild-type Ax4 strain. Blue column: Ax4-GFP-Atg1b-HA that corresponds to the overexpression of Atg1 without the kinase domain. Red column: Knockout of GFP-Atg1 and green column: overexpression of Atg1-GFP. Significance of the differences were determined by the Student´s *t*-test (***P<0.001). Right: Glucose-6-phosphate dehydrogenase activity in different Dictyostelium Ax4 strains (same as in the left panel).

Our result indicates that genetic alterations in Dd Atg1 have an effect in TK activity. There is an increase in activity when cells overexpress Atg1. In contrast TK activity decreases in cells in which Atg1 has been deleted or express an Atg1-C-terminal construct that lacks the kinase domain. An Atg1 kinase mutant has been shown previously to act as a dominant negative in Dictyostelium. [105]

We found slight changes in G6PDH activity but they are not statistically significant.

## 9.2. Transketolase Activity measurements in HEK293T cells.

Next, we wanted to determine if the modulation of TK activity by Atg1 has been conserved in human cells. An alteration of human TK activity by ULK1 (the equivalent of Atg1 in humans) would be a very relevant finding since the pentose phosphate pathway and human TK have been found to be altered in tumor cells. [116] To address this

question we performed a series of activity measurements in Human Embryonic Kidney (HEK293T) cells in which ULK1 was overexpressed.

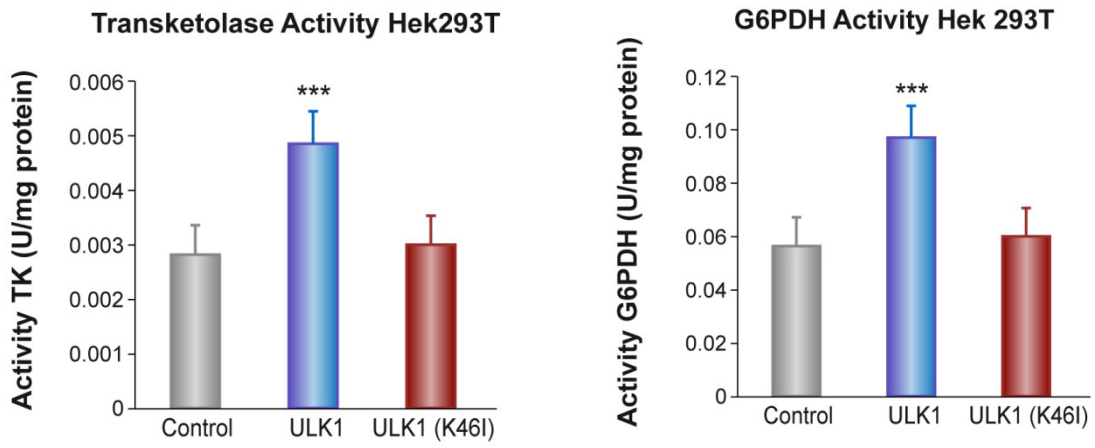


**Figure 27.** Left: Transketolase Activity in HEK293T cells in DMEM complete medium transfected with ULK1 and a form of ULK1 in which the kinase domain was mutated (ULK1 K46I). Control samples were transfected with empty pmx-IP vector. The overexpression of ULK1 kinase leads to an increase in TK activity (blue). Significance of the differences were determined by the Student´s *t*-test (***P<0.001). Left: Glucose-6-phosphate dehydrogenase activity in HEK293T cells expressing empty pmX-IP vector; ULK1 or ULK1(K46I). Cells maintained in DMEM complete medium. Significance of the differences were determined by the Student´s *t*-test (***P<0.01).

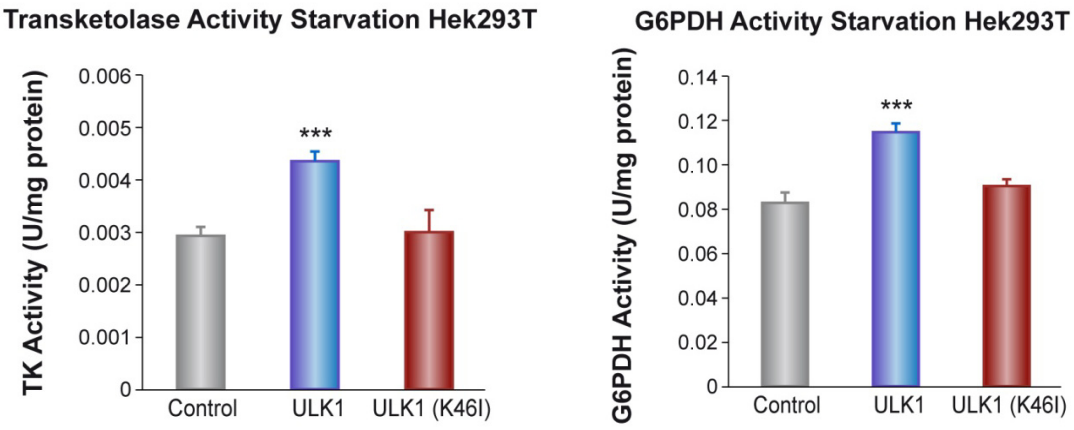


**Figure 28.** Left: Transketolase Activity in HEK293T cells in EBSS starvation media. Cells were transfected with empty pmx-IP vector, ULK1 or ULK1(K46I). Right: G6DPH Activity in HEK293T cells in starvation EBSS media. Samples overexpressing empty vector (control), ULK1 and ULK1 with mutated kinase (K46I) were analyzed. Significance of the differences were determined by the Student´s *t*-test (***P<0.001).

The results displayed in Figures 27 and 28 lead us to conclude that human ULK1 positively regulates transketolase activity and that this regulation depends on Ulk1 kinase activity since the mutated kinase strain has the same activity as the control. Other surprising finding is that this effect is independent of ULK1 activation by starvation since modulation of transketolase activity by ULK1 occurs in starved and non-starved cells.

Glucose-6-phosphate dehydrogenase activity is also altered in cells overexpressing ULK1 both in complete and starvation media. This suggests that the oxidative branch of the pentose phosphate pathway is also affected by the overexpression of ULK1 in HEK293T.

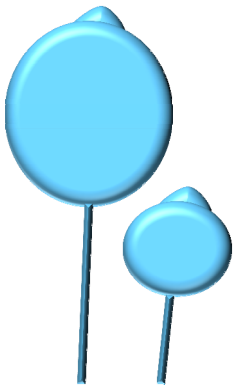

# DISCUSSION

# DISCUSSION

## 1. Analysis of Atg8 interactors reveals a high conservation and putative new regulators.

Atg8 is an ubiquitin-like protein that is a fundamental component in the autophagy machinery, as referred earlier in this work. The function of this protein depends on its association with several other proteins in a cascade of ubiquitin-like reactions that eventually conjugate Atg8 to the autophagosome membrane. Therefore, the identification of these proteins in Dictyostelium is the first step in comprehending the organization of the two subsequent ubiquitin-like conjugation systems responsible for the autophagosome elongation phase.

We were able to identify the interaction between Atg8 and Atg4, protease that exposes the carboxyl terminal glycine residue of Atg8 that then will be ligated to PE by the E1-like activating enzyme Atg7 and the E2-like conjugating enzyme Atg3. Atg 7 was proven to interact with Atg8 in Dictyostelium by both yeast two-hybrid and mass spectrometry techniques and Atg3 was also identified in the last one.

The presence of other conjugation system allows the formation of the complex Atg12-Atg5-Atg16 that is recruited to the autophagosome membrane and it is believed to be essential for Atg8 lipidation functioning as an E3-like enzyme. The interaction between Atg5 and Atg16 was recognized in our analysis, which indicates that the E3-like reaction that these proteins catalyze is probably conserved in Dictyostelium. Atg7 is also involved in this conjugation and although we identified the interaction between Atg12-Atg7 we were not able to detect Atg12 ligated to Atg5. [117] However, the formation of a conjugate between Atg12-Atg5 was detected previously in Dictyostelium by others. [81]

All together these results support the idea that the two ubiquitin-like conjugations are conserved in the Dictyostelium model (Figure 29).

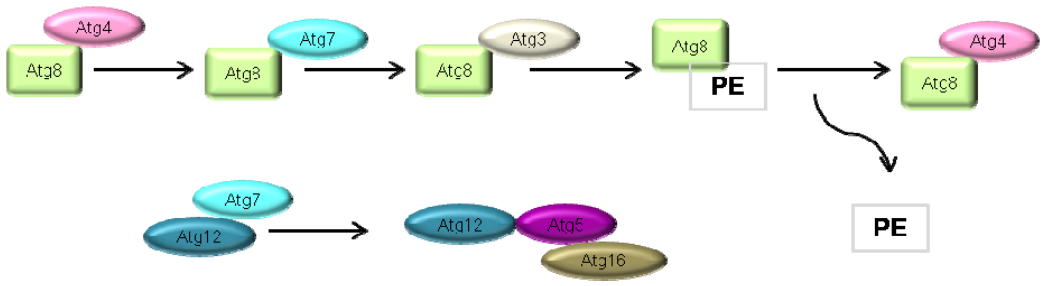


**Figure 29.** Ubiquitin-like conjugation systems conserved in *Dictyostelium discoideum.*

A homologue of the p62 in Dictyostelium was identified as part of ubiquitinated protein aggregates present in cells deficient in Vmp1, an ER-transmembrane protein required for autophagy. These aggregates also contained the autophagy marker GFP-Atg8. [118] We have now confirmed the interaction between p62 and Atg8 as described in other organisms. This interaction is believed to mediate the degradation of protein aggregates by autophagy.

Apart from these expected Atg8 interacting proteins we also encountered new interactors. The identification of such diversity of proteins highlights the complexity of the autophagy-interacting network.

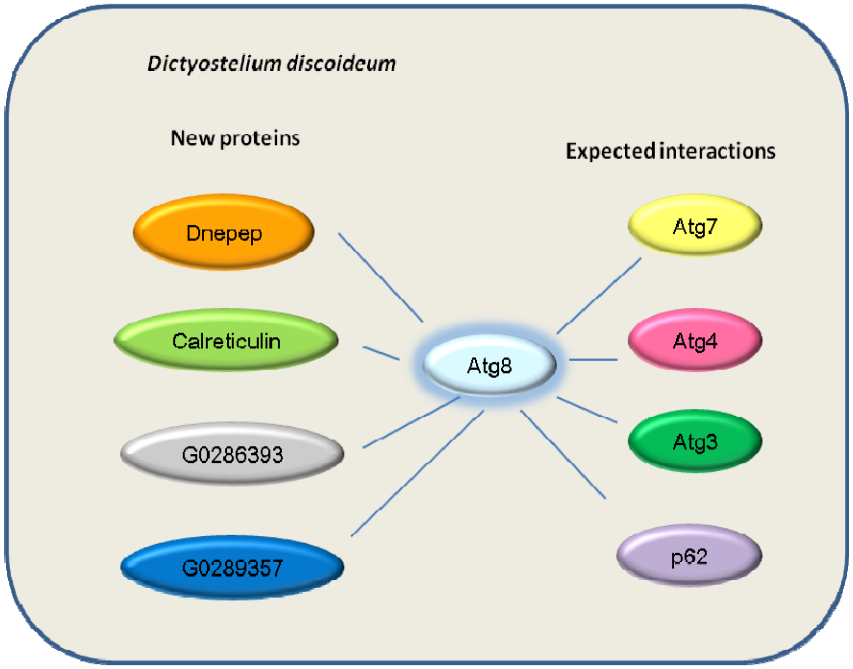


**Figure 30**. Interaction network identified for Atg8.

Atg8 interacting proteins commonly have in their sequence a motif associated with selective autophagy, called LIR motif (LC3 interaction region). Due to the importance of this motif in selective autophagy several studies have been performed to understand more about its mode of action and composition. The LIR binding interface is a major entry point for controlling autophagy since they mediate the binding of autophagy adaptors to Atg8/LC3. The consensus sequence of a LIR motif is [W/F/Y]XX[L/I/V], in which two sets of hydrophobic residues interact with two hydrophobic surfaces in Atg8. [119]

A very informative tool in the identification of putative LIR domains is iLIR, an online search engine that enables the identification of this motifs based in the analysis of the amino acid sequence of a protein of interest. [120,121]

Figure 30 represents the Atg8 interacting proteins identified in yeast two-hybrid and mass spectrometry analysis. We used the iLIR bioinformatic program to address whether these proteins have putative LIR motifs. In fact, this bioinformatic approach predicts that all the new identified Atg8 interactors (DDB_G0289357, Calreticulin, CnrK, DDB_G0286393 and Dnpep) contain LIR domains that support their interaction with Atg8.

Calreticulin is a molecular chaperone in the endoplasmic reticulum that also has a function in calcium homeostasis. [122] Although this protein is ER located, it has been detected in other cellular locations as mitochondria, nucleus and the cytosol and associated to new roles in processes like apoptosis or inflammation and with our new findings possibly autophagy. [123-125] Interestingly, there is a mammalian LC3 homologue, known as GABARAP that has been identified as an interactor of calreticulin in mammalian cells [126] being the functional significance of this interaction still unknown. The conservation of the interaction between calreticulin and Atg8/LC3 in Dictyostelium and mammalian cells gives weight to the hypothesis that this protein might act as an autophagy regulator, an issue that will need further investigation.

Aspartyl aminopeptidase, DNPEP belongs to the M18 metallopeptidase family. In a general way, aminopeptidases catalyze the removal of amino acids from the N-terminus of protein substrates, a process necessary for intracellular metabolism that has been implicated in several human diseases. These enzymes are widely encountered in eukaryotes and prokaryotes as membrane or cytosolic proteins. The fact that the homologues of DNPEP have usually 90% or higher homology rate may be indicative of an important conserved role of this protein, although its specific function is still unknown.

DNPEP has a high activity especially in the brain and testis and is commonly known to be cytosolic. [127,128]

CnrK (Cell Number Regulator) is a protein originally described as a suppressor of SmlA, a protein of unknown function whose disruption generates Dictyostelium aggregates of small size. [81] CnrK has protein similarity (E-value $3e^{-20}$) to several E3 ubiquitin protein ligases containing the typical RING zinc finger domain and the IBR domain. Interestingly the first hit when compared to the human proteome is ARIH1 (also known as HHARI, human homologue of Ariadne). This E3-ligase has been recently proposed to serve redundant roles with Parkin, another E3-ligase that has been shown to play an essential role in mitophagy (the specific degradation of mitochondria by autophagy). [129]

The Dictyostelium proteins DDB_G0289357 and DDB_G0286393 show no clear homology to any protein from yeast or mammalian cells, although the presence of LIR motifs and the interaction with Atg8 still position these two proteins as possible autophagy related proteins.

## 2. The core Atg1 complex is conserved in the Dictyostelium model.

The protein composition of the Atg1 complex has been conserved in different species as shown in Figure 31. However there are some subunits that appear to have been diverged in evolution. The core of the complex seems to be formed by the kinase Atg1, which shows high amino acid conservation in all analyzed species, including Dictyostelium [77] and the Atg13 protein.

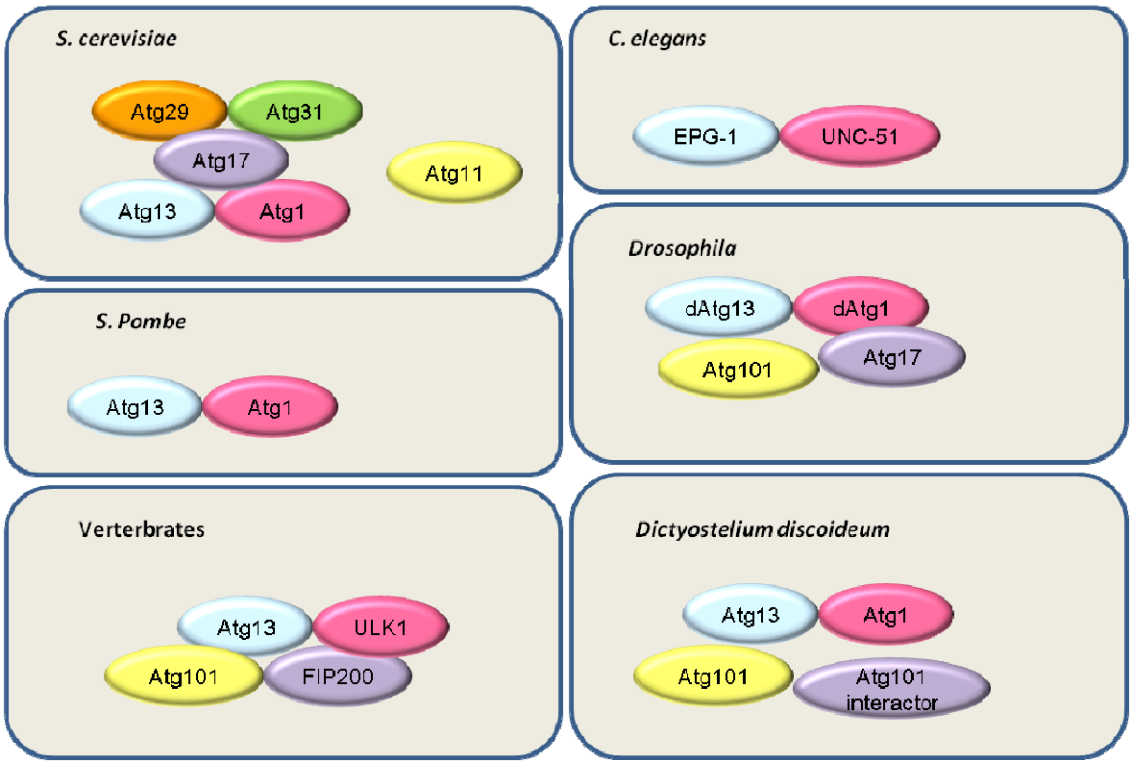


**Figure 31. Composition of complex Atg1/Ulk1 kinase in different model organisms.** (Adapted from [130-132]) *S. cerevisiae* Atg1 complex contains, besides Atg1 and Atg13, three additional proteins that are not present in any of the other organisms. In the other side we have *S. Pombe,* in which the only identified proteins are Atg1 and Atg13. In vertebrates*, Drosophila, C. elegans and Dictyostelium discoideum* the complex contains at least Atg1 (EPG-1 in *Drosophila*), Atg13 and the protein Atg101. In vertebrates FIP200 has been proposed to be the functional counterpart of Atg17 from yeast. We can speculate that Atg101-interactor could be a divergent form of Atg17/FIP200 in *Dictyostelium discoideum*.

Atg13, however, has shown a very low similarity at the amino-acid level in the different species, which makes the identification of the homologues a real problem. As a matter of fact, the Dictyostelium Atg13 protein do not show an overall significant similarity to the yeast or mammalian Atg13 but was annotated in Dictybase as having a short sequence of similarity to Atg13. This led us to include this protein in our analysis. The interaction

analysis and the functional studies presented here indicate that the putative Dictyostelium Atg13 is a bona fide homologue.

Atg13 function has been always related to a direct regulation of Atg1 kinase, thus it is expected that the disruption of the gene results in the very similar defects as the ones observed in the different Atg1/ULK1 mutants. Our results are consistent with this idea since the observed phenotype, the lack of aggregation, is similar to the one observed in Atg1 mutants. [77] This contrasts with the most common multitip phenotype observed in other autophagic mutants. [78]

In *S. cerevisiae* the disruption of the gene coding for Atg13 does not affect the viability of cells in rich nutrient conditions but this cells loose viability when exposed to prolonged starvation, the defects induced by the mutation of this gene are fully recovered by the overexpression of Atg1. [133,134]

Studies in *Drosophila* using the mutant Atg13 revealed that this strain is incapable of inducing autophagy and autophagosome markers do not detect puncta structures. [135]

Knockdown of Atg13 in HEK283T cells, in concordance with the other model organisms in which these proteins were mutated caused the inhibition of LC3 lipidation during both growth and starvation conditions. [136]

Atg101 is a small protein recently discovered in mammalian cells that seems to be absent in yeast. This protein was first identified in mammalian cells where it interacts with ULK1 in an Atg13 dependent manner stabilizing the expression of Atg13 in the cell and protecting it from proteasomal degradation. The knockdowns of this protein in mammalian cells strongly impair autophagy. [24,137]

Atg101 silencing in *Drosophila* revealed the importance of this protein both in starvation-induced and in basal autophagy, since in these mutants there is a strong accumulation of proteins like Atg8 that tends to form misshaped aggregates. [24]

In our experiments with *atg101*$^{-}$ we observed a characteristic multitip phenotype that indicates an autophagy blockage but not at the extent observed in atg13$^{-}$ or *atg1*$^{-}$. With the help of confocal microscopy we could see that there are some aggregates of GFP-Atg8 in this strain but also some autophagosomes, although fewer than in the wild-type. The autophagy machinery appears to be functional to a lesser extent as shown in the autophagic flux measurements, where autophagy is decreased by approximately 40% in comparison to the wild-type.

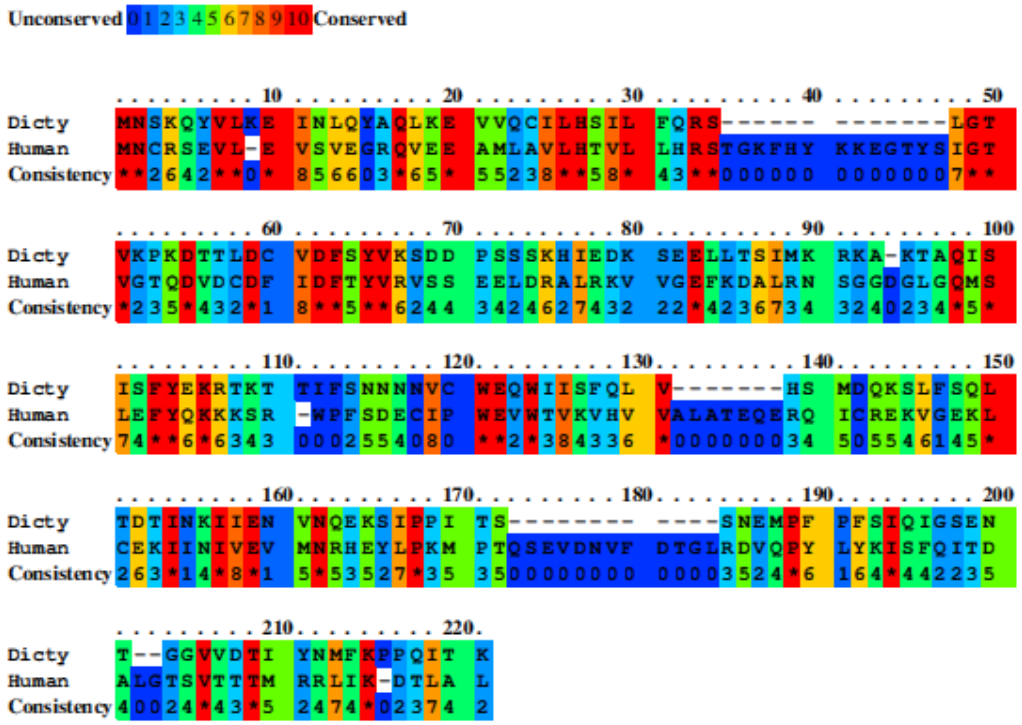


**Figure 32. Amino acid conservation scheme for human and Dd Atg101.** The conservation scoring is performed by PRALINE. The scoring scheme works from 0 for the least conserved alignment position, up to 10 for the most conserved alignment position.

The analysis of protein interactors between the putative Atg1-complex subunits confirmed that the core complex is formed by the proteins Atg1, Atg13 and Atg101 in *Dictyostelium discoideum*. This finding tells us that this complex has been conserved in evolution between Dictyostelium and mammalian cells.

In our analysis of protein-protein interactions we had to divide both Atg1 and Atg13 in two fragments due to their repetitive sequence. This enabled us to restrict the interaction regions between these two proteins and Atg101. The Atg13 N-terminal fragment is sufficient to interact with Atg1 C-terminal fragment and also with Atg101. Atg101 interacts with the N-terminal region of Atg1, which is the region that contains the kinase domain.

## 3. The putative Dictyostelium protein Atg17 is not the functional Atg17 homologue.

Atg17 was described in yeast as a modulator of the size of autophagosomes since Atg17 mutant showed fewer and smaller autophagosomes. [134]

The interaction analysis was a very rich source of data, although further validation of the functional role of the presented proteins was necessary. In the case of the putative Dictyostelium Atg17, we did not find any interacting protein among the ones used in this study, nevertheless a knockout analysis was fundamental to address the role of this protein. Unfortunately, the strain *atg17*<sup>-</sup> in *Dictyostelium discoideum* showed a wild-type and no significant alteration in autophagy flux. With all this, we believe that the putative Atg17 described in this work is not the functional homologue of the yeast Atg17.

## 4. Dictyostelium FIP200 functions as a negative regulator of autophagy.

Different studies of FIP200 in various types of mammalian cells showed the pivotal role of this protein in autophagy and other cellular mechanisms. Starvation induced autophagy is almost completely null in mouse embryonic fibroblast lacking FIP200. These cells also showed the accumulation of the protein p62 which added to the previous results indicate that autophagy is profoundly impaired. [25] Additional work using hematopoietic cells lacking FIP200 showed a rise in the number of mitochondria and p62 but and also an increase in the level o reactive oxygen species. [138]

These observations are not consistent with the ones we have observed for the putative FIP200 from *Dictyostelium discoideum*. The knockout of the putative FIP200 leads to the activation of the autophagy pathway as demonstrated by the increase in the autophagic flux and the size and number of puncta observed by the use of GFP-Atg8 and GFP-Atg18 markers. The low similarity at the level of amino acid sequence between Dictyostelium and mammalian FIP200 makes it conceivable that this protein has largely diverged in evolution and might play a different role in Dictyostelium autophagy.

We can conclude that the organization of Dictyostelium Atg1 kinase complex is very similar to the ones in animals, in contrast with the Atg1 complex of the yeast *S.cerevisiae.*

## 5. A novel Atg101 interacting protein regulates autophagy.

Atg101-interactor is a new Atg1 complex protein that has not yet been described in other model organisms. The Atg101-interactor mutant strain is phenotypically similar to the wild-type and the observation of autophagosome markers GFP-Atg8 and GFP-Atg18 did not reveal obvious alterationa in autophagosome shape and size. Despite these

similarities with wild-type we can observe that the autophagy flux in these cells is slightly reduced, which can be indicative of a regulative but not fundamental role of this protein in the complex.

Similarity analysis of this protein using BLAST did not recognize clear homologues in mammalian cells or yeast. However it contains two conserved domains, a B-Box zinc finger domain, a FNIP domain and a domain of unknown function called DUF4559. The first two domains are believed to mediate protein-protein interaction in proteins of diverse functions and thus, are not informative about a possible biochemical function. The DUF4559 motif is present in the human protein of unknown function CXorf38. We also analyzed possible similarities at the structural level using the HHpred (homology detection and structure prediction at http://toolkit.tuebingen.mpg.de/hhpred). The results of the best hits are shown in the figure 34. All of them correspond to homologies to the B-box domain. Interestingly, the first hits are protein of the TRIM family of ubiquitin E3 ligases. The possibility of Atg101-interactor being a TRIM protein open new possibilities of study and regulation since these proteins have important roles in a vast range of biological processes like cell proliferation, differentiation, development, apoptosis, oncogenesis and immunity. [139]

These bioinformatic analyses do not allow us to propose a function or a clear homologue in other organisms, although the possible function as an E3-ligase would be the clearest hypothesis to explore in future studies. It is possible that this protein could function as Atg17 in yeast or FIP200 in mammalian cells as a scaffold to modulate the activity of the complex. In fact Atg17 and FIP200 do not show similarities at the amino-acid or structural levels and they seem nevertheless to function in a similar way.

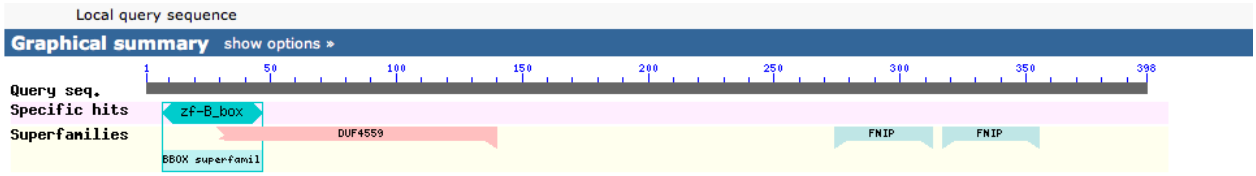


| No | Hit | | Prob | E-value | P-value | Score |
|---|---|---|---|---|---|---|
| 1 | 4tn3_A | TRIM5/cyclophilin A fus | 99.7 | 7.7E-16 | 2.3E-20 | 154.1 |
| 2 | 4nqj_A | E3 ubiquitin-protein li | 99.0 | 2E-08 | 6E-13 | 88.7 |
| 3 | 3ddt_A | E3 ubiquitin-protein li | 98.9 | 3E-10 | 8.9E-15 | 78.3 |
| 4 | 2yvr_A | Transcription intermedi | 98.9 | 8.1E-10 | 2.4E-14 | 76.9 |
| 5 | 2yrg_A | Tripartite motif-contai | 98.8 | 1.3E-09 | 3.8E-14 | 78.4 |
| 6 | 1fre_A | Nuclear factor XNF7; zi | 98.8 | 1.3E-09 | 3.9E-14 | 72.7 |
| 7 | 2did_A | Tripartite motif protei | 98.6 | 2.8E-08 | 8.4E-13 | 69.7 |
| 8 | 4ltb_A | Tripartite motif-contai | 98.5 | 4E-06 | 1.2E-10 | 74.7 |
| 9 | 2d8u_A | Ubiquitin ligase TRIM63 | 98.5 | 3.3E-08 | 9.9E-13 | 72.2 |
| 10 | 2csv_A | Tripartite motif protei | 98.4 | 9.3E-08 | 2.8E-12 | 71.5 |
| 11 | 2dja_A | Midline-2; tripartite m | 98.4 | 1.7E-07 | 5.2E-12 | 72.2 |
| 12 | 2egm_A | Tripartite motif-contai | 98.2 | 2.4E-07 | 7.1E-12 | 66.2 |
| 13 | 2jun_A | Midline-1; B-BOX, TRIM, | 98.1 | 1.1E-06 | 3.2E-11 | 70.1 |
| 14 | 4puf_A | E3 ubiquitin-protein li | 96.2 | 0.077 | 2.3E-06 | 55.9 |
| 15 | 4puf_A | E3 ubiquitin-protein li | 96.2 | 0.059 | 1.8E-06 | 56.8 |

**Figure 34.** HHpred (homology detection and structure prediction at http://toolkit.tuebingen.mpg.de/hhpred).

## 6. Transketolase and autophagy.

Atg1 kinase protein interacts with the pentose phosphate pathway enzyme transketolase (TK). For this interaction to take place it is only needed the C-terminal domain of Atg1 although as we refer in the results section this interaction seems to be much stronger when the kinase domain is present. Due to the importance of these two proteins in their respective routes we decided to investigate this relation in more detail.

Imaging studies using confocal microscopy proved that TK has no effect in autophagy, excluding this enzyme as a direct modulator of this pathway in our system.

Our results (summarized in figures 35 and 36) indicate that alterations in Atg1 levels affects TK activity in a way that suggests a direct regulation, although we have not been able to prove a possible phosphorylation of TK by the kinase Atg1.

Starvation triggers Dictyostelium development, which takes place in the absence of cell growth. However, developing cells are metabolically very active, as they need to accomplish high energy-demanding tasks, such as cell chemotaxis during aggregation and cell differentiation. It is possible that the pentose phosphate pathway provides NADPH and nucleotides required for these processes. In fact it has been described that an active pentose phosphate pathway exists during Dictyostelium development. [140] It has also been described that there is an increase in NADPH during Dictyostelium development. [141]

The increase in TK activity might facilitate the need to recycle the excess of Ribose-5-phosphate, a metabolite that could be accumulated as a result of the low requirement of requirement of nucleic acid synthesis during Dictyostelium development. The activity of TK would generate intermediates for glycolysis or Glucose-6-phosphate that can enter again the oxidative phase to generate more NADPH. Since autophagy is activated during development to support the recycling and the energy requirements of the cell, it is tempting to speculate that Atg1 might regulate this important pathway in concert with autophagy.

We have also seen the effects of Atg1 levels on TK activity in mammalian HEK293T suggesting a conservation of this pathway that might have important implications in cellular metabolism.

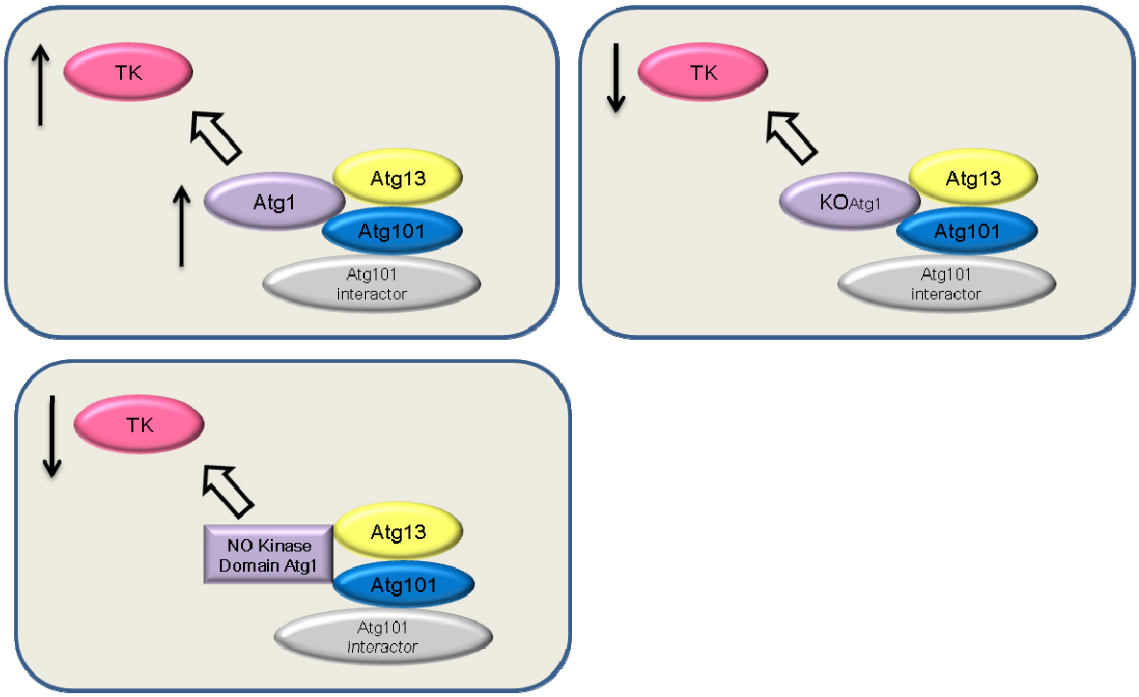


**Figure 35.** Effects of Atg1 overexpression, knockout and lack of kinase domain in transketolase activity in *Dictyosteliym discoideum.*

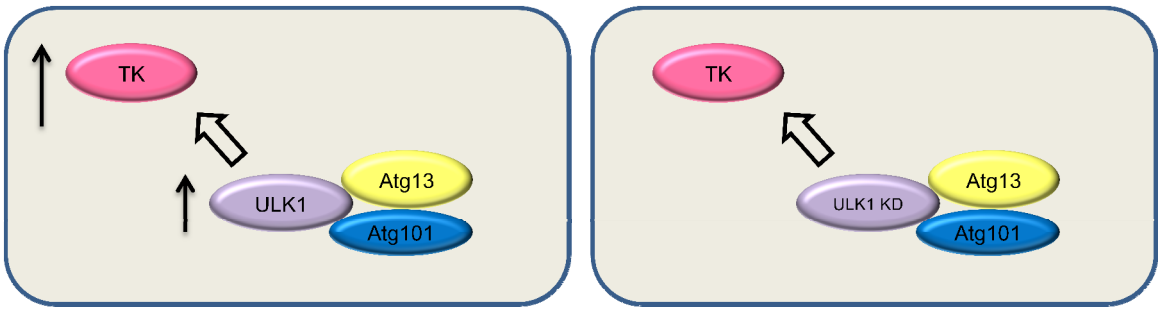


**Figure 36.** Effects of overexpression of ULK1 with and without mutated kinase.

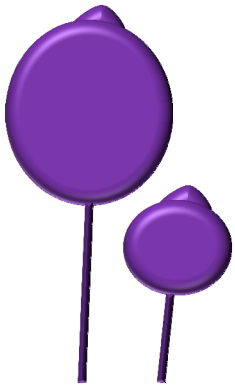

# BIBLIOGRAPHY

# BIBLIOGRAPHY


1. Abeliovich H (2014) Regulation of autophagy by amino acid availability in S. cerevisiae and mammalian cells. Amino Acids.
2. Kroemer G, Marino G, Levine B (2010) Autophagy and the integrated stress response. Mol Cell 40: 280-293.
3. Foldvari-Nagy L, Ari E, Csermely P, Korcsmaros T, Vellai T (2014) Starvation-response may not involve Atg1-dependent autophagy induction in non-unikont parasites. Sci Rep 4: 5829.
4. Klionsky DJ (2005) The molecular machinery of autophagy: unanswered questions. J Cell Sci 118: 7-18.
5. Kaushik S, Cuervo AM (2012) Chaperone-mediated autophagy: a unique way to enter the lysosome world. Trends Cell Biol 22: 407-417.
6. Li WW, Li J, Bao JK (2012) Microautophagy: lesser-known self-eating. Cell Mol Life Sci 69: 1125-1136.
7. Mijaljica D, Prescott M, Devenish RJ (2011) Microautophagy in mammalian cells: revisiting a 40-year-old conundrum. Autophagy 7: 673-682.
8. Lipinski MM, Hoffman G, Ng A, Zhou W, Py BF, et al. (2010) A genome-wide siRNA screen reveals multiple mTORC1 independent signaling pathways regulating autophagy under normal nutritional conditions. Dev Cell 18: 1041-1052.
9. Feng Y, He D, Yao Z, Klionsky DJ (2014) The machinery of macroautophagy. Cell Res 24: 24-41.
10. Tsuyuki S, Takabayashi M, Kawazu M, Kudo K, Watanabe A, et al. (2014) Detection of WIPI1 mRNA as an indicator of autophagosome formation. Autophagy 10: 497-513.
11. Kaufmann A, Wollert T (2014) Scaffolding the expansion of autophagosomes. Autophagy 10: 1343-1345.
12. Kishi-Itakura C, Koyama-Honda I, Itakura E, Mizushima N (2014) Ultrastructural analysis of autophagosome organization using mammalian autophagy-deficient cells. J Cell Sci 127: 4089-4102.
13. Nakahira K, Choi AM (2013) Autophagy: a potential therapeutic target in lung diseases. Am J Physiol Lung Cell Mol Physiol 305: L93-107.
14. Shimizu S, Honda S, Arakawa S, Yamaguchi H (2014) Alternative macroautophagy and mitophagy. Int J Biochem Cell Biol 50: 64-66.
15. Murrow L, Debnath J (2013) Autophagy as a stress-response and quality-control mechanism: implications for cell injury and human disease. Annu Rev Pathol 8: 105-137.
16. Ikeda Y, Sciarretta S, Nagarajan N, Rubattu S, Volpe M, et al. (2014) New insights into the role of mitochondrial dynamics and autophagy during oxidative stress and aging in the heart. Oxid Med Cell Longev 2014: 210934.
17. Hyttinen JM, Amadio M, Viiri J, Pascale A, Salminen A, et al. (2014) Clearance of misfolded and aggregated proteins by aggrephagy and implications for aggregation diseases. Ageing Res Rev 18C: 16-28.
18. Veljanovski V, Batoko H (2014) Selective autophagy of non-ubiquitylated targets in plants: looking for cognate receptor/adaptor proteins. Front Plant Sci 5: 308.
19. Nair U, Klionsky DJ (2005) Molecular mechanisms and regulation of specific and nonspecific autophagy pathways in yeast. J Biol Chem 280: 41785-41788.
20. Nakatogawa H, Ohbayashi S, Sakoh-Nakatogawa M, Kakuta S, Suzuki SW, et al. (2012) The autophagy-related protein kinase Atg1 interacts with the ubiquitin-like protein Atg8 via the Atg8 family interacting motif to facilitate autophagosome formation. J Biol Chem 287: 28503-28507.
21. Kamada Y, Funakoshi T, Shintani T, Nagano K, Ohsumi M, et al. (2000) Tor-mediated induction of autophagy via an Apg1 protein kinase complex. J Cell Biol 150: 1507-1513.

22. Pattingre S, Espert L, Biard-Piechaczyk M, Codogno P (2008) Regulation of macroautophagy by mTOR and Beclin 1 complexes. Biochimie 90: 313-323.
23. Tanida I (2011) Autophagy basics. Microbiol Immunol 55: 1-11.
24. Hegedus K, Nagy P, Gaspari Z, Juhasz G (2014) The putative HORMA domain protein Atg101 dimerizes and is required for starvation-induced and selective autophagy in Drosophila. Biomed Res Int 2014: 470482.
25. Hara T, Takamura A, Kishi C, Iemura S, Natsume T, et al. (2008) FIP200, a ULK-interacting protein, is required for autophagosome formation in mammalian cells. J Cell Biol 181: 497-510.
26. Alers S, Loffler AS, Paasch F, Dieterle AM, Keppeler H, et al. (2011) Atg13 and FIP200 act independently of Ulk1 and Ulk2 in autophagy induction. Autophagy 7: 1423-1433.
27. Kabeya Y, Kamada Y, Baba M, Takikawa H, Sasaki M, et al. (2005) Atg17 functions in cooperation with Atg1 and Atg13 in yeast autophagy. Mol Biol Cell 16: 2544-2553.
28. Liu F, Lee JY, Wei H, Tanabe O, Engel JD, et al. (2010) FIP200 is required for the cell-autonomous maintenance of fetal hematopoietic stem cells. Blood 116: 4806-4814.
29. Mao K, Chew LH, Yip CK, Klionsky DJ (2013) The role of Atg29 phosphorylation in PAS assembly. Autophagy 9: 2178-2179.
30. Chew LH, Setiaputra D, Klionsky DJ, Yip CK (2013) Structural characterization of the Saccharomyces cerevisiae autophagy regulatory complex Atg17-Atg31-Atg29. Autophagy 9: 1467-1474.
31. Randall-Demllo S, Chieppa M, Eri R (2013) Intestinal epithelium and autophagy: partners in gut homeostasis. Front Immunol 4: 301.
32. Kobayashi T, Suzuki K, Ohsumi Y (2012) Autophagosome formation can be achieved in the absence of Atg18 by expressing engineered PAS-targeted Atg2. FEBS Lett 586: 2473-2478.
33. Obara K, Sekito T, Niimi K, Ohsumi Y (2008) The Atg18-Atg2 complex is recruited to autophagic membranes via phosphatidylinositol 3-phosphate and exerts an essential function. J Biol Chem 283: 23972-23980.
34. Dooley HC, Razi M, Polson HE, Girardin SE, Wilson MI, et al. (2014) WIPI2 links LC3 conjugation with PI3P, autophagosome formation, and pathogen clearance by recruiting Atg12-5-16L1. Mol Cell 55: 238-252.
35. Polson HE, de Lartigue J, Rigden DJ, Reedijk M, Urbe S, et al. (2010) Mammalian Atg18 (WIPI2) localizes to omegasome-anchored phagophores and positively regulates LC3 lipidation. Autophagy 6: 506-522.
36. Seglen PO, Gordon PB (1982) 3-Methyladenine: specific inhibitor of autophagic/lysosomal protein degradation in isolated rat hepatocytes. Proc Natl Acad Sci U S A 79: 1889-1892.
37. Yang YP, Liang ZQ, Gu ZL, Qin ZH (2005) Molecular mechanism and regulation of autophagy. Acta Pharmacol Sin 26: 1421-1434.
38. Russell RC, Yuan HX, Guan KL (2014) Autophagy regulation by nutrient signaling. Cell Res 24: 42-57.
39. Lorin S, Hamai A, Mehrpour M, Codogno P (2013) Autophagy regulation and its role in cancer. Semin Cancer Biol 23: 361-379.
40. Fu LL, Cheng Y, Liu B (2013) Beclin-1: autophagic regulator and therapeutic target in cancer. Int J Biochem Cell Biol 45: 921-924.
41. Fogel AI, Dlouhy BJ, Wang C, Ryu SW, Neutzner A, et al. (2013) Role of membrane association and Atg14-dependent phosphorylation in beclin-1-mediated autophagy. Mol Cell Biol 33: 3675-3688.
42. Matsunaga K, Saitoh T, Tabata K, Omori H, Satoh T, et al. (2009) Two Beclin 1-binding proteins, Atg14L and Rubicon, reciprocally regulate autophagy at different stages. Nat Cell Biol 11: 385-396.
43. Takahashi Y, Meyerkord CL, Wang HG (2009) Bif-1/endophilin B1: a candidate for crescent driving force in autophagy. Cell Death Differ 16: 947-955.

44. Kang R, Zeh HJ, Lotze MT, Tang D (2011) The Beclin 1 network regulates autophagy and apoptosis. Cell Death Differ 18: 571-580.
45. Wang DB, Uo T, Kinoshita C, Sopher BL, Lee RJ, et al. (2014) Bax interacting factor-1 promotes survival and mitochondrial elongation in neurons. J Neurosci 34: 2674-2683.
46. Nishida K, Yamaguchi O, Otsu K (2008) Crosstalk between autophagy and apoptosis in heart disease. Circ Res 103: 343-351.
47. Funderburk SF, Wang QJ, Yue Z (2010) The Beclin 1-VPS34 complex--at the crossroads of autophagy and beyond. Trends Cell Biol 20: 355-362.
48. Tanida I (2011) Autophagosome formation and molecular mechanism of autophagy. Antioxid Redox Signal 14: 2201-2214.
49. Wild P, McEwan DG, Dikic I (2014) The LC3 interactome at a glance. J Cell Sci 127: 3-9.
50. Maruyama Y, Sou YS, Kageyama S, Takahashi T, Ueno T, et al. (2014) LC3B is indispensable for selective autophagy of p62 but not basal autophagy. Biochem Biophys Res Commun 446: 309-315.
51. Lippai M, Low P (2014) The role of the selective adaptor p62 and ubiquitin-like proteins in autophagy. Biomed Res Int 2014: 832704.
52. Birgisdottir AB, Lamark T, Johansen T (2013) The LIR motif - crucial for selective autophagy. J Cell Sci 126: 3237-3247.
53. Kaufmann A, Beier V, Franquelim HG, Wollert T (2014) Molecular mechanism of autophagic membrane-scaffold assembly and disassembly. Cell 156: 469-481.
54. Noda NN, Ohsumi Y, Inagaki F (2010) Atg8-family interacting motif crucial for selective autophagy. FEBS Lett 584: 1379-1385.
55. Bernard A, Klionsky DJ (2014) Defining the membrane precursor supporting the nucleation of the phagophore. Autophagy 10: 1-2.
56. Liu C, Ma H, Wu J, Huang Q, Liu JO, et al. (2013) Arginine68 is an essential residue for the C-terminal cleavage of human Atg8 family proteins. BMC Cell Biol 14: 27.
57. Ichimura Y, Imamura Y, Emoto K, Umeda M, Noda T, et al. (2004) In vivo and in vitro reconstitution of Atg8 conjugation essential for autophagy. J Biol Chem 279: 40584-40592.
58. Romanov J, Walczak M, Ibiricu I, Schuchner S, Ogris E, et al. (2012) Mechanism and functions of membrane binding by the Atg5-Atg12/Atg16 complex during autophagosome formation. EMBO J 31: 4304-4317.
59. Klionsky DJ, Abdalla FC, Abeliovich H, Abraham RT, Acevedo-Arozena A, et al. (2012) Guidelines for the use and interpretation of assays for monitoring autophagy. Autophagy 8: 445-544.
60. Sokollik C, Ang M, Jones N (2011) Autophagy: a primer for the gastroenterologist/hepatologist. Can J Gastroenterol 25: 667-674.
61. Florey O, Overholtzer M (2012) Autophagy proteins in macroendocytic engulfment. Trends Cell Biol 22: 374-380.
62. Xiao G (2007) Autophagy and NF-kappaB: fight for fate. Cytokine Growth Factor Rev 18: 233-243.
63. Geng J, Klionsky DJ (2008) The Atg8 and Atg12 ubiquitin-like conjugation systems in macroautophagy. 'Protein modifications: beyond the usual suspects' review series. EMBO Rep 9: 859-864.
64. Sucgang R, Kuo A, Tian X, Salerno W, Parikh A, et al. (2011) Comparative genomics of the social amoebae Dictyostelium discoideum and Dictyostelium purpureum. Genome Biol 12: R20.
65. Schilde C, Schaap P (2013) The Amoebozoa. Methods Mol Biol 983: 1-15.
66. Rollins AW, Landolt JC, Stephenson SL (2010) Dictyostelid cellular slime molds associated with grasslands of the central and western United States. Mycologia 102: 996-1003.
67. Schaap P (2011) Evolution of developmental cyclic adenosine monophosphate signaling in the Dictyostelia from an amoebozoan stress response. Dev Growth Differ 53: 452-462.

68. Eichinger L, Pachebat JA, Glockner G, Rajandream MA, Sucgang R, et al. (2005) The genome of the social amoeba Dictyostelium discoideum. Nature 435: 43-57.
69. Flowers JM, Li SI, Stathos A, Saxer G, Ostrowski EA, et al. (2010) Variation, sex, and social cooperation: molecular population genetics of the social amoeba Dictyostelium discoideum. PLoS Genet 6: e1001013.
70. Loomis WF (2013) Comparative genomics of the dictyostelids. Methods Mol Biol 983: 39-58.
71. Tian X, Strassmann JE, Queller DC (2013) Dictyostelium development shows a novel pattern of evolutionary conservation. Mol Biol Evol 30: 977-984.
72. Roberge-White E, Katoh-Kurasawa M (2011) Plasticity in the development and dedifferentiation of Dictyostelium discoideum. Dev Growth Differ 53: 587-596.
73. Williams JG (2010) Dictyostelium finds new roles to model. Genetics 185: 717-726.
74. Myre MA (2012) Clues to gamma-secretase, huntingtin and Hirano body normal function using the model organism Dictyostelium discoideum. J Biomed Sci 19: 41.
75. Weijer CJ (2004) Dictyostelium morphogenesis. Curr Opin Genet Dev 14: 392-398.
76. Schaap P (2011) Evolutionary crossroads in developmental biology: Dictyostelium discoideum. Development 138: 387-396.
77. Otto GP, Wu MY, Kazgan N, Anderson OR, Kessin RH (2004) Dictyostelium macroautophagy mutants vary in the severity of their developmental defects. J Biol Chem 279: 15621-15629.
78. Calvo-Garrido J, Carilla-Latorre S, Kubohara Y, Santos-Rodrigo N, Mesquita A, et al. (2010) Autophagy in Dictyostelium: genes and pathways, cell death and infection. Autophagy 6: 686-701.
79. King JS (2012) Autophagy across the eukaryotes: is S. cerevisiae the odd one out? Autophagy 8: 1159-1162.
80. Calvo-Garrido J, Escalante R (2010) Autophagy dysfunction and ubiquitin-positive protein aggregates in Dictyostelium cells lacking Vmp1. Autophagy 6: 100-109.
81. Otto GP, Wu MY, Kazgan N, Anderson OR, Kessin RH (2003) Macroautophagy is required for multicellular development of the social amoeba Dictyostelium discoideum. J Biol Chem 278: 17636-17645.
82. Mesquita A, Calvo-Garrido J, Carilla-Latorre S, Escalante R (2013) Monitoring autophagy in Dictyostelium. Methods Mol Biol 983: 461-470.
83. Patra KC, Hay N (2014) The pentose phosphate pathway and cancer. Trends Biochem Sci 39: 347-354.
84. Horecker BL (2002) The pentose phosphate pathway. J Biol Chem 277: 47965-47971.
85. Kruger NJ, von Schaewen A (2003) The oxidative pentose phosphate pathway: structure and organisation. Curr Opin Plant Biol 6: 236-246.
86. Boada J, Roig T, Perez X, Gamez A, Bartrons R, et al. (2000) Cells overexpressing fructose-2,6-bisphosphatase showed enhanced pentose phosphate pathway flux and resistance to oxidative stress. FEBS Lett 480: 261-264.
87. Pekovich SR, Martin PR, Singleton CK (1996) Thiamine pyrophosphate-requiring enzymes are altered during pyrithiamine-induced thiamine deficiency in cultured human lymphoblasts. J Nutr 126: 1791-1798.
88. Manganelli G, Masullo U, Passarelli S, Filosa S (2013) Glucose-6-phosphate dehydrogenase deficiency: disadvantages and possible benefits. Cardiovasc Hematol Disord Drug Targets 13: 73-82.
89. Stanton RC (2012) Glucose-6-phosphate dehydrogenase, NADPH, and cell survival. IUBMB Life 64: 362-369.
90. Schenk G, Duggleby RG, Nixon PF (1998) Properties and functions of the thiamin diphosphate dependent enzyme transketolase. Int J Biochem Cell Biol 30: 1297-1318.
91. Fullam E, Pojer F, Bergfors T, Jones TA, Cole ST (2012) Structure and function of the transketolase from Mycobacterium tuberculosis and comparison with the human enzyme. Open Biol 2: 110026.

92. Kochetov GA, Solovjeva ON (2014) Structure and functioning mechanism of transketolase. Biochim Biophys Acta 1844: 1608-1618.
93. Michalak S, Michalowska-Wender G, Adamcewicz G, Wender MB (2013) Erythrocyte transketolase activity in patients with diabetic and alcoholic neuropathies. Folia Neuropathol 51: 222-226.
94. Meshalkina LE, Solovjeva ON, Kochetov GA (2011) Interaction of transketolase from human tissues with substrates. Biochemistry (Mosc) 76: 1061-1064.
95. Wang J, Zhang X, Ma D, Lee WN, Xiao J, et al. (2013) Inhibition of transketolase by oxythiamine altered dynamics of protein signals in pancreatic cancer cells. Exp Hematol Oncol 2: 18.
96. Vicente JJ, Galardi-Castilla M, Escalante R, Sastre L (2008) Structural and functional studies of a family of Dictyostelium discoideum developmentally regulated, prestalk genes coding for small proteins. BMC Microbiol 8: 1.
97. Yang X, Hubbard EJ, Carlson M (1992) A protein kinase substrate identified by the two-hybrid system. Science 257: 680-682.
98. Hosokawa N, Sasaki T, Iemura S, Natsume T, Hara T, et al. (2009) Atg101, a novel mammalian autophagy protein interacting with Atg13. Autophagy 5: 973-979.
99. Pankiv S, Clausen TH, Lamark T, Brech A, Bruun JA, et al. (2007) p62/SQSTM1 binds directly to Atg8/LC3 to facilitate degradation of ubiquitinated protein aggregates by autophagy. J Biol Chem 282: 24131-24145.
100. Behrends C, Sowa ME, Gygi SP, Harper JW (2010) Network organization of the human autophagy system. Nature 466: 68-76.
101. Klionsky DJ, Schulman BA (2014) Dynamic regulation of macroautophagy by distinctive ubiquitin-like proteins. Nat Struct Mol Biol 21: 336-345.
102. Metlagel Z, Otomo C, Ohashi K, Takaesu G, Otomo T (2014) Structural insights into E2-E3 interaction for LC3 lipidation. Autophagy 10: 522-523.
103. Carroll B, Korolchuk VI, Sarkar S (2014) Amino acids and autophagy: cross-talk and co-operation to control cellular homeostasis. Amino Acids.
104. Nath S, Dancourt J, Shteyn V, Puente G, Fong WM, et al. (2014) Lipidation of the LC3/GABARAP family of autophagy proteins relies on a membrane-curvature-sensing domain in Atg3. Nat Cell Biol 16: 415-424.
105. Tekinay T, Wu MY, Otto GP, Anderson OR, Kessin RH (2006) Function of the Dictyostelium discoideum Atg1 kinase during autophagy and development. Eukaryot Cell 5: 1797-1806.
106. Stege JT, Laub MT, Loomis WF (1999) tip genes act in parallel pathways of early Dictyostelium development. Dev Genet 25: 64-77.
107. Tung SM, Unal C, Ley A, Pena C, Tunggal B, et al. (2010) Loss of Dictyostelium ATG9 results in a pleiotropic phenotype affecting growth, development, phagocytosis and clearance and replication of Legionella pneumophila. Cell Microbiol 12: 765-780.
108. Iwai-Kanai E, Yuan H, Huang C, Sayen MR, Perry-Garza CN, et al. (2008) A method to measure cardiac autophagic flux in vivo. Autophagy 4: 322-329.
109. Bauvy C, Meijer AJ, Codogno P (2009) Assaying of autophagic protein degradation. Methods Enzymol 452: 47-61.
110. Calvo-Garrido J, Carilla-Latorre S, Mesquita A, Escalante R (2011) A proteolytic cleavage assay to monitor autophagy in Dictyostelium discoideum. Autophagy 7: 1063-1068.
111. Hara T, Mizushima N (2009) Role of ULK-FIP200 complex in mammalian autophagy: FIP200, a counterpart of yeast Atg17? Autophagy 5: 85-87.
112. Welter E, Thumm M, Krick R (2010) Quantification of nonselective bulk autophagy in S. cerevisiae using Pgk1-GFP. Autophagy 6: 794-797.
113. Nair U, Thumm M, Klionsky DJ, Krick R (2011) GFP-Atg8 protease protection as a tool to monitor autophagosome biogenesis. Autophagy 7: 1546-1550.

114. Krick R, Henke S, Tolstrup J, Thumm M (2008) Dissecting the localization and function of Atg18, Atg21 and Ygr223c. Autophagy 4: 896-910.
115. Itakura E, Mizushima N (2010) Characterization of autophagosome formation site by a hierarchical analysis of mammalian Atg proteins. Autophagy 6: 764-776.
116. Meshalkina LE, Drutsa VL, Koroleva ON, Solovjeva ON, Kochetov GA (2013) Is transketolase-like protein, TKTL1, transketolase? Biochim Biophys Acta 1832: 387-390.
117. Xie Z, Nair U, Klionsky DJ (2008) Atg8 controls phagophore expansion during autophagosome formation. Mol Biol Cell 19: 3290-3298.
118. Calvo-Garrido J, Carilla-Latorre S, Escalante R (2008) Vacuole membrane protein 1, autophagy and much more. Autophagy 4: 835-837.
119. Yamaguchi M, Noda NN, Nakatogawa H, Kumeta H, Ohsumi Y, et al. (2010) Autophagy-related protein 8 (Atg8) family interacting motif in Atg3 mediates the Atg3-Atg8 interaction and is crucial for the cytoplasm-to-vacuole targeting pathway. J Biol Chem 285: 29599-29607.
120. Leckie BJ, McConnell A (1975) Proceedings: Activation of renin in human plasma and in rabbit kidney extracts. J Endocrinol 65: 7P.
121. Weissenhorn W, Fauvarque MO (2014) A small switch has a large effect on autophagy. Structure 22: 1-2.
122. Gold LI, Eggleton P, Sweetwyne MT, Van Duyn LB, Greives MR, et al. (2010) Calreticulin: non-endoplasmic reticulum functions in physiology and disease. FASEB J 24: 665-683.
123. Zhou R, Yazdi AS, Menu P, Tschopp J (2011) A role for mitochondria in NLRP3 inflammasome activation. Nature 469: 221-225.
124. Pinton P, Giorgi C, Siviero R, Zecchini E, Rizzuto R (2008) Calcium and apoptosis: ER-mitochondria Ca2+ transfer in the control of apoptosis. Oncogene 27: 6407-6418.
125. Zhang M, Wei J, Li Y, Shan H, Yan R, et al. (2014) Novel distribution of calreticulin to cardiomyocyte mitochondria and its increase in a rat model of dilated cardiomyopathy. Biochem Biophys Res Commun 449: 62-68.
126. Mohrluder J, Stangler T, Hoffmann Y, Wiesehan K, Mataruga A, et al. (2007) Identification of calreticulin as a ligand of GABARAP by phage display screening of a peptide library. FEBS J 274: 5543-5555.
127. Chaikuad A, Pilka ES, De Riso A, von Delft F, Kavanagh KL, et al. (2012) Structure of human aspartyl aminopeptidase complexed with substrate analogue: insight into catalytic mechanism, substrate specificity and M18 peptidase family. BMC Struct Biol 12: 14.
128. Wilk S, Wilk E, Magnusson RP (1998) Purification, characterization, and cloning of a cytosolic aspartyl aminopeptidase. J Biol Chem 273: 15961-15970.
129. Parelkar SS, Cadena JG, Kim C, Wang Z, Sugal R, et al. (2012) The parkin-like human homolog of Drosophila ariadne-1 (HHARI) can induce aggresome formation in mammalian cells and is immunologically detectable in Lewy bodies. J Mol Neurosci 46: 109-121.
130. Alers S, Loffler AS, Wesselborg S, Stork B (2012) The incredible ULKs. Cell Commun Signal 10: 7.
131. Nagy P, Karpati M, Varga A, Pircs K, Venkei Z, et al. (2014) Atg17/FIP200 localizes to perilysosomal Ref(2)P aggregates and promotes autophagy by activation of Atg1 in Drosophila. Autophagy 10: 453-467.
132. Liang Q, Yang P, Tian E, Han J, Zhang H (2012) The C. elegans ATG101 homolog EPG-9 directly interacts with EPG-1/Atg13 and is essential for autophagy. Autophagy 8: 1426-1433.
133. Funakoshi T, Matsuura A, Noda T, Ohsumi Y (1997) Analyses of APG13 gene involved in autophagy in yeast, Saccharomyces cerevisiae. Gene 192: 207-213.
134. Cheong H, Yorimitsu T, Reggiori F, Legakis JE, Wang CW, et al. (2005) Atg17 regulates the magnitude of the autophagic response. Mol Biol Cell 16: 3438-3453.

135. Chang YY, Neufeld TP (2009) An Atg1/Atg13 complex with multiple roles in TOR-mediated autophagy regulation. Mol Biol Cell 20: 2004-2014.
136. Chan EY, Longatti A, McKnight NC, Tooze SA (2009) Kinase-inactivated ULK proteins inhibit autophagy via their conserved C-terminal domains using an Atg13-independent mechanism. Mol Cell Biol 29: 157-171.
137. Mercer CA, Kaliappan A, Dennis PB (2009) A novel, human Atg13 binding protein, Atg101, interacts with ULK1 and is essential for macroautophagy. Autophagy 5: 649-662.
138. Liu F, Guan JL (2011) FIP200, an essential component of mammalian autophagy is indispensible for fetal hematopoiesis. Autophagy 7: 229-230.
139. Mandell MA, Jain A, Arko-Mensah J, Chauhan S, Kimura T, et al. (2014) TRIM Proteins Regulate Autophagy and Can Target Autophagic Substrates by Direct Recognition. Dev Cell 30: 394-409.
140. THOMAS DA (1978) Pentose Phosphate Metabolism during Differentiation in Dictyostelium discoideum. Journal of General Microbiology 113: 357-368.
141. Wright BE, Wassarman ME (1964) Pyridine Nucleotide Levels in Dictyostelium Discoideum during Differentiation. Biochim Biophys Acta 90: 423-424.

# ANNEX

# ANNEX 1: SUPPLEMENTAL DATA

## Atg1 C-terminal mass Spectrometry

| | |
|---|---|
| DDB0185178 | Protein\|gene: atg1 on chromosome: 6 position 1694801 to 1697129 - [DDB_G0292390] |
| DDB0191337 | Protein\|gene: mvpB on chromosome: 5 position 5070813 to 5073466 - [DDB_G0291127] |
| DDB0191259 | Protein\|gene: mvpA on chromosome: 1 position 3649783 to 3652408 - [DDB_G0269156] |
| DDB0185040 | Protein\|gene: pdi1 on chromosome: 2 position 6548168 to 6549349 - [DDB_G0276141] |
| DDB0219929 | Protein\|gene: hspA on chromosome: 5 position 1238068 to 1240089 - [DDB_G0288181] |
| DDB0232125 | Protein\|gene: hspG6 on chromosome: 2 position 7574080 to 7574712 - [DDB_G0276949] |
| DDB0232127 | Protein\|gene: hspG8 on chromosome: 2 position 7578926 to 7579561 - [DDB_G0277119] |
| DDB0232124 | Protein\|gene: hspG7 on chromosome: 2 position 7575967 to 7576590 - [DDB_G0276951] |
| DDB0308249 | Protein\|gene: DDB_G0279941 on chromosome: 3 position 2718242 to 2721164 - [DDB_G0279941] |
| DDB0308149 | Protein\|gene: DDB_G0275519 on chromosome: 2 position 6062122 to 6063145 - [DDB_G0275519] |
| DDB0229941 | Protein\|gene: shkB on chromosome: 5 position 1745652 to 1747854 - [DDB_G0288617] |
| DDB0185029 | Protein\|gene: chcA on chromosome: 2 position 7717198 to 7722630 - [DDB_G0277221] |
| DDB0305134 | Protein\|gene: DDB_G0286289 on chromosome: 4 position 4300974 to 4303039 - [DDB_G0286289] |
| DDB0232122 | Protein\|gene: hspG9 on chromosome: 2 position 7581914 to 7582519 - [DDB_G0276953] |
| DDB0307261 | Protein\|gene: DDB_G0275359 on chromosome: 2 position 5424566 to 5425954 - [DDB_G0275359] |
| DDB0231483 | Protein\|gene: mmsdh on chromosome: 5 position 2337171 to 2339014 - [DDB_G0289085] |
| DDB0233359 | Protein\|gene: pabpc1A on chromosome: 6 position 3041877 to 3044187 - [DDB_G0293558] |
| DDB0306711 | Protein\|gene: DDB_G0290971 on chromosome: 5 position 4814825 to 4816254 - [DDB_G0290971] |
| DDB0185058 | Protein\|gene: pppB on chromosome: 2 position 6106886 to 6107851 - [DDB_G0275619] |
| DDB0238507 | Protein\|gene: DDB_G0287859 on chromosome: 5 position 694189 to 699162 - [DDB_G0287859] |
| DDB0230063 | Protein\|gene: pccA on chromosome: 2 position 5413401 to 5415816 - [DDB_G0275355] |
| DDB0230208 | Protein\|gene: udkB on chromosome: 2 position 4144032 to 4144859 - [DDB_G0274559] |
| DDB0346635 | Protein\|gene: DDB_G0293328 on chromosome: 6 position 2760211 to 2760718 - [DDB_G0293328] |
| DDB0305376 | Protein\|gene: iliO on chromosome: 6 position 473965 to 475269 - [DDB_G0291520] |
| DDB0231686 | Protein\|gene: DD8-14 on chromosome: 5 position 2821081 to 2823256 - [DDB_G0289467] |
| DDB0230171 | Protein\|gene: ada on chromosome: 5 position 206705 to 209270 - [DDB_G0287371] |
| DDB0230086 | Protein\|gene: purL on chromosome: 5 position 1141268 to 1145420 - [DDB_G0288145] |
| DDB0232129 | Protein\|gene: hspK on chromosome: 2 position 5922492 to 5923304 - [DDB_G0275525] |
| DDB0185208 | Protein\|gene: paxB on chromosome: 2 position 4174381 to 4176090 - [DDB_G0274109] |
| DDB0230145 | Protein\|gene: DDB_G0271904 on chromosome: 2 position 1058890 to 1061065 - [DDB_G0271904] |
| DDB0231358 | Protein\|gene: scsB on chromosome: 2 position 4574977 to 4576552 - [DDB_G0274449] |
| DDB0231600 | Protein\|gene: DDB_G0289047 on chromosome: 5 position 2299492 to 2302095 - [DDB_G0289047] |
| DDB0231321 | Protein\|gene: gluS on chromosome: 5 position 295392 to 297778 - [DDB_G0287467] |
| DDB0308515 | Protein\|gene: DDB_G0273247 on chromosome: 2 position 2794534 to 2799419 - [DDB_G0273247] |
| DDB0216177 | Protein\|gene: dymA on chromosome: 3 position 252381 to 255025 - [DDB_G0277849] |
| DDB0305321 | Protein\|gene: iliC on chromosome: 1 position 4633487 to 4634149 - [DDB_G0271068] |
| DDB0238324 | Protein\|gene: DDB_G0290575 on chromosome: 5 position 4299544 to 4301062 - [DDB_G0290575] |
| DDB0306998 | Protein\|gene: DDB_G0282867 on chromosome: 3 position 6322173 to 6323255 - [DDB_G0282867] |
| DDB0238603 | Protein\|gene: cyc1 on chromosome: 6 position 1821453 to 1822974 - [DDB_G0292594] |
| DDB0232132 | Protein\|gene: hspG2 on chromosome: 2 position 6164176 to 6164778 - [DDB_G0276003] |
| DDB0230198 | Protein\|gene: odhB on chromosome: 2 position 5316981 to 5318500 - [DDB_G0275029] |
| DDB0232133 | Protein\|gene: hspG4 on chromosome: 2 position 7028602 to 7029201 - [DDB_G0276587] |
| DDB0306131 | Protein\|gene: DDB_G0270618 on chromosome: 1 position 3364045 to 3365508 - [DDB_G0270618] |
| DDB0191476 | Protein\|gene: rab1A on chromosome: 4 position 1241175 to 1242406 - [DDB_G0283757] |
| DDB0231339 | Protein\|gene: rpl7a on chromosome: 2 position 8280728 to 8282193 - [DDB_G0277629] |
| DDB0237755 | Protein\|gene: odc on chromosome: 3 position 4069177 to 4070741 - [DDB_G0281109] |
| DDB0229398 | Protein\|gene: rab1D on chromosome: 4 position 2756032 to 2757408 - [DDB_G0284985] |
| DDB0231150 | Protein\|gene: rpl32 on chromosome: 2 position 1095789 to 1096190 - [DDB_G0271976] |
| DDB0234112 | Protein\|gene: eif2s2 on chromosome: 3 position 5298628 to 5299779 - [DDB_G0282035] |

| | |
|---|---|
| DDB0234116 | Protein\|gene: cand1 on chromosome: 2 position 4865578 to 4869561 - [DDB_G0274167] |
| DDB0215357 | Protein\|gene: hmgB on chromosome: 2 position 7053641 to 7055221 - [DDB_G0276615] |
| DDB0191104 | Protein\|gene: cxeA on chromosome: 1 position 3937103 to 3937960 - [DDB_G0269118] |
| DDB0306488 | Protein\|gene: DDB_G0267744 on chromosome: 1 position 767152 to 768575 - [DDB_G0267744] |
| DDB0231317 | Protein\|gene: proS on chromosome: 4 position 1680128 to 1681774 - [DDB_G0284197] |
| DDB0346617 | Protein\|gene: DDB_G0291798 on chromosome: 6 position 762390 to 766299 - [DDB_G0291798] |
| DDB0306981 | Protein\|gene: DDB_G0283971 on chromosome: 4 position 1401996 to 1405050 - [DDB_G0283971] |
| DDB0216282 | Protein\|gene: nek2 on chromosome: 1 position 4847143 to 4848761 - [DDB_G0270814] |
| DDB0215016 | Protein\|gene: ddj1 on chromosome: 3 position 3103912 to 3105333 - [DDB_G0280037] |
| DDB0235361 | Protein\|gene: DDB_G0278341 on chromosome: 3 position 722601 to 724035 - [DDB_G0278341] |
| DDB0308107 | Protein\|gene: DDB_G0273493 on chromosome: 2 position 3018032 to 3019030 - [DDB_G0273493] |
| DDB0185072 | Protein\|gene: vilB on chromosome: 2 position 6792443 to 6795412 - [DDB_G0276453] |
| DDB0233992 | Protein\|gene: cct2 on chromosome: 6 position 177191 to 179304 - [DDB_G0291358] |
| DDB0230123 | Protein\|gene: shkC on chromosome: 3 position 836437 to 838779 - [DDB_G0278409] |
| DDB0229908 | Protein\|gene: aco1 on chromosome: 3 position 1708174 to 1711261 - [DDB_G0279159] |
| DDB0219924 | Protein\|gene: hgsA on chromosome: 5 position 1582464 to 1584009 - [DDB_G0288461] |
| DDB0230170 | Protein\|gene: udpB on chromosome: 3 position 3914149 to 3915176 - [DDB_G0280985] |
| DDB0266327 | Protein\|gene: dohh-2 on chromosome: 2 position 3747735 to 3748763 - [DDB_G0274079] |
| DDB0232397 | Protein\|gene: ponM on chromosome: 3 position 5221448 to 5221843 - [DDB_G0281989] |
| DDB0266791 | Protein\|gene: dnpep on chromosome: 4 position 4132917 to 4134488 - [DDB_G0286149] |
| DDB0233994 | Protein\|gene: cct5 on chromosome: 3 position 5012149 to 5014049 - [DDB_G0281849] |
| DDB0229401 | Protein\|gene: rab5A on chromosome: 2 position 1113320 to 1114208 - [DDB_G0271984] |
| DDB0191442 | Protein\|gene: eif5a on chromosome: 4 position 2766075 to 2766554 - [DDB_G0284861] |
| DDB0230149 | Protein\|gene: rpl23a on chromosome: 6 position 2967908 to 2968721 - [DDB_G0293502] |
| DDB0214932 | Protein\|gene: arcA on chromosome: 3 position 304397 to 306034 - [DDB_G0277825] |
| DDB0185061 | Protein\|gene: rabC on chromosome: 2 position 718547 to 719569 - [DDB_G0271736] |
| DDB0229442 | Protein\|gene: pdhB on chromosome: 2 position 6888601 to 6890166 - [DDB_G0276417] |
| DDB0214996 | Protein\|gene: forA on chromosome: 3 position 2388583 to 2393474 - [DDB_G0279607] |
| DDB0214953 | Protein\|gene: psmA4 on chromosome: 3 position 4147505 to 4148552 - [DDB_G0280969] |
| DDB0231478 | Protein\|gene: oatA on chromosome: 5 position 841784 to 843034 - [DDB_G0287913] |
| DDB0308208 | Protein\|gene: DDB_G0291740 on chromosome: 6 position 678305 to 679554 - [DDB_G0291740] |
| DDB0237794 | Protein\|gene: osbH on chromosome: 4 position 1009391 to 1010770 - [DDB_G0283709] |
| DDB0191255 | Protein\|gene: gpaA on chromosome: 4 position 547836 to 549106 - [DDB_G0283349] |
| DDB0348080 | Protein\|gene: DDB_G0283097 on chromosome: 4 position 214573 to 215986 - [DDB_G0283097] |
| DDB0231059 | Protein\|gene: rps19 on chromosome: 3 position 1760514 to 1760960 - [DDB_G0279207] |
| DDB0231305 | Protein\|gene: serS on chromosome: 2 position 2243539 to 2245192 - [DDB_G0272660] |
| DDB0252562 | Protein\|gene: sqrdl on chromosome: 6 position 1300465 to 1301905 - [DDB_G0292250] |
| DDB0191348 | Protein\|gene: pgmA on chromosome: 5 position 1620141 to 1621859 - [DDB_G0288483] |
| DDB0191511 | Protein\|gene: tifA on chromosome: 1 position 3537960 to 3539386 - [DDB_G0269192] |
| DDB0191276 | Protein\|gene: hspH on chromosome: 5 position 3818443 to 3820972 - [DDB_G0290187] |
| DDB0214894 | Protein\|gene: alaS on chromosome: 3 position 919657 to 922497 - [DDB_G0277823] |
| DDB0305056 | Protein\|gene: DDB_G0268360 on chromosome: 1 position 948334 to 948612 - [DDB_G0268360] |
| DDB0266744 | Protein\|gene: culE on chromosome: 3 position 1485914 to 1488923 - [DDB_G0278991] |
| DDB0304584 | Protein\|gene: zpr1 on chromosome: 1 position 2767401 to 2768924 - [DDB_G0269438] |
| DDB0233323 | Protein\|gene: DDB_G0279755 on chromosome: 3 position 2510417 to 2512172 - [DDB_G0279755] |
| DDB0307132 | Protein\|gene: DDB_G0271816 on chromosome: 2 position 825354 to 829079 - [DDB_G0271816] |
| DDB0234128 | Protein\|gene: DDB_G0286603 on chromosome: 4 position 4689118 to 4691291 - [DDB_G0286603] |
| DDB0216236 | Protein\|gene: cinC on chromosome: 5 position 689907 to 692602 - [DDB_G0287685] |
| DDB0235357 | Protein\|gene: pccB on chromosome: 2 position 6663471 to 6665132 - [DDB_G0276341] |
| DDB0214823 | Protein\|gene: rac1C on chromosome: 3 position 6045140 to 6045859 - [DDB_G0282365] |

| | |
|---|---|
| DDB0309089 | Protein\|gene: DDB_G0286271 on chromosome: 4 position 4271583 to 4273892 - [DDB_G0286271] |
| DDB0191188 | Protein\|gene: gxcC on chromosome: 4 position 2552011 to 2555903 - [DDB_G0284845] |
| DDB0234061 | Protein\|gene: pdx2 on chromosome: 5 position 1361910 to 1362748 - [DDB_G0288305] |
| DDB0238048 | Protein\|gene: pex5 on chromosome: 4 position 3973237 to 3975427 - [DDB_G0286033] |
| DDB0232925 | Protein\|gene: DDB_G0285709 on chromosome: 4 position 3622848 to 3624630 - [DDB_G0285709] |
| DDB0231061 | Protein\|gene: rps21 on chromosome: 6 position 3013335 to 3014141 - [DDB_G0293700] |
| DDB0238758 | Protein\|gene: DDB_G0269462 on chromosome: 1 position 2825931 to 2833171 - [DDB_G0269462] |
| DDB0235343 | Protein\|gene: spkA-2 on chromosome: 2 position 3060166 to 3062409 - [DDB_G0273531] |
| DDB0233899 | Protein\|gene: adcA on chromosome: 6 position 2277184 to 2279014 - [DDB_G0292924] |
| DDB0216430 | Protein\|gene: sir2A on chromosome: 4 position 1272110 to 1273864 - [DDB_G0283917] |
| DDB0306677 | Protein\|gene: DDB_G0289679 on chromosome: 5 position 3090972 to 3091571 - [DDB_G0289679] |
| DDB0216422 | Protein\|gene: DDB_G0277405 on chromosome: 2 position 7966950 to 7968159 - [DDB_G0277405] |
| DDB0185025 | Protein\|gene: casK on chromosome: 2 position 7370887 to 7372679 - [DDB_G0276885] |
| DDB0235256 | Protein\|gene: oxct on chromosome: 5 position 1121891 to 1123618 - [DDB_G0288105] |
| DDB0233513 | Protein\|gene: DDB_G0276361 on chromosome: 2 position 6745195 to 6747564 - [DDB_G0276361] |
| DDB0233866 | Protein\|gene: DDB_G0288947 on chromosome: 5 position 2162285 to 2166798 - [DDB_G0288947] |
| DDB0348083 | Protein\|gene: DDB_G0283003 on chromosome: 4 position 141272 to 141856 - [DDB_G0283003] |
| DDB0214827 | Protein\|gene: rasC on chromosome: 3 position 4519070 to 4520084 - [DDB_G0281385] |
| DDB0191099 | Protein\|gene: fhbA on chromosome: 6 position 1649565 to 1650758 - [DDB_G0292378] |
| DDB0347240 | Protein\|gene: DDB_G0281775 on chromosome: 3 position 4948067 to 4949528 - [DDB_G0281775] |
| DDB0307155 | Protein\|gene: DDB_G0272322 on chromosome: 2 position 1285359 to 1286321 - [DDB_G0272322] |
| DDB0230207 | Protein\|gene: abpF on chromosome: 6 position 145941 to 153138 - [DDB_G0291229] |
| DDB0230205 | Protein\|gene: cda on chromosome: 5 position 2144804 to 2145603 - [DDB_G0288933] |
| DDB0231298 | Protein\|gene: DDB_G0291926 on chromosome: 6 position 959253 to 960582 - [DDB_G0291926] |
| DDB0306882 | Protein\|gene: DDB_G0278547 on chromosome: 3 position 1050062 to 1052275 - [DDB_G0278547] |
| DDB0233905 | Protein\|gene: DDB_G0268064 on chromosome: 1 position 1393387 to 1394274 - [DDB_G0268064] |
| DDB0231269 | Protein\|gene: valS1 on chromosome: 2 position 8402743 to 8406060 - [DDB_G0277733] |
| DDB0231288 | Protein\|gene: idhA on chromosome: 2 position 68200 to 69521 - [DDB_G0271344] |
| DDB0201650 | Protein\|gene: hydA on chromosome: 5 position 4230498 to 4232233 - [DDB_G0290479] |
| DDB0306426 | Protein\|gene: DDB_G0287929 on chromosome: 5 position 861720 to 863096 - [DDB_G0287929] |
| DDB0233032 | Protein\|gene: cyp524A1 on chromosome: 1 position 2256023 to 2257759 - [DDB_G0269016] |
| DDB0233925 | Protein\|gene: eif3E on chromosome: 6 position 2402071 to 2403845 - [DDB_G0293052] |
| DDB0232958 | Protein\|gene: psmB2 on chromosome: 1 position 2839118 to 2839714 - [DDB_G0269472] |
| DDB0191505 | Protein\|gene: vacA on chromosome: 5 position 2888908 to 2890870 - [DDB_G0289485] |
| DDB0231253 | Protein\|gene: leuS on chromosome: 4 position 3240792 to 3244287 - [DDB_G0285451] |
| DDB0238518 | Protein\|gene: DDB_G0287005 on chromosome: 4 position 5193960 to 5195815 - [DDB_G0287005] |
| DDB0215348 | Protein\|gene: cnxA on chromosome: 2 position 216838 to 218448 - [DDB_G0271144] |
| DDB0215387 | Protein\|gene: pdhC on chromosome: 3 position 1063899 to 1066276 - [DDB_G0277847] |
| DDB0191197 | Protein\|gene: adprt4 on chromosome: 1 position 243053 to 245068 - [DDB_G0267468] |
| DDB0347428 | Protein\|gene: DDB_G0292080 on chromosome: 6 position 1159633 to 1160758 - [DDB_G0292080] |
| DDB0231400 | Protein\|gene: fumH on chromosome: 3 position 3451016 to 3452416 - [DDB_G0280495] |
| DDB0306782 | Protein\|gene: DDB_G0293032 on chromosome: 6 position 2351624 to 2356321 - [DDB_G0293032] |
| DDB0233990 | Protein\|gene: cct3 on chromosome: 3 position 4903167 to 4904990 - [DDB_G0281741] |
| DDB0215010 | Protein\|gene: glpV on chromosome: 3 position 4540912 to 4543611 - [DDB_G0281383] |
| DDB0238179 | Protein\|gene: sgtA on chromosome: 3 position 3286144 to 3287386 - [DDB_G0280345] |
| DDB0231372 | Protein\|gene: DDB_G0269046 on chromosome: 1 position 1853006 to 1856574 - [DDB_G0269046] |
| DDB0305871 | Protein\|gene: DDB_G0284681 on chromosome: 4 position 2334842 to 2335972 - [DDB_G0284681] |
| DDB0302549 | Protein\|gene: ndufa9 on chromosome: 2 position 1449219 to 1450573 - [DDB_G0272266] |
| DDB0215363 | Protein\|gene: alrA on chromosome: 6 position 3404974 to 3406128 - [DDB_G0293850] |
| DDB0308333 | Protein\|gene: DDB_G0267754 on chromosome: 1 position 786322 to 788000 - [DDB_G0267754] |
| DDB0306572 | Protein\|gene: DDB_G0269452 on chromosome: 1 position 2799520 to 2802510 - [DDB_G0269452] |

## Atg8 mass Spectrometry

| | |
|---|---|
| DDB0191259 | Protein\|gene: mvpA on chromosome: 1 position 3649783 to 3652408 - [DDB_G0269156] |
| DDB0191337 | Protein\|gene: mvpB on chromosome: 5 position 5070813 to 5073466 - [DDB_G0291127] |
| DDB0214819 | Protein\|gene: atg7 on chromosome: 2 position 20345 to 22738 - [DDB_G0271096] |
| DDB0191413 | Protein\|gene: atg8 on chromosome: 4 position 4321108 to 4321704 - [DDB_G0286191] |
| DDB0305138 | Protein\|gene: DDB_G0286393 on chromosome: 4 position 4403606 to 4404448 - [DDB_G0286393] |
| DDB0214936 | Protein\|gene: rpl28 on chromosome: 3 position 6061184 to 6061582 - [DDB_G0282379] |
| DDB0230149 | Protein\|gene: rpl23a on chromosome: 6 position 2967908 to 2968721 - [DDB_G0293502] |
| DDB0231339 | Protein\|gene: rpl7a on chromosome: 2 position 8280728 to 8282193 - [DDB_G0277629] |
| DDB0252605 | Protein\|gene: atg3 on chromosome: 2 position 7690557 to 7691968 - [DDB_G0277319] |
| DDB0214837 | Protein\|gene: adprt1B on chromosome: 3 position 1744004 to 1746597 - [DDB_G0279195] |
| DDB0230024 | Protein\|gene: rps7 on chromosome: 5 position 2252902 to 2253483 - [DDB_G0289025] |
| DDB0231483 | Protein\|gene: mmsdh on chromosome: 5 position 2337171 to 2339014 - [DDB_G0289085] |
| DDB0231358 | Protein\|gene: scsB on chromosome: 2 position 4574977 to 4576552 - [DDB_G0274449] |
| DDB0305344 | Protein\|gene: crip on chromosome: 1 position 4620271 to 4621128 - [DDB_G0270314] |
| DDB0306721 | Protein\|gene: DDB_G0291175 on chromosome: 5 position 5097563 to 5100774 - [DDB_G0291175] |
| DDB0191488 | Protein\|gene: zipA on chromosome: 4 position 5171363 to 5174437 - [DDB_G0286985] |
| DDB0237782 | Protein\|gene: atp5C1 on chromosome: 6 position 1438508 to 1440245 - [DDB_G0292306] |
| DDB0232091 | Protein\|gene: DDB_G0287407 on chromosome: 5 position 263392 to 268500 - [DDB_G0287407] |
| DDB0307261 | Protein\|gene: DDB_G0275359 on chromosome: 2 position 5424566 to 5425954 - [DDB_G0275359] |
| DDB0234117 | Protein\|gene: ogdh on chromosome: 5 position 1102242 to 1105954 - [DDB_G0288127] |
| DDB0306677 | Protein\|gene: DDB_G0289679 on chromosome: 5 position 3090972 to 3091571 - [DDB_G0289679] |
| DDB0233077 | Protein\|gene: uqcrh on chromosome: 2 position 890518 to 891898 - [DDB_G0271774] |
| DDB0231059 | Protein\|gene: rps19 on chromosome: 3 position 1760514 to 1760960 - [DDB_G0279207] |
| DDB0234112 | Protein\|gene: eif2s2 on chromosome: 3 position 5298628 to 5299779 - [DDB_G0282035] |
| DDB0346635 | Protein\|gene: DDB_G0293328 on chromosome: 6 position 2760211 to 2760718 - [DDB_G0293328] |
| DDB0214823 | Protein\|gene: rac1C on chromosome: 3 position 6045140 to 6045859 - [DDB_G0282365] |
| DDB0185208 | Protein\|gene: paxB on chromosome: 2 position 4174381 to 4176090 - [DDB_G0274109] |
| DDB0191476 | Protein\|gene: rab1A on chromosome: 4 position 1241175 to 1242406 - [DDB_G0283757] |
| DDB0306782 | Protein\|gene: DDB_G0293032 on chromosome: 6 position 2351624 to 2356321 - [DDB_G0293032] |
| DDB0231061 | Protein\|gene: rps21 on chromosome: 6 position 3013335 to 3014141 - [DDB_G0293700] |
| DDB0308249 | Protein\|gene: DDB_G0279941 on chromosome: 3 position 2718242 to 2721164 - [DDB_G0279941] |
| DDB0214931 | Protein\|gene: limC on chromosome: 3 position 309381 to 310345 - [DDB_G0277881] |
| DDB0306067 | Protein\|gene: DDB_G0282713 on chromosome: 3 position 6189456 to 6191092 - [DDB_G0282713] |
| DDB0238518 | Protein\|gene: DDB_G0287005 on chromosome: 4 position 5193960 to 5195815 - [DDB_G0287005] |
| DDB0233990 | Protein\|gene: cct3 on chromosome: 3 position 4903167 to 4904990 - [DDB_G0281741] |
| DDB0232995 | Protein\|gene: psmD12 on chromosome: 3 position 3979792 to 3981586 - [DDB_G0281051] |
| DDB0230145 | Protein\|gene: DDB_G0271904 on chromosome: 2 position 1058890 to 1061065 - [DDB_G0271904] |
| DDB0231305 | Protein\|gene: serS on chromosome: 2 position 2243539 to 2245192 - [DDB_G0272660] |
| DDB0191364 | Protein\|gene: pfkA on chromosome: 2 position 4510635 to 4513139 - [DDB_G0274111] |
| DDB0233359 | Protein\|gene: pabpc1A on chromosome: 6 position 3041877 to 3044187 - [DDB_G0293558] |
| DDB0237755 | Protein\|gene: odc on chromosome: 3 position 4069177 to 4070741 - [DDB_G0281109] |
| DDB0266791 | Protein\|gene: dnpep on chromosome: 4 position 4132917 to 4134488 - [DDB_G0286149] |
| DDB0219929 | Protein\|gene: hspA on chromosome: 5 position 1238068 to 1240089 - [DDB_G0288181] |
| DDB0185019 | Protein\|gene: rpl36 on chromosome: 2 position 733224 to 733804 - [DDB_G0271668] |
| DDB0267025 | Protein\|gene: rpl37 on chromosome: 4 position 3886590 to 3887209 - [DDB_G0285971] |
| DDB0307317 | Protein\|gene: DDB_G0277327 on chromosome: 2 position 7723793 to 7727267 - [DDB_G0277327] |
| DDB0231067 | Protein\|gene: rps28 on chromosome: 4 position 3428530 to 3429424 - [DDB_G0285597] |
| DDB0191401 | Protein\|gene: limD1 on chromosome: 5 position 361279 to 361988 - [DDB_G0287507] |
| DDB0308149 | Protein\|gene: DDB_G0275519 on chromosome: 2 position 6062122 to 6063145 - [DDB_G0275519] |
| DDB0235253 | Protein\|gene: impa1 on chromosome: 3 position 4261304 to 4262400 - [DDB_G0281239] |
| DDB0237515 | Protein\|gene: DDB_G0293070 on chromosome: 6 position 2426564 to 2433958 - [DDB_G0293070] |
| DDB0185029 | Protein\|gene: chcA on chromosome: 2 position 7717198 to 7722630 - [DDB_G0277221] |
| DDB0191157 | Protein\|gene: H3a on chromosome: 1 position 1520754 to 1521173 - [DDB_G0267402] |
| DDB0302555 | Protein\|gene: DDB_G0272318 on chromosome: 2 position 1278811 to 1280712 - [DDB_G0272318] |
| DDB0231150 | Protein\|gene: rpl32 on chromosome: 2 position 1095789 to 1096190 - [DDB_G0271976] |
| DDB0231480 | Protein\|gene: DDB_G0276305 on chromosome: 2 position 6612090 to 6614240 - [DDB_G0276305] |

# ANNEX 2: PUBLICATION LIST

**Article:** Monitoring Autophagy in Dictyostelium.

Ana Mesquita, Javier Calvo-Garrido, Sergio Carilla-Latorre, Ricardo Escalante

PMID: 23494324

**Article:** A proteolytic cleavage assay to monitor autophagy in Dictyostelium discoideum.

Calvo-Garrido J, Carilla-Latorre S, **Mesquita A**, Escalante R.

PMID: 21876387

**Chapter:** Dictyostelium discoideum as a model in Biomedical Research.

In book: Dictyostelids. Evolution, Genomics and Cell Biology, Chapter: Dictyostelium dscoideum as a model in Biomedical Research, Publisher: Springer, Editors: María Romeralo; Sandra Baldaulf and Ricardo Escalante, pp.1-34, 01/2013.

**Article:** Autophagy in Dictyostelium: genes and pathways, cell death and infection.

Javier Calvo-Garrido, Sergio Carilla-Latorre, Yuzuru Kubohara, Natalia Santos-Rodrigo, **Ana Mesquita**, Thierry Soldati, Pierre Golstein, Ricardo Escalante.

PMID: 20603609